USGS
science for a changing world

Geologic Field-Trip Guide to Volcanism and its Interaction with Snow and Ice at Mount Rainier, Washington

Scientific Investigations Report 2017–5022–A

U.S. Department of the Interior
U.S. Geological Survey

COVER.

Northeastern flank of Mount Rainier from near Sunrise, Washington. Photograph by Jim Vallance, U.S. Geological Survey.

Geologic Field-Trip Guide to Volcanism and its Interaction with Snow and Ice at Mount Rainier, Washington

By James W. Vallance and Thomas W. Sisson

Scientific Investigations Report 2017–5022–A

U.S. Department of the Interior
U.S. Geological Survey

U.S. Geological Survey, Reston, Virginia: 2022

Suggested citation:
Vallance, J.W., and Sisson, T.W., 2022, Geologic field-trip guide to volcanism and its interaction with snow and ice at Mount Rainier, Washington: U.S. Geological Survey Scientific Investigations Report 2017–5022–A, 76 p., https://doi.org/10.3133/sir20175022A.

ISSN 2328-0328 (online)

Preface

The North American Cordillera is home to a greater diversity of volcanic provinces than any comparably sized region in the world. The interplay between changing plate-margin interactions, tectonic complexity, intra-crustal magma differentiation, and mantle melting have resulted in a wealth of volcanic landscapes. Field trips in this series visit many of these landscapes, including (1) active subduction-related arc volcanoes in the Cascade Range; (2) flood basalts of the Columbia Plateau; (3) bimodal volcanism of the Snake River Plain-Yellowstone volcanic system; (4) some of the world's largest known ignimbrites from southern Utah, central Colorado, and northern Nevada; (5) extension-related volcanism in the Rio Grande Rift and Basin and Range Province; and (6) the spectacular eastern Sierra Nevada featuring Long Valley Caldera and the iconic Bishop Tuff. Some of the field trips focus on volcanic eruptive and emplacement processes, calling attention to the fact that the western United States provides opportunities to examine a wide range of volcanological phenomena at many scales.

The 2017 Scientific Assembly of the International Association of Volcanology and Chemistry of the Earth's Interior (IAVCEI) in Portland, Oregon, marks the first time that the U.S. volcanological community has hosted this quadrennial meeting since 1989, when it was held in Santa Fe, New Mexico. The 1989 field-trip guides are still widely used by students and professionals alike. This new set of field guides is similarly a legacy collection that summarizes decades of advances in our understanding of magmatic and tectonic processes of volcanic western North America.

The field of volcanology has flourished since the 1989 IAVCEI meeting, and it has profited from detailed field investigations coupled with emerging new analytical methods. Mapping has been enhanced by plentiful major- and trace-element whole-rock and mineral data, technical advances in radiometric dating and collection of isotopic data, GPS (Global Positioning System) advances, and the availability of lidar (light detection and ranging) imagery. Spectacularly effective microbeam instruments, geodetic and geophysical data collection and processing, paleomagnetic determinations, and modeling capabilities have combined with mapping to provide new information and insights over the past 30 years. The collective works of the international community have made it possible to prepare wholly new guides to areas across the western United States. These comprehensive field guides are available, in large part, because of enormous contributions from many experienced geologists who have devoted entire careers to their field areas. Early career scientists are carrying forward and refining their foundational work with impressive results.

Our hope is that future generations of scientists as well as the general public will use these field guides as introductions to these fascinating areas and will be enticed toward further exploration and field-based research.

Michael Dungan, University of Oregon
Judy Fierstein, U.S. Geological Survey
Cynthia Gardner, U.S. Geological Survey
Dennis Geist, National Science Foundation
Anita Grunder, Oregon State University
John Wolff, Washington State University

Field-trip committee, IAVCEI 2017

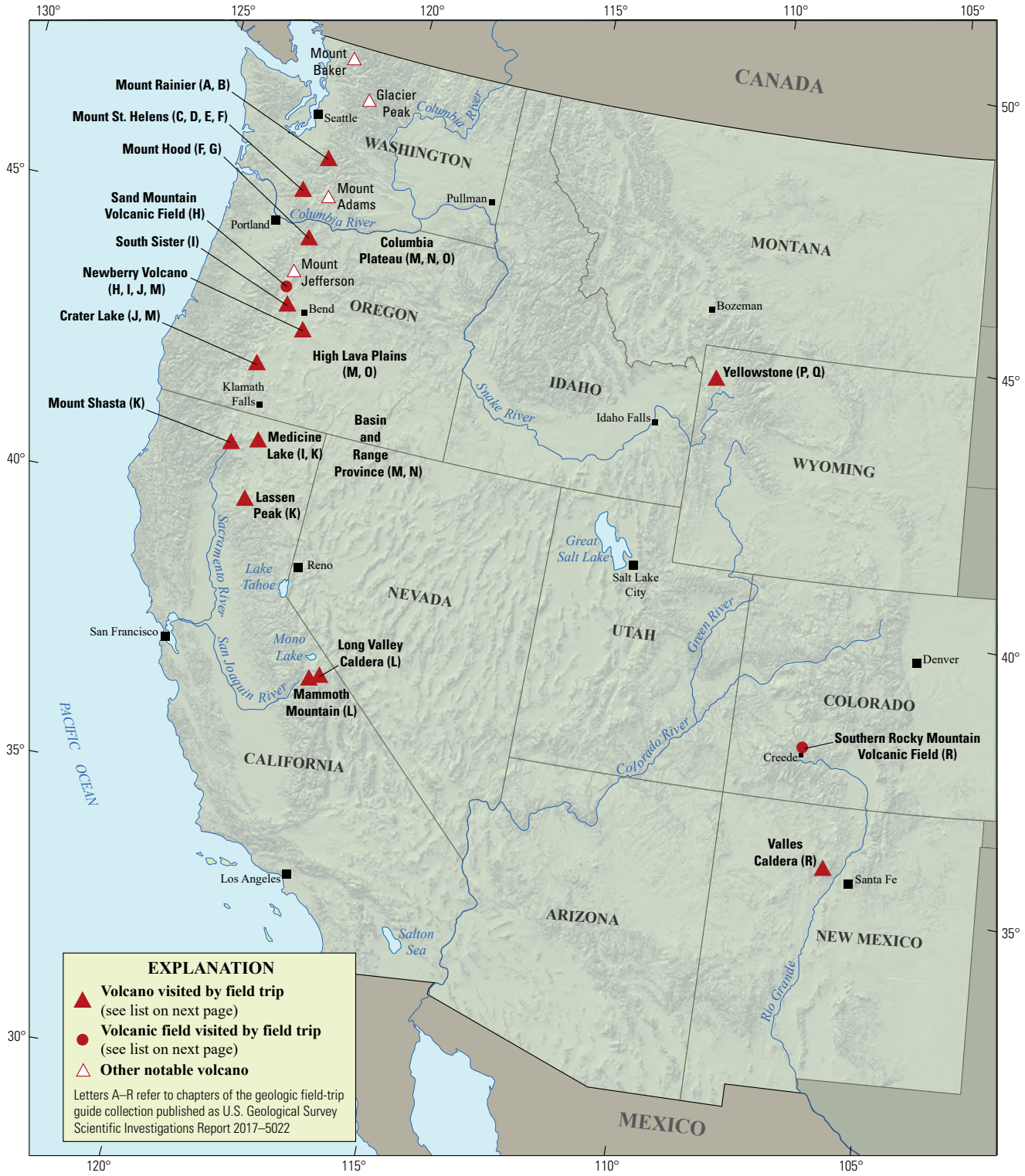

Shaded-relief base from U.S. Geological Survey National Elevation Dataset 30-meter digital elevation model data.

Map of the western United States showing volcanoes and volcanic fields visited by geologic field trips scheduled in conjunction with the 2017 meeting of the International Association of Volcanology and Chemistry of the Earth's Interior (IAVCEI) in Portland, Oregon, and available as chapters in U.S. Geological Survey Scientific Investigations Report 2017–5022.

Contributing Authors

Boise State University
Brittany D. Brand
Nicholas Pollock

Colgate University
Karen Harpp
Alison Koleszar

Durham University
Richard J. Brown

Eastern Oregon University
Mark L. Ferns

ETH Zurich
Olivier Bachmann

Georgia Institute of Technology
Josef Dufek

GNS Science, New Zealand
Natalia I. Deligne

Hamilton College
Richard M. Conrey

Massachusetts Institute of Technology
Timothy Grove

National Science Foundation
Dennis Geist (also with Colgate University and University of Idaho)

New Mexico Bureau of Geology and Mineral Resources
Paul W. Bauer
William C. McIntosh
Matthew J. Zimmerer

New Mexico State University
Emily R. Johnson

Northeastern University
Martin E. Ross

Oregon Department of Geology and Mineral Industries
William J. Burns
Lina Ma
Ian P. Madin
Jason D. McClaughry

Oregon State University
Adam J.R. Kent

Portland State University
Jonathan H. Fink (also with University of British Columbia)
Martin J. Streck
Ashley R. Streig

San Diego State University
Victor E. Camp

Smithsonian Institution
Lee Siebert

Universidad Nacional Autónoma de San Luis Potosi
Damiano Sarocchi

University of California, Davis
Kari M. Cooper

University of Liverpool
Peter B. Kokelaar

University of Northern Colorado
Steven W. Anderson

University of Oregon
Ilya N. Binderman
Michael A. Dungan
Daniele McKay (also with Oregon State University and Oregon State University, Cascades)

University of Portland
Kristin Sweeney

University of Tasmania
Martin Jutzeler
Jocelyn McPhie

University of Utah
Jamie Farrell

U.S. Army Corps of Engineers
Keith I. Kelson

U.S. Forest Service
Gordon E. Grant (also with Oregon State University
Robert A. Jensen

U.S. Geological Survey
Charles R. Bacon
Andrew T. Calvert
Christine F. Chan
Robert L. Christiansen
Michael A. Clynne
Michael A. Cosca
Julie M. Donnelly-Nolan
Benjamin J. Drenth
William C. Evans
Judy Fierstein
Cynthia A. Gardner
V.J.S. Grauch
Christopher J. Harpel
Wes Hildreth
Richard P. Hoblitt
Peter W. Lipman
Jacob B. Lowenstern
Jon J. Major
Seth C. Moran
Lisa A. Morgan
Leah E. Morgan
L.J. Patrick Muffler
James E. O'Connor
John S. Pallister
Thomas C. Pierson
Joel E. Robinson
Juliet Ryan-Davis
Kevin M. Scott
William E. Scott
Wayne (Pat) Shanks
David R. Sherrod
Thomas W. Sisson
Mark Evan Stelten
Weston Thelen
Ren A. Thompson
Kenzie J. Turner
James W. Vallance
Alexa R. Van Eaton
Jorge A. Vazquez
Richard B. Waitt
Heather M. Wright

U.S. Nuclear Regulatory Commission
Stephen Self (also with University of California, Berkeley)

Washington State University
Joseph R. Boro
Owen K. Neill
Stephen P. Reidel
John A. Wolff

Acknowledgments
Juliet Ryan-Davis and Kate Sullivan created the overview map, and Vivian Nguyen created the cover design for this collection of field-trip guide books. The field trip committee is grateful for their contributions.

Contents

Figures

Table

Conversion Factors

International System of Units to U.S. customary units

Multiply	By	To obtain
	Length	
centimeter (cm)	0.3937	inch (in.)
millimeter (mm)	0.03937	inch (in.)
meter (m)	3.281	foot (ft)
kilometer (km)	0.6214	mile (mi)
kilometer (km)	0.5400	mile, nautical (nmi)
meter (m)	1.094	yard (yd)
	Area	
square meter (m^2)	0.0002471	acre
square kilometer (km^2)	247.1	acre
square kilometer (km^2)	0.3861	square mile (mi^2)
	Volume	
cubic meter (m^3)	264.2	gallon (gal)
cubic meter (m^3)	0.0002642	million gallons (Mgal)
cubic meter (m^3)	35.31	cubic foot (ft^3)
cubic meter (m^3)	1.308	cubic yard (yd^3)
cubic kilometer (km^3)	0.2399	cubic mile (mi^3)
cubic meter (m^3)	0.0008107	acre-foot (acre-ft)
	Flow rate	
cubic meter per second (m^3/s)	70.07	acre-foot per day (acre-ft/d)
meter per second (m/s)	3.281	foot per second (ft/s)
cubic meter per second (m^3/s)	35.31	cubic foot per second (ft^3/s)
cubic meter per second (m^3/s)	22.83	million gallons per day (Mgal/d)
millimeter per year (mm/yr)	0.03937	inch per year (in/yr)

Abbreviations

cal. yr B.P.	calendar years before present, where present is 1950
DRE	dense rock equivalent
ka	kilo-annum
Ma	mega-annum
MIS	marine isotope stage
ppm	part per million
QMI	quenched magmatic inclusion
SR	State Route
SVG	sparsely vesicular glassy
USGS	U.S. Geological Survey
UTM	Universal Transverse Mercator
VEI	volcanic explosivity index

Geologic Field-Trip Guide to Volcanism and its Interaction with Snow and Ice at Mount Rainier, Washington

By James W. Vallance and Thomas W. Sisson

Introduction

Mount Rainier is the Pacific Northwest's iconic volcano. At 4,393 meters (m) (14,410 feet [ft]) and situated in the south-central Cascade Range of Washington State, it towers over cities of the Puget Lowland (figs. 1 and 2). It was known among Native Americans as Tacoma or Tahoma. In 1792, Captain George Vancouver dubbed it by its present official name after his friend, Rear Admiral Peter Rainier. Just prior to Super Bowl XLVIII, the Washington State Senate temporarily renamed it Mount Seattle Seahawks. More serious debate periodically arises about returning to the original name, Mount Tahoma.

As the highest summit in the Cascade Range, Mount Rainier hosts 26 glaciers and numerous permanent snow fields covering 87 square kilometers (km^2) and having a snow and ice volume of about 3.8 cubic kilometers (km^3). It remains by far the most heavily glacier-clad mountain in the conterminous United States despite having lost about 14 percent of its ice volume between 1970 and 2008 (Sisson and others, 2011). The largest of its glaciers descend 6–10 kilometers (km) in all directions from the summit into deeply incised valleys (as much as 1,000 m relief) that are relics of Pleistocene glaciations. Termini of the largest glaciers typically lie between 1,100 (north) and 1,600 m (south and west) elevation.

Five major rivers head at Mount Rainier (fig. 1). Because Mount Rainier is situated west of the Cascade Range crest, all of these rivers eventually turn and drain westward. The White, Carbon, Puyallup, and Nisqually Rivers head on the northeast, north, west, and south flanks of the mountain and eventually empty into Puget Sound. In contrast, the Cowlitz River, which drains the southeast quadrant of the volcano, empties into the Columbia River.

The Puget Lowland, situated west to northwest of Mount Rainier, is the Pacific Northwest's most densely populated area, including Seattle, Tacoma, and Olympia, the capital of Washington State (fig. 1). The Puget Lowland is now home to a population of more than 4.5 million and a vibrant economy in which new industries such as aerospace (Boeing), technology (Microsoft), and service (Amazon) superseded older resource extraction (especially timber) and shipping industries.

Mount Rainier is one of the most hazardous volcanoes in the United States, not so much because of its explosivity, but rather because of its frequent eruptions, its propensity to produce voluminous far-traveled lahars, and its proximity to large population centers of the Puget Lowland (fig. 2) (Crandell, 1971; Sisson and Vallance, 2009). Steep-sided, glacially carved valleys serve as lahar conduits, and even mild eruptions commonly produced large lahars that traveled into areas now populated by hundreds of thousands of people. Because of its prominence and its threat to communities downstream, Mount Rainier was targeted for intensive study as a Decade Volcano in the 1990s as part of the United Nations' International Decade for Natural Disaster Reduction, and Mount Rainier has continued to be a focus for scientific research since that time.

Tectonic Setting

Subduction of the Juan de Fuca Plate beneath the western margin of the North American Plate gives rise to the present, north-south-trending, Cascades volcanic arc, extending ~1,400 km from Silverthrone Mountain in southern British Columbia to Lassen Peak in northern California. At the latitude of Mount Rainier, the Juan de Fuca Plate moves ~4.3 centimeters per year east-northeastward relative to North America. In contrast, the Pacific Plate moves north relative to the North American Plate, causing right-lateral strike slip on the fault systems north and south of the subducting Juan de Fuca Plate. Because the Juan de Fuca spreading ridge is merely 250–450 km from the axis of the volcanic arc (fig. 3), the subducting oceanic crust of the Cascades volcanic arc is among the youngest (10–15 million years old [Ma]) and hottest worldwide (Hyndman and Wang, 1993).

Northward translation of the Sierra Nevada block and impingement of the Basin and Range Province at the south end of the Cascades volcanic arc combine with a Coast Mountains buttress to the north to fragment elements of the Pacific Northwest portion of the North American Plate and influence volcanism along the arc. Pacific Plate motion along the San Andreas Fault System combined with opening of the Basin and Range Province pulls the Sierra Nevada block northwestward, causing rotation of an Oregon coastal block and compressing the Washington block against the northern Coast Mountains of British Columbia so that the arc grades from transtensional to transpressional from south to north (fig. 4). From south to north, increasing compression corresponds to diminished volcanic productivity along the arc, with extensive volcanic fields surrounding more numerous stratovolcanoes in the south versus isolated stratovolcanoes to the north. Mount Rainier is at the far north end of the more productive southern segment of the arc.

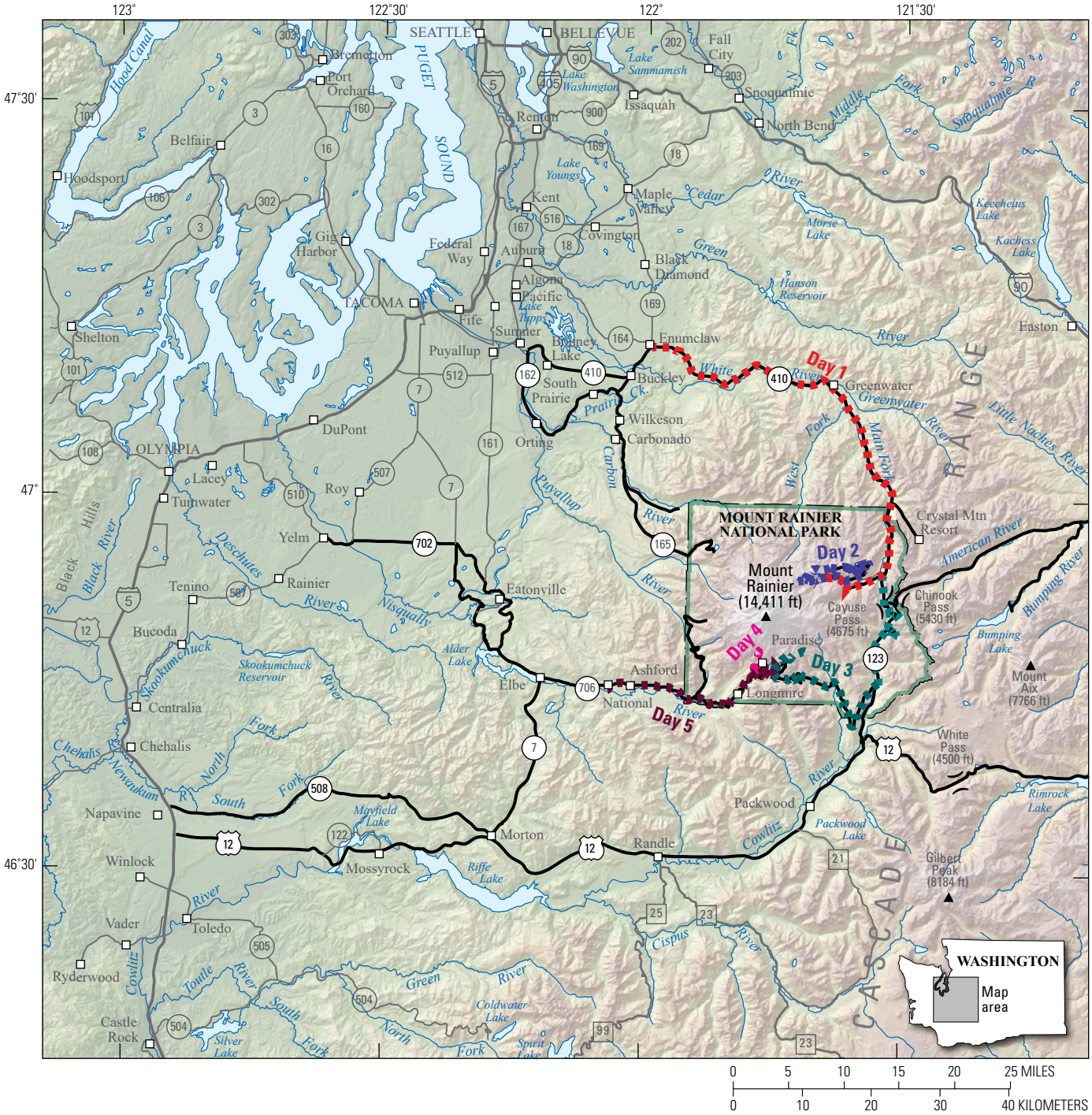

Figure 1. Map of Mount Rainier and the Puget Lowland showing the route the field trip will take on each of five days. Map modified from Pringle (2008).

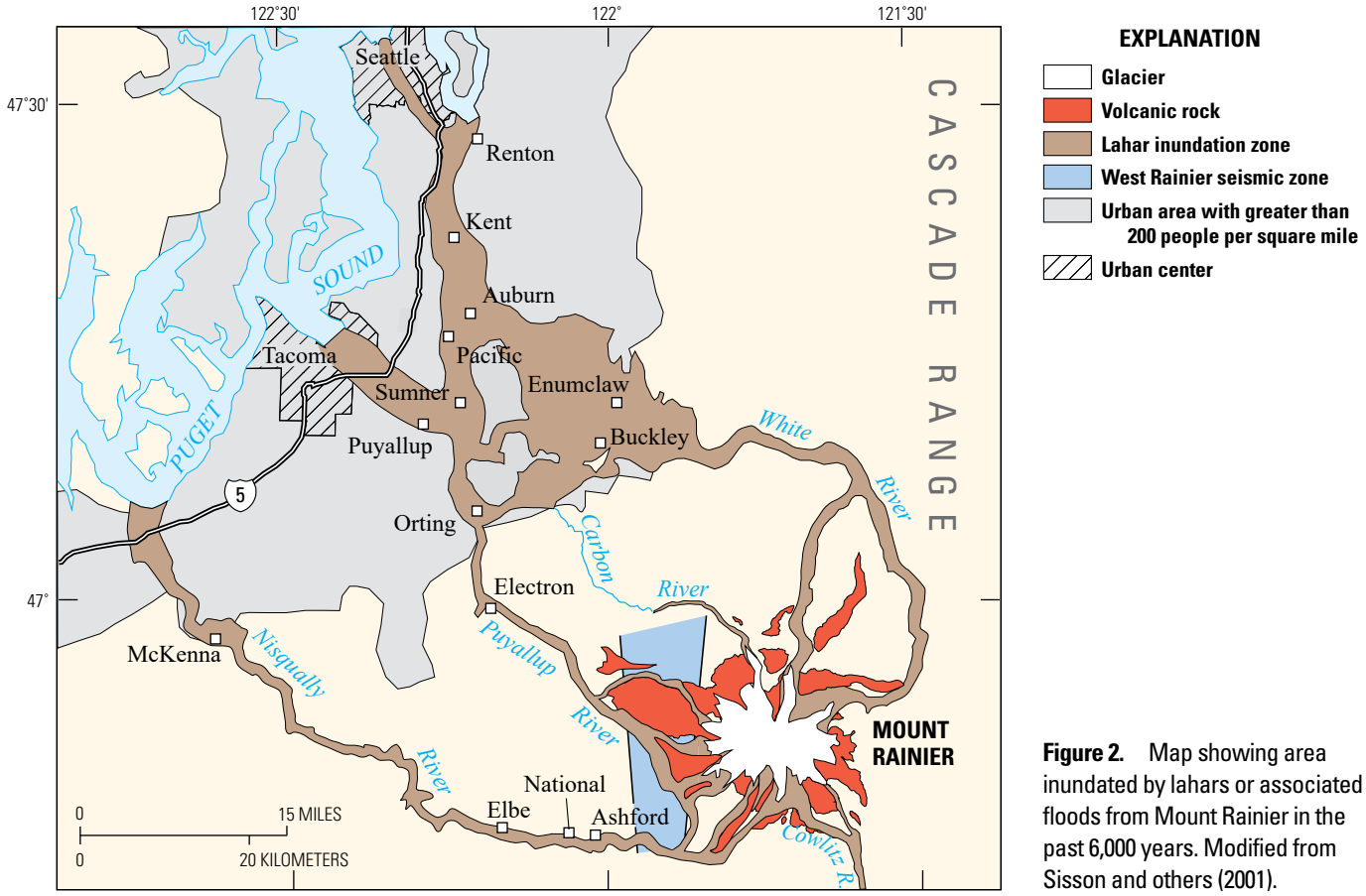

Figure 2. Map showing area inundated by lahars or associated floods from Mount Rainier in the past 6,000 years. Modified from Sisson and others (2001).

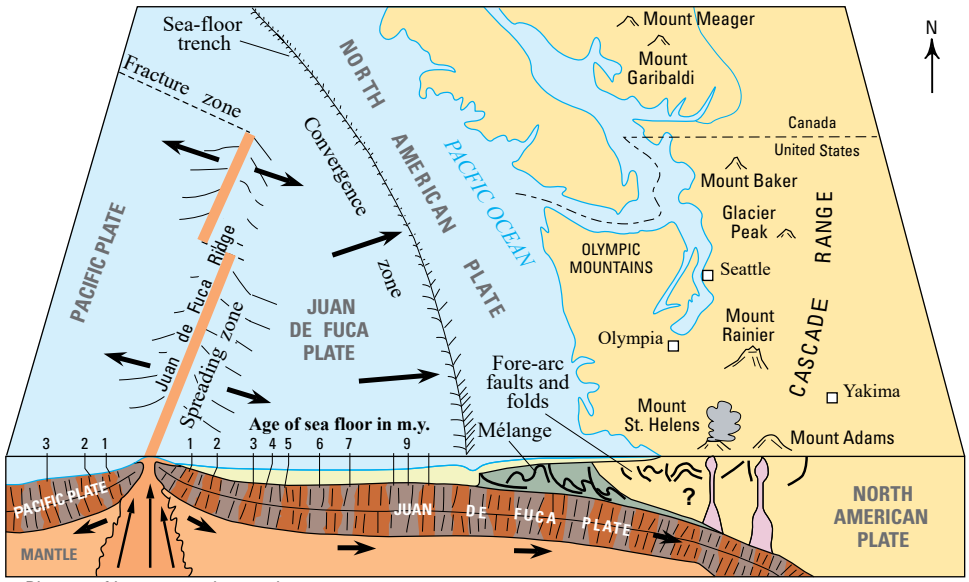

Figure 3. Schematic block diagram of the Juan de Fuca spreading ridge and the Cascadia subduction zone (the area from the trench east to where the Juan de Fuca Plate sinks beneath the North American Plate). Striping in the cross section of the sea floor indicates the magnetic orientation of the sea floor recorded at the Juan de Fuca spreading ridge: brown areas indicate times when rock was created with a magnetic orientation of north; red-brown segments have reversed polarity. Notice that the age (in million years [m.y.]) of the ocean floor is progressively older with distance from the spreading zone. The pattern of ages approximately parallels the ridge on both sides. The mélange is a jumbled mixture of continental shelf blocks and oceanic sediments that is faulted and sheared at shallow depths in the subduction zone. The fore-arc faults and folds occur in a zone of crustal deformation between the subducting sea floor and the Cascade Range volcanic arc. Redrawn from Foxworthy and Hill (1982) and Uyeda (1978) by Pringle (2008) and modified slightly here.

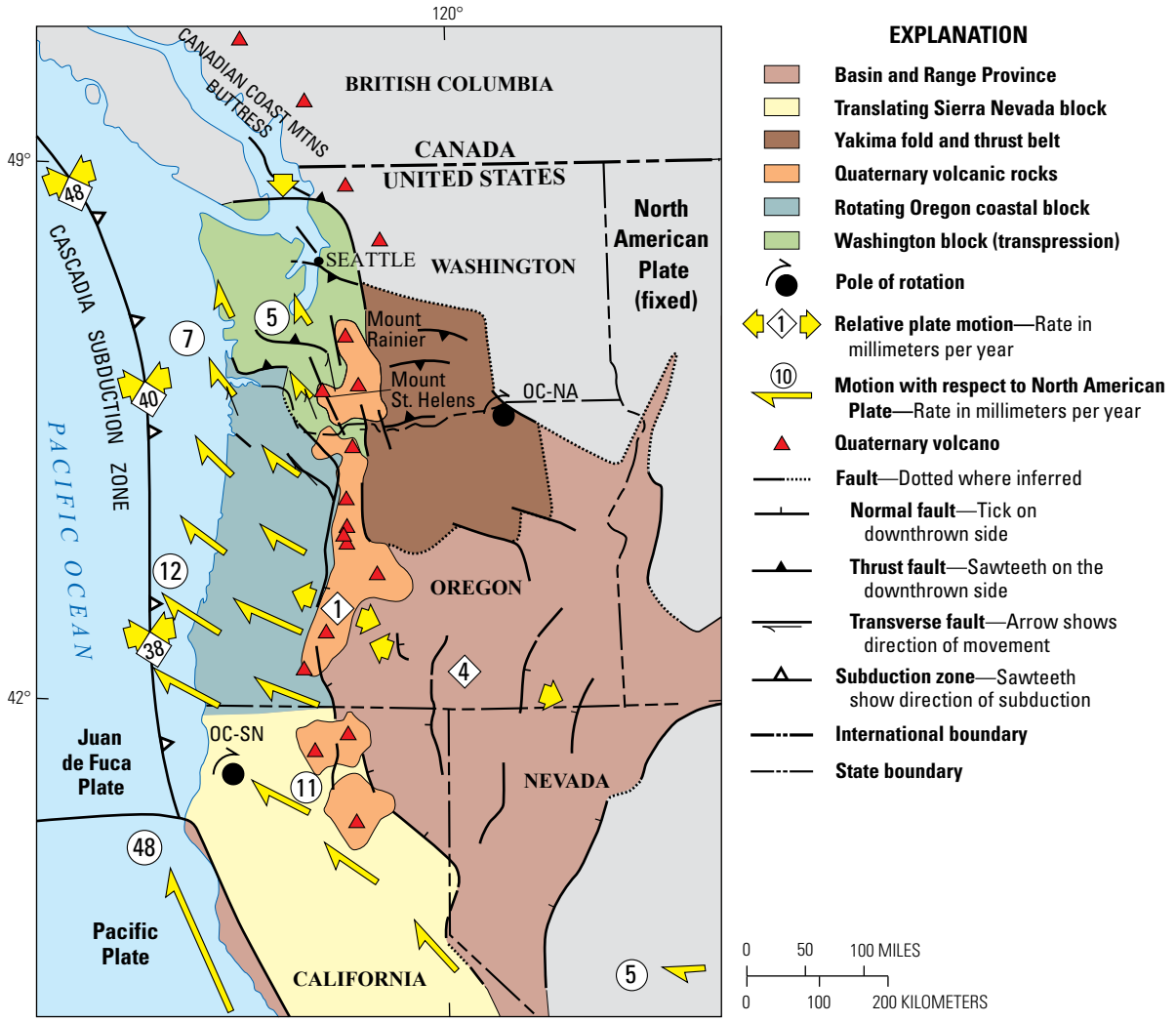

Figure 4. Generalized map of the tectonic setting of Cascadia. The Juan de Fuca Plate is subducting along the Cascadia subduction zone. The migrating Cascadia fore-arc terrane is divided into Washington, Oregon coastal (OC), and Sierra Nevada (SN) blocks. The velocity (in millimeters per year [mm/yr]) of the tectonic blocks (yellow arrows) is calculated from a pole of rotation at point OC-NA (North America). The Oregon coastal block is also rotating around pole OC-SN. The velocity of the Oregon Coastal block is calculated for the post-Eocene. The north end of the Oregon block squeezes the fore-arc area of Washington (green) against the buttress-like mass of crystalline rocks in the Canadian Coast Mountains. This relative movement causes north-south compression, uplift, thrust faulting, and consequent earthquakes. Modified from Pringle (2008) and Wells and others (1998, 2002).

Regional Geology

Regional Cascade Range Geology

Over the past approximately 200 million years, the west coast of North America was the site of subduction magmatism and the accretion of terranes, both by direct collision and by strike-slip faulting. These processes expanded the continental margin westward by as much as 600 km. In the Mount Rainier region, volcanic, sedimentary, and plutonic rocks of the past 37 million years generally overlie and conceal accreted terranes. Regional crustal domains (fig. 5) include the Paleocene to early Eocene Siletzia submarine basalt province that floors the forearc basin west of the active arc from southernmost Vancouver Island southward through Oregon's Willamette Valley (Duncan, 1982). Younger rocks conceal Siletzia's eastern margin, but the north-trending terrane boundary has been inferred from seismic velocity sections to underlie the Mount St. Helens seismic zone (Parsons and others, 1998), which passes beneath Mount St. Helens and about 15 km to the west of Mount Rainier as the west Mount Rainier seismic zone (Stanley and others, 1999). In Washington, the unexposed deep basement abutting Siletzia on the east is probably Mesozoic tectonite mélange correlative with the western and eastern mélange belts that border the western margin of the North Cascades crystalline core to the north of Mount Rainier (Frizzell and others, 1987). Quartz-rich sands and silts from the North American continental interior, and possibly the North Cascades terrane, spread across present-day southern Washington and northern to central Oregon during the

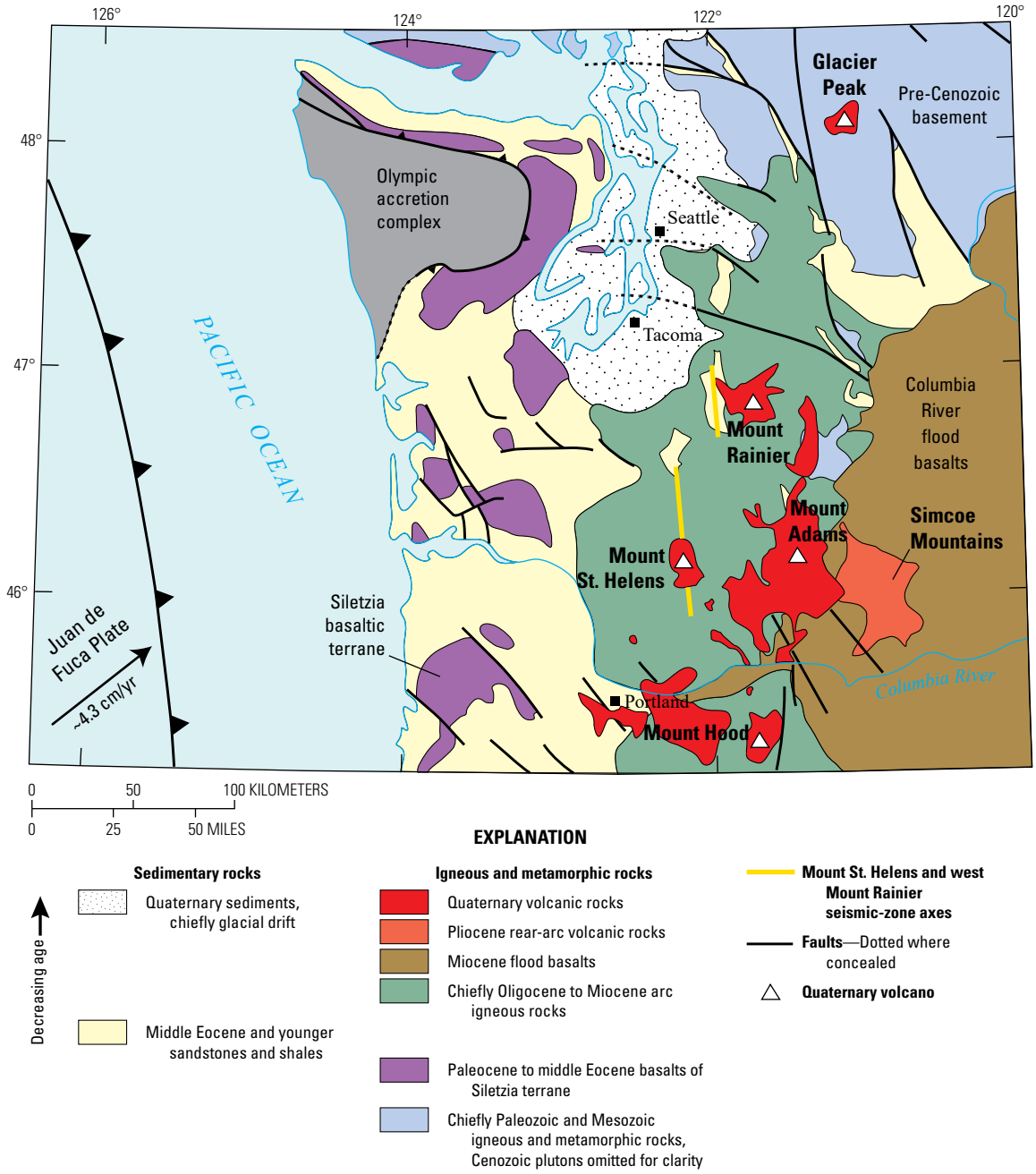

Figure 5. Map showing the regional geologic setting of Mount Rainier volcano. Triangles show locations of Mount Rainier, Mount Adams, Mount St. Helens, Mount Hood, and Glacier Peak. Axes of Mount St. Helens and west Mount Rainier seismic zones (yellow lines) are coincident with anticlinal exposures of Eocene sedimentary rocks that may mark the buried eastern margin of the Siletzia terrane. Arrow in Pacific Ocean shows convergence direction and velocity (in centimeters per year [cm/yr]) of the Juan de Fuca Plate relative to the North American Plate interior. Map simplified from Schuster (2005) and Walker and MacLeod (1991) by Sisson and others (2013) and modified slightly here.

Eocene and partly buried the mélange and Siletzia basalts with fluvial, deltaic, and shallow-marine sediments. These continent-derived sedimentary rocks form the Puget Group in southwest Washington, and the widespread Tyee Formation, among others, in Oregon (Buckovic, 1979; Heller and others, 1985).

Cascades Arc volcanism commenced intermittently and locally in the middle Eocene and became extensive and voluminous in the Oligocene and Miocene (Armentrout, 1987). Oligocene volcanism in southwest Washington is manifest as the widespread andesitic Ohanapecosh Formation, overlain unconformably in the Mount Rainier region by silicic ash-flow tuffs of the 25 Ma rhyolitic Stevens Ridge Formation and the 22 Ma rhyodacitic tuff of Clear West Peak caldera (Vance and others, 1987; Tabor and others, 2000). These late Oligocene and early Miocene ash-flow tuffs are largely overlain by, but also interfinger with, andesitic volcanic rocks

of the chiefly Miocene Fifes Peak Formation. Granodioritic plutons then intruded the Tertiary volcanic section, represented at Mount Rainier by the 19–14 Ma Tatoosh intrusive suite and White River and Carbon River stocks (Mattinson, 1977; du Bray and others, 2011). The late Miocene and Pliocene record of subduction-related volcanism is limited, at least in part owing to rapid uplift and incision of the Washington Cascade Range and Olympic Mountains that commenced perhaps as early as 15.6 Ma, with widespread exhumation ages of about 12–10 Ma (Reiners and others, 2000). Late Miocene volcanism is recorded on the Cascade Range flanks by the volcaniclastic Ellensburg and Mashel Formations but stratified late Miocene deposits are absent from the range interior as uplift and erosion outstripped deposition. Uplift shallowly unroofed the plutons, tilted the 16 Ma Columbia River flood basalts that onlap the eastern margin of the Cascade Range, and incised the deep unconformity upon which the Quaternary volcanoes grew.

Geology of the Mount Rainier Area

Mount Rainier sits atop a broad, north-northwest-trending, internally folded synclinorium of Tertiary arc volcanic rocks, intruded by the Tatoosh plutonic suite, and is flanked on the west and southeast by steep-sided, north-northwest-striking anticlinoria (fig. 6). To the west is the Carbon River anticlinorium cored by middle Eocene Puget Group arkoses, carbonaceous black shales, and local coal seams that dip steeply beneath and floor the Tertiary arc volcanic section. The base of the Puget Group is not exposed in the Carbon River area, but Stanley and others (1994) presented geologic and geophysical evidence for a deformed

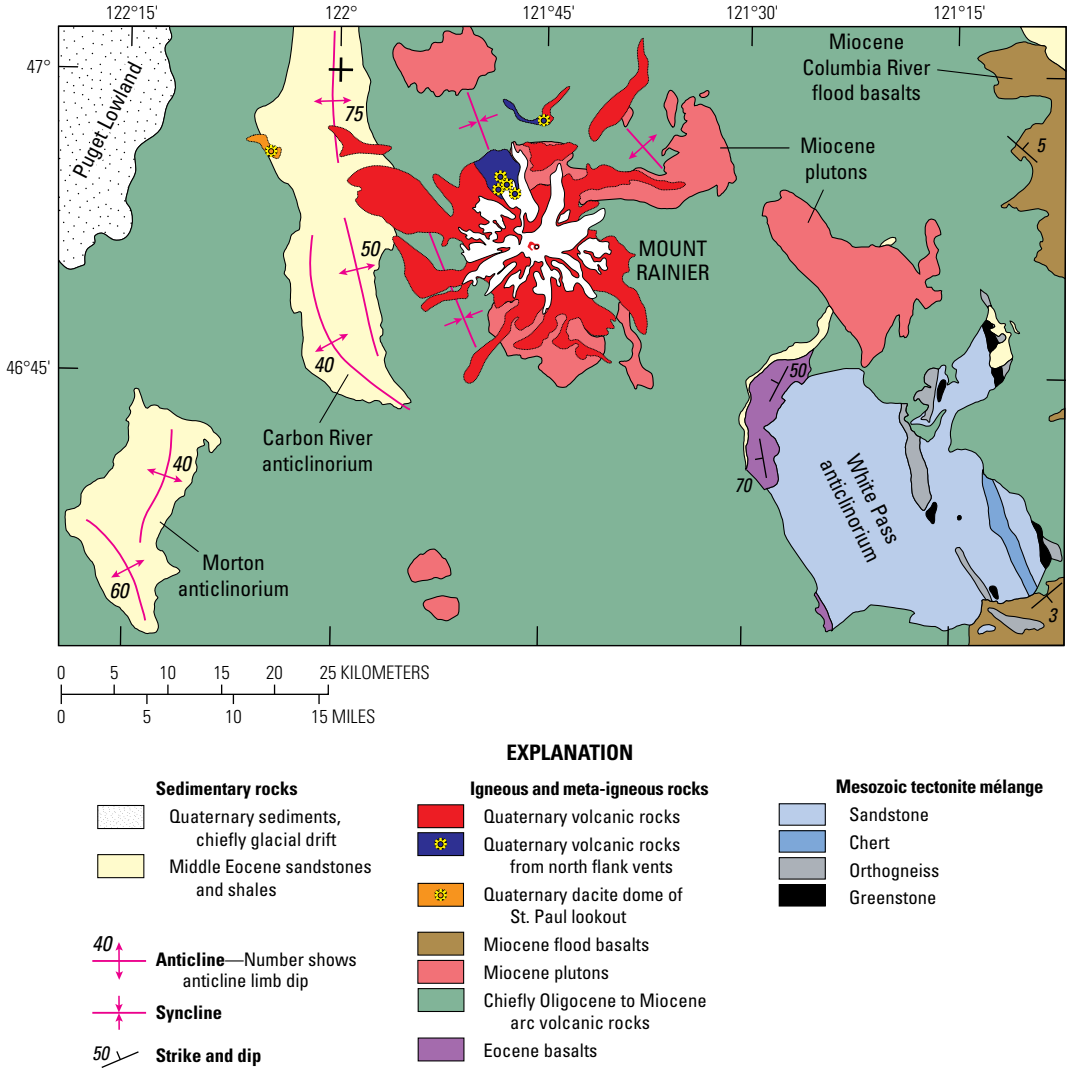

Figure 6. Map showing the local geologic setting of Mount Rainier volcano. Quaternary volcanic rocks of the White Pass area are omitted for clarity. Ice on Mount Rainier is shown as white. Map simplified by Sisson and others (2013) from Fiske and others (1963), Tabor and others (2000), Schasse (1987), and Miller (1989) and modified slightly here.

thickness of 10–20 km, including postulated underlying marine shales that together create the southern Washington Cascade Range (electrical) conductor. The Carbon River anticlinorium coincides with the west Mount Rainier seismic zone, and seismic velocity sections (Stanley and others, 1999) show that it probably overlies the buried eastern margin of Siletzia, similar to the Morton anticlinorium and Mount St. Helens seismic zone to the south (Parsons and others, 1998).

To the southeast is the White Pass anticlinorium (fig. 6), which is cored by the Late Jurassic to Early Cretaceous Rimrock Lake inlier of tectonite mélange. The mélange is composed of sheared dirty arkoses to graywackes, greenstone, minor chert, and tectonically bounded blocks and belts of intrusive rocks ranging from hornblende dioritic orthogneiss to cataclastically deformed biotite granodiorite (Miller, 1989). Mesozoic mélange rocks are overlain unconformably on the west limb of the anticlinorium by the steeply west-dipping Eocene Summit Creek basalt, which is overlain by the arkosic Eocene Summit Creek sandstone, and then Oligocene andesitic rocks of the Ohanapecosh Formation (Vance and others, 1987). Thus, Eocene continent-derived sedimentary rocks dip steeply beneath Mount Rainier both from the west and the southeast (fig. 6) and are probably continuous beneath the volcano in the middle and perhaps lower crust, possibly underlain by Paleocene to Eocene non-arc basalts, all floored by Mesozoic sedimentary and igneous tectonite mélange and disrupted by Tertiary and Quaternary igneous intrusions.

Glacial Geology of Puget Sound and Mount Rainier Areas

Continental Glaciation

During the repeated glaciations of the Pleistocene (fig. 7), ice from the Cordilleran ice sheet advanced into the Puget Lowland and coated the area with glacial drift. In the area west of Mount Rainier, the most prominent of these deposits are those of the most recent Vashon advance (fig. 8). During this advance, the Puget lobe of the ice sheet advanced to about 24 km south of Olympia (fig. 8), and filled the lowland between the Olympic Mountains and Cascade Range to depths of 1,000–2,000 m. The Vashon glacier reached its maximum extent by 17 thousand years ago (ka) and then began to retreat (Porter and Swanson, 1998).

West of Mount Rainier, the Puget lobe banked up against the Cascade Range, damming rivers and forcing them to run southwestward along ice margins and greatly increasing discharge above that of today through meltwater runoff (fig. 8). These conditions created ice-marginal features like lakes in backed-up tributaries, meltwater channels cut through bedrock along the Cascade Range front, and thick ice-marginal deposits. As the Puget lobe retreated, it deposited multiple levels of kame terrace sediments along the Cascade Range front, several of which now crop out between Sumner and Mud Mountain Dam (Crandell, 1963). The early Holocene course of the White River

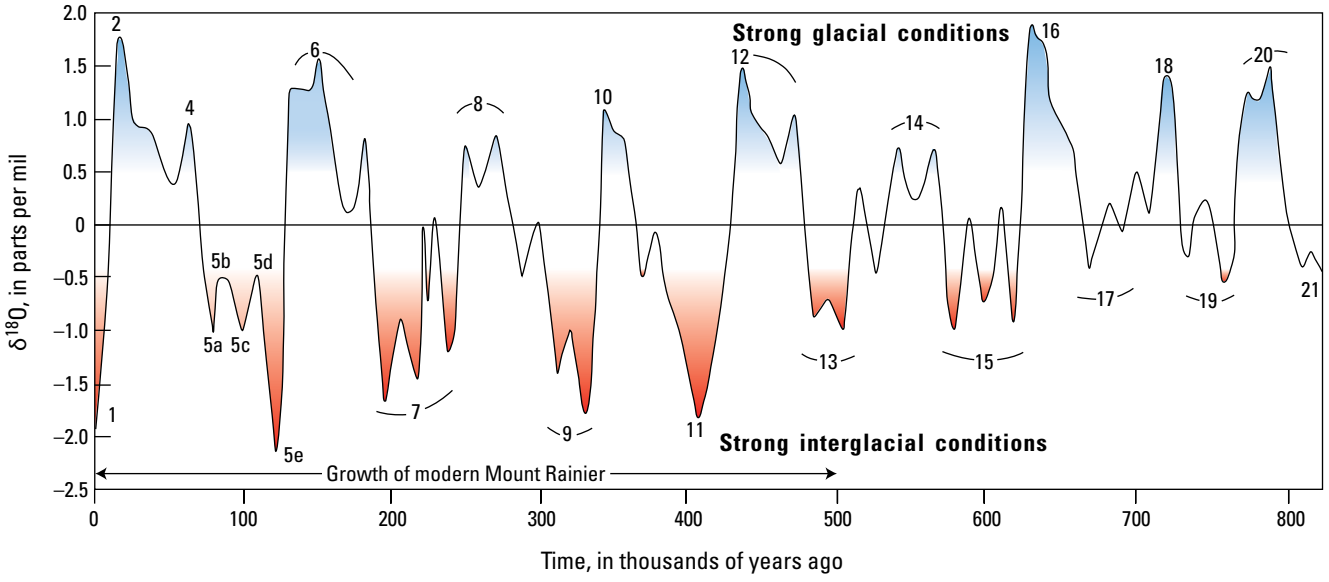

Figure 7. Plot of marine oxygen-isotope stages for the last 800,000 years. The graph shows variations between $^{18}O/^{16}O$ over time measured in marine foraminifera (values shown in parts per mil deviations from a standard). Evaporation preferentially removes ^{16}O from the oceans, which then returns to the oceans in the waters of rivers and streams. Growth of large glaciers interrupts this return, so the $^{18}O/^{16}O$ of the oceans increases, and this is recorded in the shells and skeletons of marine lifeforms, providing a proxy record of the total amount of glacial ice worldwide. The numbers within the graph are Marine Isotope Stage numbers; the even-numbered peaks (blue shading at top) are glacial maxima, and the odd-numbered troughs (at bottom) are interglacial minima. The red areas indicate interglacial episodes, based on a cutoff at –0.5 $\delta^{18}O$ oxygen-isotope values (equivalent to Holocene interglacial values—the relatively milder climate of the last 10,000 years). Note that the last 800,000 years of the Quaternary is dominated by times of glaciation. Modified from Pringle (2008) and Morrison (1991).

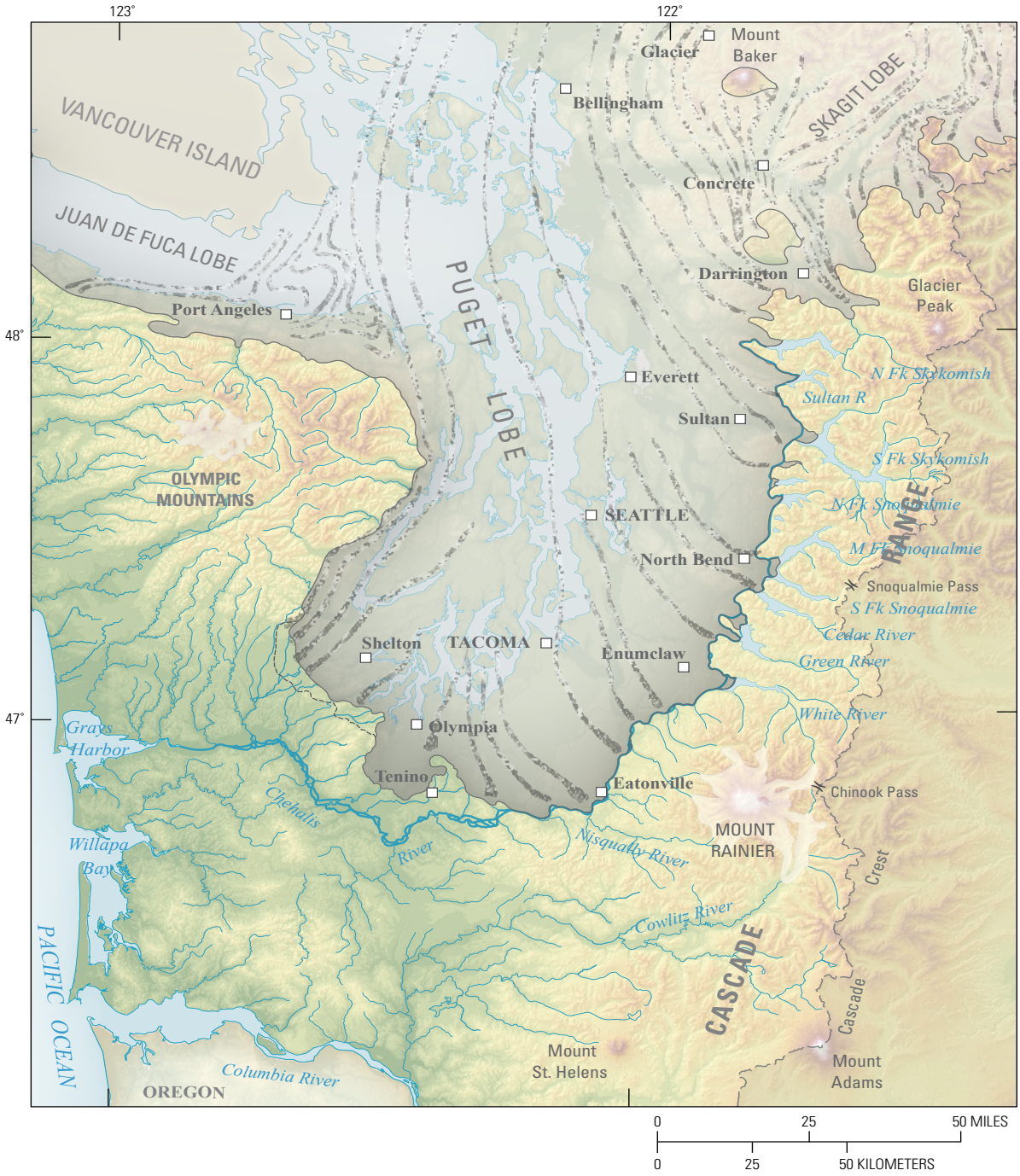

Figure 8. Map of the Puget lobe of the Cordilleran ice sheet, showing its maximum extent about 16,000 years ago. Ice was about 5,000 feet (ft; 1,524 meters [m]) thick at Bellingham, 3,500 ft (1,067 m) thick at Seattle, and 2,000 ft (610 m) thick at Tacoma (Pringle, 2008). The ice had reached Olympia, and valley glaciers (which are not shown in this figure) from Mount Rainier extended many miles downstream from the national park owing to expansion of glaciers in alpine areas. Water from all the rivers draining Mount Rainier, except those of the Cowlitz River system, flowed into lakes dammed at the ice margin; overflow was shunted around the toe of the Puget lobe. The water then merged with meltwater from the Puget lobe, gathering all the drainage north and west of Mount Rainier into a stream near Eatonville that was about the size of the Columbia River at Grand Coulee Dam. Flow continued out to the Pacific Ocean via the Chehalis River valley. The Columbia River has an average gradient of about 1 foot per mile (ft/mi; 0.2 meter per kilometer [m/km]); this paleostream had an average gradient of about 9 ft/mi (1.7 m/km). This figure shows the modern coastline, but when the ice was this far south, sea level was more than 300 ft (~100 m) lower, and the coast then was 30 to 50 miles (48–81 km) west of its present position. Not shown are late Pleistocene ice fields or ice caps in the Cascade Range and Olympic Mountains. Redrawn by Pringle (2008) from Cary (1966) and slightly modified here.

downstream from the Cascade Range foothills followed a relic path southwestward along what is now South Prairie Creek and only switched to its present course owing to the Osceola Mudflow 5,600 years ago (Crandell, 1963).

Alpine Glaciations

During the Pleistocene, alpine ice also repeatedly coalesced along the crest of the Cascade Range and in the Mount Rainier area and then advanced westward onto parts of adjoining lowland areas. In the southern Washington Cascade Range, these glaciers originated in the highlands near Mounts Rainier, Adams, and St. Helens (fig. 9). When these glaciers were at their maximum extent, they coalesced and created an ice cap over much of the crest of the Cascade Range. During each glacial episode, the movements of these glaciers radically modified the terrain by stripping off large volumes of rock, carving cirques and large U-shaped valleys, depositing glacial debris, and, as they melted, scouring the landscape with huge quantities of sediment-laden meltwater.

The Pleistocene record preserves deposits of as many as four major episodes of alpine glaciation in the southern Washington Cascade Range, of which the two most recent, the Hayden Creek and the Evans Creek, are best preserved. The older and most extensive of these two alpine advances is the Hayden Creek glaciation that reached its greatest extent 170–130 ka (fig. 7). The most recent of these glaciations, the Evans Creek glaciation, peaked at about 17 ka, and then retreated rapidly (Waitt and Thorson, 1983).

Hayden Creek Drift

The most widespread glacial deposits around Mount Rainier have been mapped as the Hayden Creek Drift, named by Crandell (1969) for a stony till exposed along the Mowich Lake Road near Hayden Creek, about 9 miles (14.5 km) northwest of Mount Rainier's summit (fig. 9). Till mapped as Hayden Creek Drift overlies ice-marginal lava flows as young as ~250 ka, and an ice-marginal lava flow that erupted at ~170 ka is situated well above canyon floors, confirming the presence of thick ice at that time, so the peak of Hayden Creek glaciation may have been during Marine Isotope Stage (MIS) 6 (~170–130 ka). Constructional glacial landforms in the Hayden Creek Drift are only present near the distal limits which, along with the presence of ice-marginal lava flows as old as ~500 ka, raises the possibility that the as-mapped Hayden Creek Drift includes tills from prior glacial advances. Consistent with this, Evarts and others (2003) presented evidence that some deposits mapped as Hayden Creek Drift are as old as MIS 8 (~275–250 ka). Indeed, the ubiquity of ice-marginal lava flows around Mount Rainier leads to the interpretation that thick, valley-filling ice was the norm in that region during the Pleistocene and that ice-poor conditions of the strong interglacial periods were brief and atypical. During the Hayden Creek glaciation (and probably older ones), ice caps almost completely covered higher areas. The presence and configuration of U-shaped valleys show that these ice caps fed large valley glaciers that moved down the White, Mowich, Puyallup, Nisqually, and Tilton River drainages. The moraines and deposits left behind show that a large valley glacier of Hayden Creek age extended down the Cowlitz River valley for 63 miles (105 km) from Mount Rainier and along the Nisqually River valley about 30 miles (48 km) from Mount Rainier to the west end of Alder Lake (Crandell and Miller, 1974). Glaciers no doubt dammed many tributary valleys to form meltwater lakes.

Evans Creek Drift

The Evans Creek Drift was deposited from the most recent major alpine glaciation in the Mount Rainier area during the protracted glacial episode that spanned from ~110–12 ka (MIS 5d–2). Worldwide, ice achieved its greatest extent from 30–16.5 ka (MIS 2) (Lambeck and others, 2014), referred to colloquially as the last glacial maximum and known in the Pacific Northwest as the Evans Creek glaciation (fig. 9). Evans Creek deposits overlie a Mount Rainier lava flow as young as ~43 ka, but that lava flow is itself ice-marginal with its top situated high above flanking valleys, as is a lava flow erupted ~90 ka (Lescinsky and Sisson, 1998), showing that glaciers much thicker and longer than those of today filled the valleys near Mount Rainier for much of the past 100,000 years. Evans Creek glaciers were less extensive than those of Hayden Creek time, but at their peak, Evans Creek glaciers extended from Mount Rainier down the Cowlitz River valley for 38 miles (64 km), down the Nisqually River valley 19 miles (30 km), down the Puyallup and Mowich River valleys about 16 miles (26 km), down the White River valley 24 miles (38 km), and down the Carbon River valley 19 miles (30 km). The floors of cirques, small bowl-shaped glacial heads last occupied during Evans Creek time, are as low as 2,700 ft (824 m) elevation near Mount Rainier. Lakes now occupy some of the cirques; Mowich, Crescent, Hidden, Shriner, Deadwood, Placer, Miners, and Blue Lakes as well as Lakes Eleanor, George, Allen, and Ethel are good examples.

Latest Pleistocene to Earliest Holocene McNeeley Drift

At Mount Rainier, Crandell and Miller (1974) found small, north-facing moraines that are mantled with pumice layer R from Mount Rainier, which erupted 10,050±50 calendar years before present (cal. yr B.P. [by convention, calendar years before present refer to years before 1950]; Samolczyk and others, 2016). They named this glacial debris the McNeeley Drift for cirque moraines lying at an altitude of 5,900 ft (1,800 m) about 0.4 miles (0.7 km) south of McNeeley Peak. The drift is underlain by ground moraine of Evans Creek age and in places by bedrock scoured by Evans Creek glaciers. McNeely age deposits may also include widespread pro-talus ramparts (low ridges of talus boulders that accumulated at the feet of formerly larger steep snow slopes), but these can be difficult to distinguish from younger neoglacial deposits. Geologists and climatologists are trying to understand how ice ages begin and end and to what extent regional and local ice advances are synchronous with a specific ice age. The McNeeley Drift is of interest because of its emplacement by small glaciers during the Younger Dryas

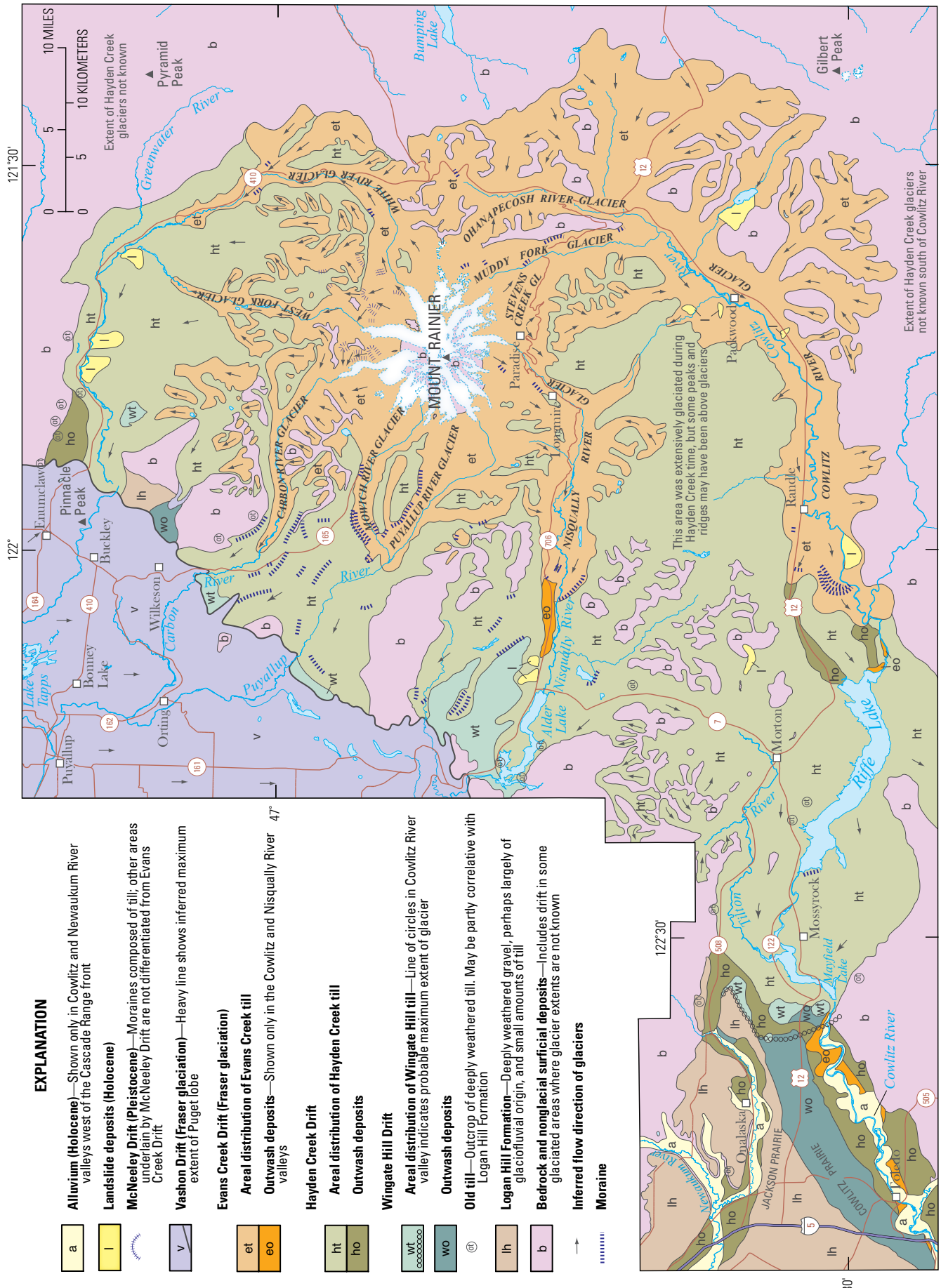

Figure 9. Map showing the distribution of surficial deposits and extents of Pleistocene glaciers from Mount Rainier and vicinity as implied by mapped units. Modified by Pringle (2008) from Crandell and Miller (1974) and Walsh and others (1987) and modified slightly here.

period, a brief reversion to cold climate after the onset of worldwide glacial retreat near the end of the Pleistocene. Age measurements for the Younger Dryas event suggest it began about 12,800 cal. yr B.P. (Southon and others, 2012; Lisiecki and Stern, 2016) and lasted for about 1,000 years; the end of the Younger Dryas marks the beginning of the Holocene.

Neoglacial Advances

At Mount Rainier, two small Holocene glacial advances are the older Burroughs Mountain and the younger Garda stades (Crandell and Miller, 1974). The Burroughs Mountain glaciers reached their maximum between 2,800 and 2,600 cal. yr B.P. The younger Garda stade at Mount Rainier is more commonly known worldwide as the Little Ice Age. It has been documented at Mount Rainier both by historical accounts and by tree ring analyses of trees growing on, or adjacent to, moraines (Sigafoos and Hendricks, 1961, 1972). The Little Ice Age lasted from about 1250 C.E. until the mid-1800s and was particularly severe between 1560 and 1850. At Mount Rainier, Garda moraines extend about 2 km farther down river valleys than present-day glaciers. Sigafoos and Hendricks (1972) found that eight of Mount Rainier's glaciers started to recede between 1830 and 1850, and they discovered moraines that had formed before 1363 C.E. By counting rings of trees along a Carbon Glacier lateral moraine, Crandell and Miller (1964) pushed the maximum age of Garda stade ice to before 1217 C.E. at Mount Rainier.

Geology of Mount Rainier

Style of Volcanism

Mount Rainier consists largely of andesitic and subordinate dacitic lava flows exposed on the incised headwalls and cleavers (ridges) of the upper volcano as seemingly thin, ribbon-like couplets consisting of a lower, dense, cliff-forming flow interior overlain by its loose, rubbly flow top (examination on the outcrop shows that rubbly flow bases are inconsistently developed and thin) (fig. 10). Repetition of these cliff-rubble couplets imparts a stair-step appearance to the rocky slopes of the upper volcano, with the lower angle rubble slopes, commonly mantled by snow, alternating with cliffs of the dark, dense flow interiors. Single flows (cliff-rubble couplets) are typically 15–25 m thick and dip outward at 20–30°. Single flows can be traced laterally (along strike) for about 0.15–1.5 km and down slope for approximately 1–5 km, giving representative single-flow volumes on the order of 0.002–0.2 km^3. Erosion is rapid on the upper mountain, but headwalls expose conformable successions of several to as many as a dozen flows each with intact rubbly tops, indicating their rapid sequential emplacement, so likely single-eruption volumes are more in the range of 0.01–1 km^3. Unconformities with low angular discordance separate the conformable successions of flows.

Rare, thicker lava flows are also present on the upper mountain, and incision of these flows can form cliffs as great as 200 m high and have true thicknesses of as much 150 m.

Figure 10. Photograph of upper southwest side of Mount Rainier showing lava flow cliff-and-bench morphology of the upper edifice. Dense interiors of the flows form cliffs, and rubbly flow tops make up the benches (see text for discussion). Photograph by Tom Sisson, U.S. Geological Survey.

These thicker upper edifice flows commonly differ from the simple cliff-rubble couplets in consisting of multiple alternating bands of dense lava and sintered autobreccia, each 2–10 m thick and broadly parallel with the flow base. Lack of internal cooling breaks typically causes these thick flows to form single cliffs, commonly with internal banding structures.

Lava flows on the lower flanks of the volcano and its surrounding ridges are considerably thicker owing to the combined effects of their greater volumes and their impoundment against Pleistocene glacial ice. At elevations below about 5,000 ft (1,500 m), lava flows are commonly 75–300 m thick and can locally approach 500 m. These lower elevation flows are 10–22 km long as measured from the present summit, although some were likely to have erupted from flank vents fed by radial dikes, which would reduce their true flow lengths by as much as about 5 km (fig. 11). Eruptive volumes cannot be determined with precision because of erosion, concealment beneath younger deposits, and uncertainty about vent locations (flank versus summit), but conservative estimates place volumes of the largest single flows at 5–7 km^3 and the smallest ridge-forming flank flows at about 0.5 km^3. Thus, eruptions from Mount Rainier, capable of producing lava flows, span nearly three orders of magnitude in volume (0.01–7 km^3).

Mount Rainier also produces pyroclastic-flow deposits, but their susceptibility for erosion in the alpine environment, as well as their syn-eruptive transformation to highly mobile lahars as they transit snow and ice, causes them to be underrepresented in the edifice rock record. Pyroclastic-flow deposits are wholly of block-and-ash type, consisting of poorly sorted angular fragments of commonly glassy, weakly inflated porphyritic silicic andesite or dacite. The deposits commonly have discontinuous internal stratification defined by intervals of more abundant coarse blocks aligned with the overall dip of the deposit. Deposit thicknesses range from about 3 to 150 m, although only one of the thicker localities is known to consist of a single cooling unit as defined by throughgoing columnar joints; other localities with thick pyroclastic flow deposits have sufficient diversity in clast types, sizes, and sorting to consist of multiple superposed flow units. Some such stratified breccia deposits can be seen to interfinger laterally with multiple thin lava flows, indicating concurrent deposition, possibly from intermittent Vulcanian explosions during periods of lava effusion or by intermittent avalanches of lava blocks cascading off the margins of lava flows moving down steep terrain. Reconnaissance fluxgate magnetometer measurements of juvenile-appearing clasts show shared magnetic directions demonstrating hot emplacement. In the absence of such measurements, or of columnar jointing, such block-and-ash-flow deposits can be difficult to distinguish from lahars. Sloughing by glacial meltwater of flow-top rubble off of active lava flows may also have produced interfingering of lava flows and adjacent monolithologic breccias.

As with all volcanoes, Mount Rainier also produces tephra. Most tephra deposits from Mount Rainier are thin (centimeters thick) even on the proximal slopes of the edifice and consist of angular-to-fluidal, poorly vesicular glassy ash grains. Such deposits probably result from small hydromagmatic explosions when largely degassed magmas transited the edifice hydrothermal system, but some are known to be ash-cloud deposits from active block-and-ash flows (Sisson and Vallance, 2009). Mount Rainier also produces pumiceous tephra, although deposits are thinner than those of nearby Mount St. Helens at similar distances from their source, indicating smaller eruptions driven by direct magmatic degassing. Mount Rainier produced eight chiefly pumiceous fall deposits in the Holocene, but their greatest preserved thicknesses do not exceed about 35 centimeters (cm) in subalpine meadows 6–8 km from the summit, and the most voluminous, the C pumice of ~2,300 cal. yr B.P., has a dense-rock equivalent (DRE) volume of 0.05–0.12 km^3 (0.15–0.35 km^3 bulk) and an estimated volcanic explosivity index (VEI) of 4. For comparison, pumiceous tephra layer Yn from Mount St. Helens exceeds 2.5 m thickness at a similar distance from its vent along its depositional axis, has a DRE of 0.9–1.2 km^3 (Nathenson, 2017), and an estimated VEI of 6. Two Pleistocene pumiceous fall deposits have been identified from Mount Rainier that rival those from Mount St. Helens. One is preserved 12 km from the summit near Sunrise as a ~2-m-thick deposit of biotite-bearing rhyodacite pumice lapilli that erupted at 230–210 ka (U-Pb zircon and $^{40}Ar/^{39}Ar$ biotite ages). The other is the prominent band of dacite pumice that spans Sunset Amphitheater headwall, visible from the Puget Lowland, that is also present as 1.5- to 2.5-m-thick exposures along the road to Sunrise and near Baker Point, 14 and 8 km from the summit, respectively. This deposit proved difficult to date reliably by $^{40}Ar/^{39}Ar$ methods, but (U-Th)/He zircon measurements indicate eruption near 85 ka (Sisson and others, 2019).

Dikes and Hydrothermal Alteration

Crandell and Waldron (1956) reported the discovery of a Holocene volcanic mudflow "of exceptional dimensions" from Mount Rainier and that this deposit, the Osceola Mudflow, is typified by altered volcanic clasts in a matrix of abundant clays, and ubiquitous pyrite, opal, and cristobalite, indicating a hydrothermally altered volcanic source. They traced the Osceola Mudflow back to the crest of Steamboat Prow on Mount Rainier's lower east-northeast face, beneath the broad expanse of the conjoined Emmons and Winthrop Glaciers, and concluded that collapse of the altered flank of the volcano caused the prodigious mudflow. Since their publication, weakening of the edifice by hydrothermal alteration has figured prominently in all studies and reports on volcanic hazards from Mount Rainier, with the analogy of a "house rotting from within" by termites or other pests, and that the volcano could collapse anywhere at any time, proving popular with the news media. Accordingly, the distribution and causes of alteration are of particular importance for assessing and mitigating risks. The summit and upper east-northeast flank of the volcano are now recognized as a young lava cone that largely fills the horseshoe-shaped Osceola collapse crater (fig. 11). Specifics of the Osceola eruption and collapse of 5,600 cal. yr B.P. are treated in detail elsewhere in this guide.

Geologic mapping, first by Fiske and others (1963) and later by us, showed that the volcano is bisected by a belt of

near-vertical radial dikes (fig. 11) and that hydrothermal alteration is restricted to the vicinity of those dikes as well as at the summit. West flank dikes strike east-northeasterly and run up Puyallup Cleaver, Sunset Ridge, and through Saint Andrews Rock into the region of Sunset Amphitheater (fig. 11). Dikes on the opposite, east flank of the volcano are only exposed below and on the south edge of the Osceola collapse amphitheater (fig. 11). East flank dikes strike northeasterly above Glacier Basin and easterly through Little Tahoma Peak, but, presumably, dikes also once abundant on the upper east to northeast flank were removed by the Osceola collapse along with associated altered rocks. Radial dikes and alteration are absent on the well exposed upper northwest, north, and south flanks of the volcano constructed during the Mowich and Kautz stages. Alteration near dikes is most strongly developed in breccias, including rubbly flow tops, because of their high permeability. The most common alteration assemblage in debris flows and exposed in situ on the edifice is the intermediate argillic smectite-pyrite association created in the magmatic hydrothermal environment where magmatic SO_2 reacts with groundwater to produce H_2SO_4 (sulfuric acid) that then reacts with minerals and glass to produce the alteration assemblage (John and others, 2008). The spatial association of alteration with dikes is probably because the dikes supplied both heat and SO_2 to their immediate surroundings during their injection. The dikes are Pleistocene, so the associated edifice-flank alteration is fossil and is not actively forming.

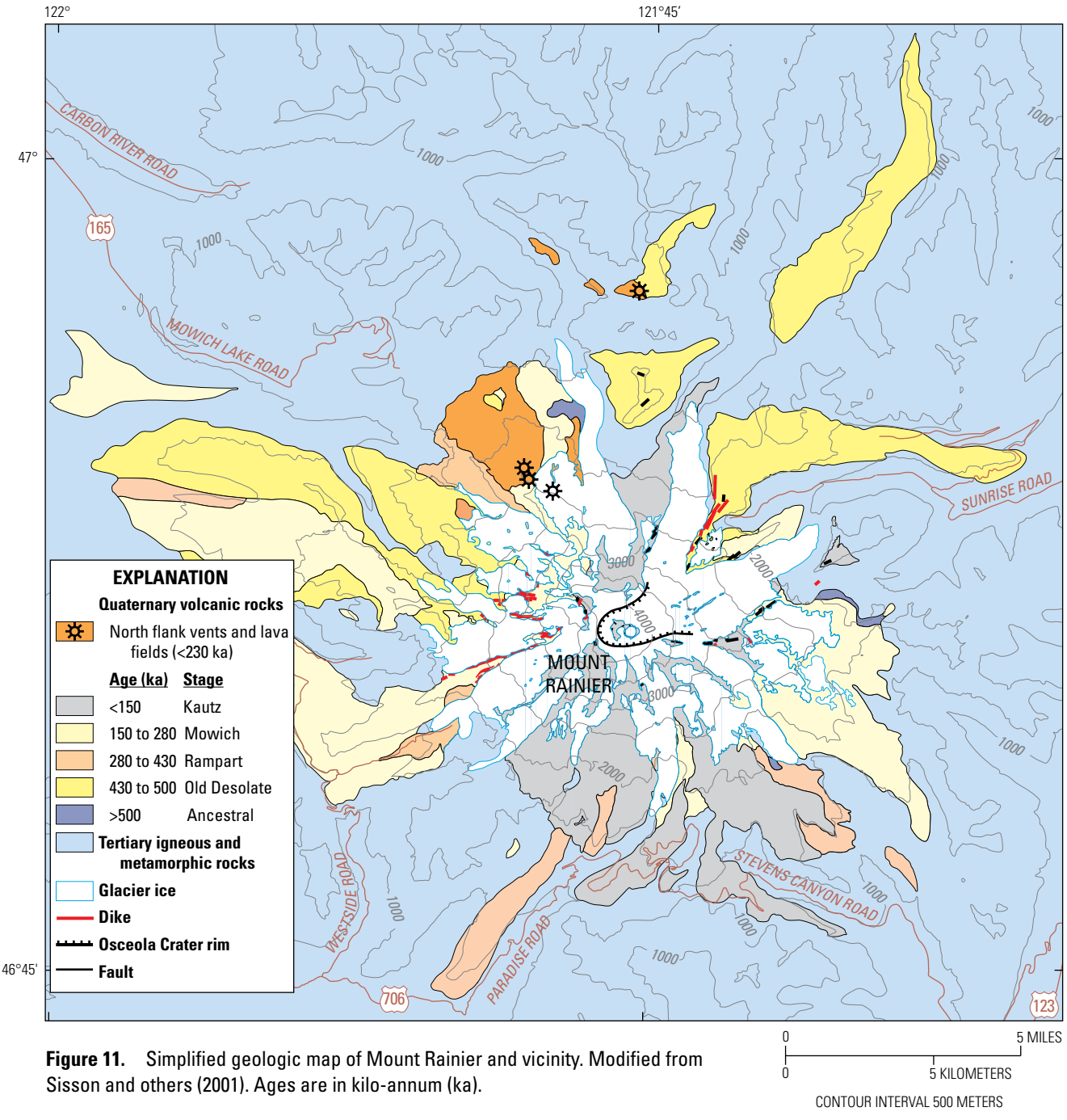

Figure 11. Simplified geologic map of Mount Rainier and vicinity. Modified from Sisson and others (2001). Ages are in kilo-annum (ka).

Active alteration is taking place in and near the young summit craters, where fumaroles vent gases at temperatures ranging from slightly above ambient to boiling point for their elevation. Vented gases are chiefly moist air with concentrations of CO_2 that range from air values (~360 parts per million [ppm]) to ~1 weight percent, concentrations of CH_4 of 1–5 ppm, detection-level traces of H_2S, and no detected SO_2 (Zimbelman and others, 2000). Summit alteration is the advanced argillic opal-kaolinite-alunite assemblage (with or without trace pyrite, anhydrite/gypsum, and sulfur) and forms in the steam-heated environment where steam generated by deeper boiling in the hydrothermal system ascends toward the surface carrying H_2S that oxidizes with air and condenses with steam to H_2SO_4 and H_2O (John and others, 2008). This acidic condensate alters the rocks of the summit craters, producing clays that reduce permeability to the extent that meltwater accumulates as one or two small lakes concealed beneath the crater-filling ice but that are accessible through fumarole-melted caves along the ice-crater interface.

Although altered rocks appear widespread at the summit, a high-resolution aeromagnetic survey shows that alteration at the summit is thin (20–50 m) (Finn and others, 2001). That survey further shows that the single greatest thickness of altered rocks lies beneath Sunset Amphitheater, where the west flank radial dikes emanate from the axial conduit system of the volcano. It appears from these geophysical results that the Osceola collapse removed the majority of altered rocks from the summit and upper east flank. Andesitic eruptions then refilled the collapse crater, but insufficient time has since passed for the steam-heated process to alter these to significant thicknesses. Based on these results, the greatest concern for collapse of upper edifice flanks is the volcano's upper west slope (Reid and others, 2001), where abundant altered rocks remain at high elevations on and above steep slopes.

Lava-Ice Interaction

A longstanding enigma for Mount Rainier's geology was the situation of thick, large-volume lava flows on the crests and sides of ridges, rather than in valley floors where lavas would be expected to have flowed. Fiske and others (1963) proposed that these flank lavas did advance down and partly fill former valleys, thereby displacing rivers that then entrenched along the margins of the flows, eventually reversing the topography and leaving the flows perched high above younger valleys. Lava benches perched at several levels approaching the floor of Stevens Canyon were interpreted as a succession of flows (deeper = younger) emplaced during prolonged entrenchment of the canyon. Such lava flows were termed "intra-canyon" to make the point that they were once within (intra) canyons or valleys, even though many are now between (inter) major valleys. This intra-canyon, reversed-topography interpretation became unsupportable as K-Ar and $^{40}Ar/^{39}Ar$ eruption-age measurements, geochemistry, and field observations accumulated during subsequent geologic mapping. Lava flows as young as 43 ka face canyons 900 ft (275 m) deep floored by hard granodiorite (Ricksecker Point), which would require incision rates averaging 0.25 inches per year (6 millimeters per year [mm/yr]) in the reversed topography model. Rates of glacial incision are not readily measured. More commonly estimated are basin-integrated rates of glacial denudation, which include headwall and sidewall erosion, and which can be more rapid than direct downcutting. Basin-integrated denudation rates exceeding 6 mm/yr are not unknown for the Holocene, but rates of 0.05–1 mm/yr are more common for Pacific Northwest glacial systems integrated over the Pleistocene (Koppes and Montgomery, 2009). The lava benches within and stepping into Stevens Canyon all proved to have the same eruption age (~90 ka), appearance (texture and quenched magmatic inclusions), and tight geochemical coherence, indicating that they are parts of the same lava flow (the dacite of Mazama Ridge), rather than a succession of flows emplaced intermittently over a long time span.

Clues for why the lava flows sit on ridge crests and flanks are areas of horizontally oriented, narrow, glassy columns that locally decorate the cliffy, canyon-facing sides of the lava flows. Lava columns generally point in the direction of cooling, and columns are generally narrower for faster rates of cooling, other factors being the same. These patches of narrow horizontal columns are commonly no more than several meters thick. They contrast with the thicker, taller, glass-poor vertical columns that typify flow interiors and show that (1) the lava flows originally had steep to vertical faces toward the now open canyons, (2) the lava flows abutted against something steep that cooled their lateral margins rapidly, and (3) the material that accomplished this cooling is now gone. The simplest interpretation (Lescinsky and Sisson, 1998) is that the canyons were filled with glacial ice to heights at least as great as the relatively flat tops of the ridge-forming and ridge-flanking lava flows, and that the lava flows mainly advanced along the margins of valley-filling glaciers, as well as atop the crests of ice-buried ridges between major ice streams, in both cases progressing farthest where the ice was thinnest and least capable of freezing and hardening the lava (fig. 12). Many such lava flows terminate at the confluences of major glacial valleys where marked increases in ice thickness may have been sufficient to arrest the lavas' further progress. During the brief strong interglacial periods, such as today, glacial termini retreated to the foot of the main edifice, emptying the canyons of ice and leaving the lava flows stranded on ridge crests and canyon walls. In the case of Stevens Canyon, the various lava benches lie just upcanyon of side valleys that supported tributary glaciers that descended steeply from the Tatoosh Range. These tributary glaciers temporarily halted lava that was advancing along the south side of the then greatly enlarged Paradise Glacier that filled Stevens Canyon. Lava accumulated behind each tributary ice dam, creating a bench, but then melted through the obstructing tributary glacier and continued down the main glacier margin until reaching the next glacial tributary and repeating the process. Subglacial lava flows are also present on Mount Rainier but are observed no farther than the foot of the main edifice, which would have marked the transition from thin alpine to thick valley glaciers. This process of ice-marginal volcanism likely accounts for ridge-forming lava flows at other glaciated volcanoes in the Cascade Range and elsewhere. Thus, dating of ice-marginal lavas provides one of the few precise measurements of the local extent and timing of Pleistocene glaciers.

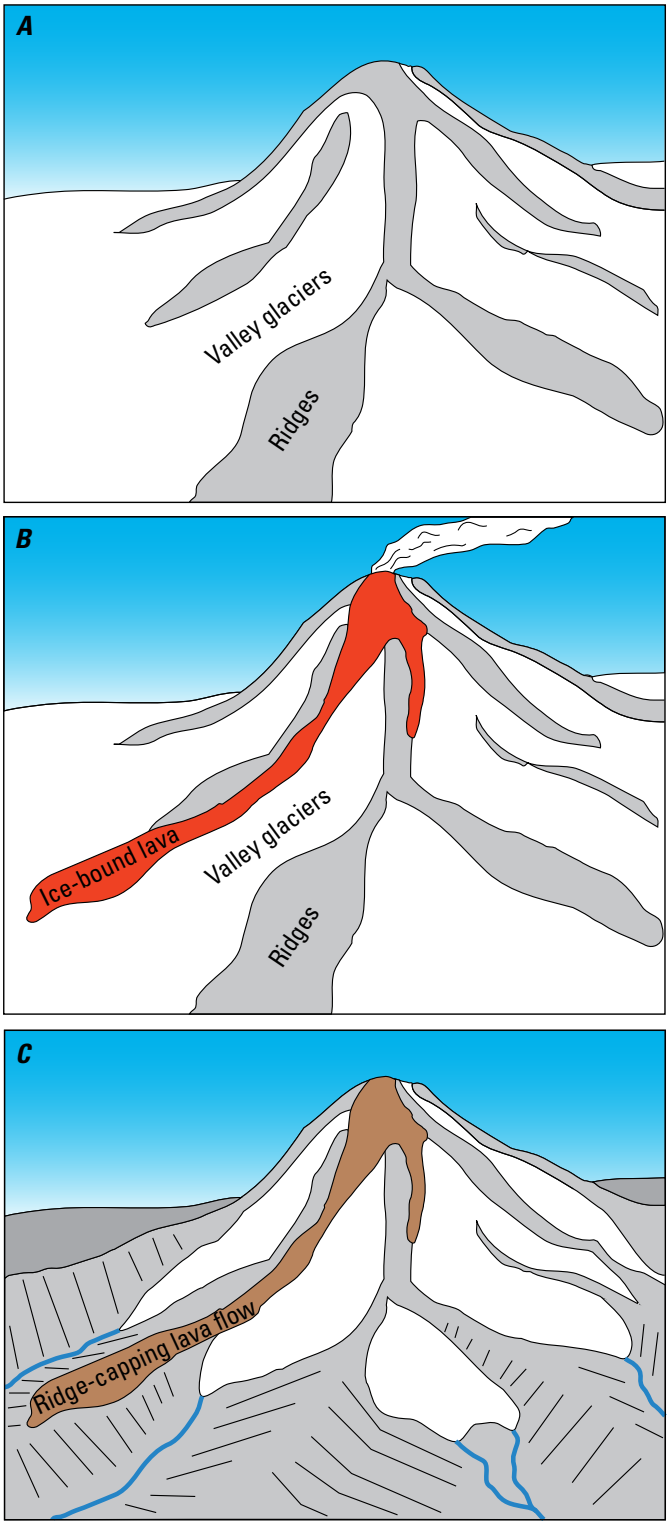

Figure 12. Schematic perspectives that show how thick ice-age glaciers affect lava flows (modified from Lescinsky and Sisson, 1998). *A*, Dormant Mount Rainier during a glacial advance. *B*, During an eruption, lava commonly flows along the margins of glaciers (that may be as thick as 1,000 meters) rather than push through the thickest ice. *C*, During interglacial periods, the ice retreats leaving lava flows perched on ridge tops and along valley sides. Detailed description of this process is given in the text.

Growth of Mount Rainier

Based on geologic mapping and radiometric dating (K-Ar and $^{40}Ar/^{39}Ar$ by A. Calvert and M. Lanphere, plus limited U-Pb and U-Th zircon by T.W. Sisson), the onset of modern Mount Rainier is estimated at close to 500 ka atop the deeply eroded remains of an ancestral Mount Rainier that occupied the same location and was chiefly active prior to 1 Ma (fig. 11). Little remains exposed of the ancestral Mount Rainier edifice except for deeply eroded remnants of hornblende dacite lava near Summerland and Panhandle Gap (1.06 Ma) and hornblende-olivine andesite lava in Glacier Basin (1.03 Ma). Sizeable laharic deposits from the ancestral volcano lie to the northwest of Mount Rainier as the Lily Creek Formation (volcanic clast ages 1.39 Ma and 1.16 Ma), and as the correlative volcanic clast-bearing Alderton and Puyallup Formations (Crandell, 1963). The Alderton and Puyallup Formations have not been dated directly but underlie the 1.15 Ma Lake Tapps tephra from the Kulshan caldera near Mount Baker (Hildreth, 1996) and are reversely magnetized (Blunt and others, 1987), indicating deposition after the Gauss-Matuyama reversal at about 2.6 Ma. Other than this reconnaissance dating, little work has been performed on ancestral Mount Rainier's products. Volcanism did not cease entirely between the ancestral and modern edifices, as shown by two widely separated, deeply eroded andesite lava flows near canyon floors that erupted near 600 ka, but inception of the modern edifice is estimated at just before 500 ka because the volcanic rock record from then to now is voluminous and has few age gaps.

Growth of the modern edifice can be divided into four broad stages defined by alternating periods of high and low volcanic eruption rates individually spanning 70,000–150,000 years as recorded by voluminous lower flank lava flows that are less susceptible to erosion than rocks of the upper edifice (figs. 11 and 13). The last 70,000 years are a substage during which the bulk of the upper north and south slopes of the volcano were erupted, but during which time only one eruption was sufficiently large to produce a lava flow that extended beyond the foot of the edifice. Other such substages probably lie within the major stages but these have not been subdivided because of poor preservation and imprecise age results yielded by the typically glassy and porous lavas of the upper edifice. Mount Rainier's Quaternary growth stages are coarser divisions of time encompassing greater geologic complexity than are the stages defined for construction of nearby Mount St. Helens (Clynne and others, 2008).

Old Desolate stage (~510–430 ka).—The earliest preserved products of modern Mount Rainier are coarse, poorly sorted, and poorly bedded fragmental deposits that constitute Steamboat Prow and that underlie the andesitic lava flows of Burroughs Mountain (506 ka) and Old Desolate (455 ka) on Mount Rainier's lower northeast and north flanks. In the Glacier Basin area, these fragmental deposits unconformably overlie Tertiary Ohanapecosh Formation, its crosscutting granodiorite, and a deeply incised ancestral Mount Rainier lava flow. Reconnaissance fluxgate magnetometer measurements of prismatically jointed juvenile-appearing clasts give consistent normally magnetized directions for outcrops at elevations above about 7,500 ft (2,300 m), but

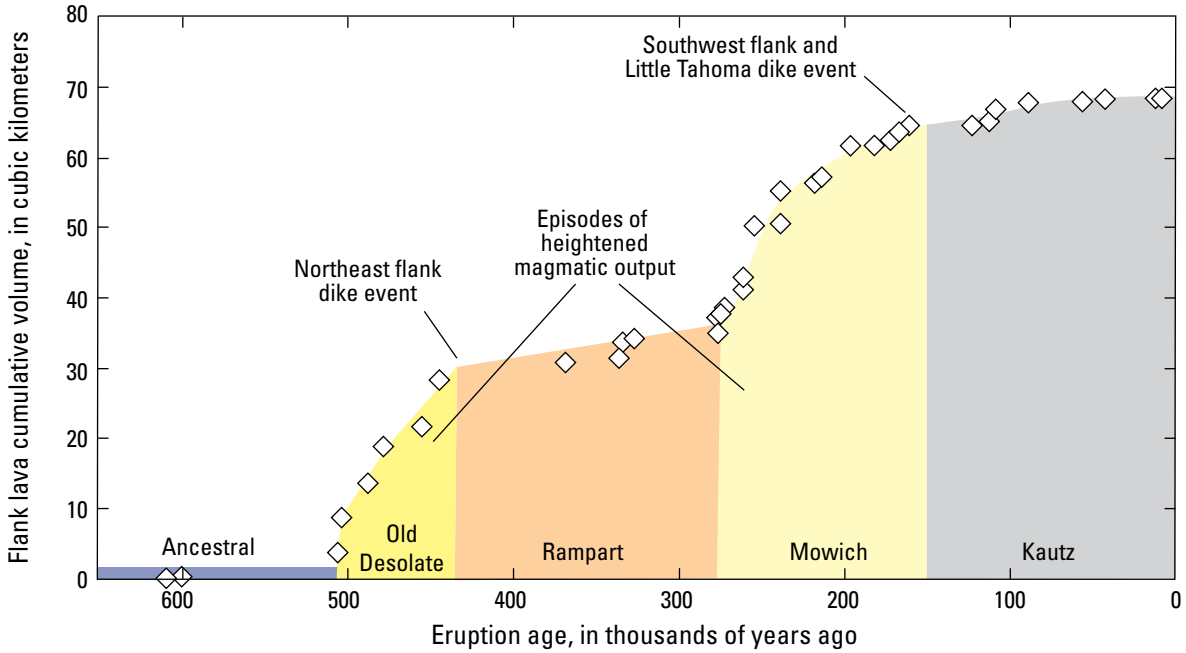

Figure 13. Cumulative growth curve for flank lavas from Mount Rainier showing stages of growth. Ages are based on geologic mapping and radiometric dating (updated with $^{40}Ar/^{39}Ar$ ages from K-Ar plot of Sisson and others, 2001). Each diamond symbol represents a mapped and dated flank flow or flow group. Events involving emplacement of large dikes are labeled. The total edifice growth curve is not shown because of imprecise volume estimates.

inconsistent directions lower and farther from the volcano. Rounded and glacially striated nonvolcanic clasts appear in the breccias with greater distance from the volcano, indicating entrainment of unconsolidated sediments. These changes in magnetism and clast makeup probably signify a transition from hot block-and-ash flows to lahars. Fragmental deposits high on Steamboat Prow are interstratified with minor thin, conformable andesitic lava flows, and the fragmental deposits and lavas dip away from the present summit location at 15–20°, consistent with rapid construction of a tall volcanic edifice early in the growth of modern Mount Rainier. The fragmental deposits are indurated on Steamboat Prow, with a few light-colored smectite-rich intervals probably marking paleo-aquifers, but the deposits transition to loose and unconsolidated with greater distance from the volcano. Their contacts with the overlying andesites of Burroughs Mountain and Old Desolate are near horizontal and lack appreciable incision, so emplacement of the lava flows is interpreted to have closely followed the initial pyroclastic eruptions (Stockstill and others, 2002).

The bulk of Mount Rainier's Old Desolate growth stage is made up of large (2.5–7 km^3) lava flows on the north side of the volcano: Burroughs Mountain (506 ka), Old Desolate (455 ka), and Grand Park (445 ka), as well as various large, ridge-forming lava flows in the headwaters of the Mowich River system (506–466 ka). These flows extend as far as 13.5 miles (22 km) from the present summit, but some were fed by northeast-striking radial dikes, one of which above Glacier Basin is dated at 445 ka and may be the source for the beheaded Grand Park flow. No Old Desolate stage rocks have been identified higher on the volcano than Steamboat Prow at 9,700 ft (2,960 m) and none are known on the volcano's south flank.

Rampart stage (430–280 ka).—Volcanic output diminished greatly after 430 ka (fig. 13), and the rock record for the following 150,000 years consists of temporally widely spaced flank lava flows (fig. 11) that do not individually exceed about 2.5 km^3. The most prominent of these are Rampart Ridge above Longmire (335 ka), a flow on the south side of Rushingwater Creek (336 ka), lower Ptarmigan Ridge (369 ka), and in the Muddy Fork Cowlitz River shortly above Box Canyon (328 ka). Other rocks from this stage are fragmental deposits that support lower Saint Andrews Rock (362 ka) and various smaller incised lava flows that do not support named, geographically prominent localities. Geographic outliers for this stage are an erosional remnant of andesite lava in an embayment on the east side of the West Fork White River (350 ka) 13.5 miles (22 km) north of the summit and lava near Lake James (341 ka) 9 miles (15 km) north of the summit. These are anomalous by their geographic (West Fork White River) and topographic (Lake James) separations from the edifice. Although eruption ages of the Rampart Ridge and Lake James flows are within uncertainty of a worldwide deglaciation from MIS 10 to 9, centered at 337 ka (Lisiecki and Raymo, 2005), both flows have well preserved ice contact columns, indicating the presence of extensive canyon-filling ice.

Mowich stage (280–150 ka).—The volcano reinvigorated after 280 ka, initially recorded by several flank flows of 0.5–1 km^3, building to several flows or flow complexes of 1–7 km^3

(260–190 ka) mainly on the volcano's west side (figs. 11 and 13). The most voluminous of these is a complex of thick flows (255 ka) that support Saint Andrews Park between the South Puyallup and North Puyallup Rivers, with well-developed ice-contact columns on its west and north margins. Another sizeable flow complex from this stage supports lower Sunset Park and the ridge descending west to the Puyallup River (232 ka). These voluminous flow complexes preceded and postdated the worldwide deglaciation from MIS 8 to 7 centered at 243 ka (Lisiecki and Raymo, 2005). Mowich stage lava flows make up the upper part of the steep Mowich Face on Mount Rainier's west flank to the highest exposed rocks (4,000 m, or 13,100 ft), including crossing a prominent angular unconformity along the crest of upper Ptarmigan Ridge. Mowich stage activity declined gradually, and its termination is somewhat arbitrarily placed at 150 ka to encompass the growth of Little Tahoma Peak (≥164 ka) and Emerald Ridge (173 ka) as well as the major radial dikes that run up Puyallup Cleaver, Tokaloo Rock, and Little Tahoma Peak, and the lava flows they fed (167–159 ka).

Kautz stage (150 ka–present).—Volcanic output has been comparatively modest over the past 150,000 years, represented on the lower flanks by the dacite of Mazama Ridge (90 ka) that continues along the south side of Stevens Canyon, and of Ricksecker Point (43 ka), and by mid-flank flows of Anvil Rock, the ridge below Cathedral Rocks, the "narrows" along Kautz Creek, Comet Falls, as well as geographically nondescript locations (figs. 11 and 13). Notable Kautz stage rocks include the north flank olivine basaltic andesite field of Spray Park that erupted from the since-eviscerated cinder cones of Echo and Observation Rocks (97 ka), an atypically thick (to 140 m), columnar-jointed pyroclastic flow deposit that fills upper Kautz Creek (bracketed between 83 and 70 ka), and the prominent white dacitic pumice of Sunset Amphitheater headwall (85 ka; Sisson and others, 2019). The pyroclastic-flow deposit in upper Kautz Creek does not extend farther than 6 miles (10 km) from the volcano, and its thickness may result from the flow having entrenched into and impounded behind ice that filled the downstream valley. Considerable erosive incision and edifice degradation must have followed the Mowich stage to account for the topographic isolation of late Mowich stage Little Tahoma Peak, which is surrounded by younger rocks. Sunset Amphitheater headwall exposes a deep unconformity incised into Mowich stage rocks, overlain and infilled by Kautz stage lava flows and the dacite pumice of Sunset Amphitheater, but observations and evidence are insufficient to determine if a single major period of edifice degradation, such as a major edifice collapse, separated the Mowich and Kautz stages.

Point Success substage (70–5.6 ka).—The Point Success substage is defined because, although no overall increase in activity is recorded by lower flank lava flows, the last 70,000 years saw emplacement of the great thicknesses of lava flows that make up the volcano's upper south and north sides. These include the stair-stepped stacks of lava flows of Point Success, Tahoma Cleaver, the Tahoma Glacier headwall, upper Curtis Ridge, the Willis Wall, and Liberty Ridge. Point Success substage rocks on the south flank overlie a deep unconformity atop Anvil Rock and below Cathedral Rocks, but a potentially corresponding unconformity on the north flank is mainly disconformable, lacking pronounced incision. The sole Point Success substage eruption sufficiently voluminous to send lava beyond the main edifice produced the dacite of Ricksecker Point (43 ka). Ice-contact columns preserved locally on its steep west and upper east faces show that the lava flow was confined between thick glaciers that filled the adjacent valleys. Several stratigraphically high upper edifice samples have ages in the range of 36–17 ka, indicating that growth of much of the present upper edifice took place approaching, and perhaps during, the last glacial maximum.

Columbia Crest substage (5.6 ka–present).—Reconfiguration of the volcano requires definition of a substage commencing with the Osceola edifice collapse at 5.6 ka and continuing to the present, even though no changes in volcanic style or overall output are apparent. The Osceola collapse beheaded outward-dipping lava flows now exposed as an arc of high points that partly encircles the new summit cone (fig. 14). These high points mark the eroded crest of the former collapse amphitheater, and most consist of lavas erupted during the Point Success substage (Gibraltar Rock, Nisqually Cleaver, Kautz Cleaver, Point Success, Tahoma Cleaver, Curtis Ridge, and Russell Cliff), but the Osceola collapse probably also beheaded earlier Kautz and Mowich stage lava flows on Liberty Cap. Subsequent lava eruptions filled the collapse crater and built the present summit cone, which is capped by older (western) and younger (eastern) craters. The youth of both craters is shown by lack of glacial incision despite their weakening by hydrothermal alteration. The oldest post-collapse lava flows are buried beneath subsequent flows, and the youngest lava flows are themselves accessible only locally owing to concealment beneath glacial ice. Small exposures through the conjoined Emmons and Winthrop Glaciers, and on the Tahoma Glacier on the opposite southwest flank, reveal andesites with distinctly high concentrations of strontium (Sr) for Mount Rainier (Sisson and Vallance, 2009); these high-Sr lava flows extend no more than about 4.5 miles (7 km) from the summit, failing to extend to the present limits of the Emmons, Winthrop, and Tahoma Glaciers. Paleomagnetic and geochemical evidence show that these high-Sr lavas correlate with high-Sr tephras that were deposited just after a ~2,400 cal. yr B.P. block-and-ash flow of ordinary-Sr andesite. Topography is appropriate for the high-Sr lava flows to have constructed Mount Rainier's west summit crater. An andesite lava flow that supports the rim and outer wall of the younger east summit crater has paleomagnetic direction consistent with eruption at ~2,000 cal. yr B.P. This andesite has normal Sr concentrations for Mount Rainier, and its eruption probably shortly followed the eruption of the mixed-Sr C tephra of ~2,300 cal. yr B.P. This ~2,000 cal. yr B.P. andesite along the rim of the east summit crater is the youngest lava from Mount Rainier. Its flows descended no more than about 1.25 miles (less than 2 km) down the cone's upper slopes, and their termini are wholly concealed by ice.

Later eruptive products of the Columbia Crest substage consist of thin tephras, voluminous laharic deposits, and minor landslides described elsewhere in this guide. The last eruption of Mount Rainier for which there is unambiguous physical evidence

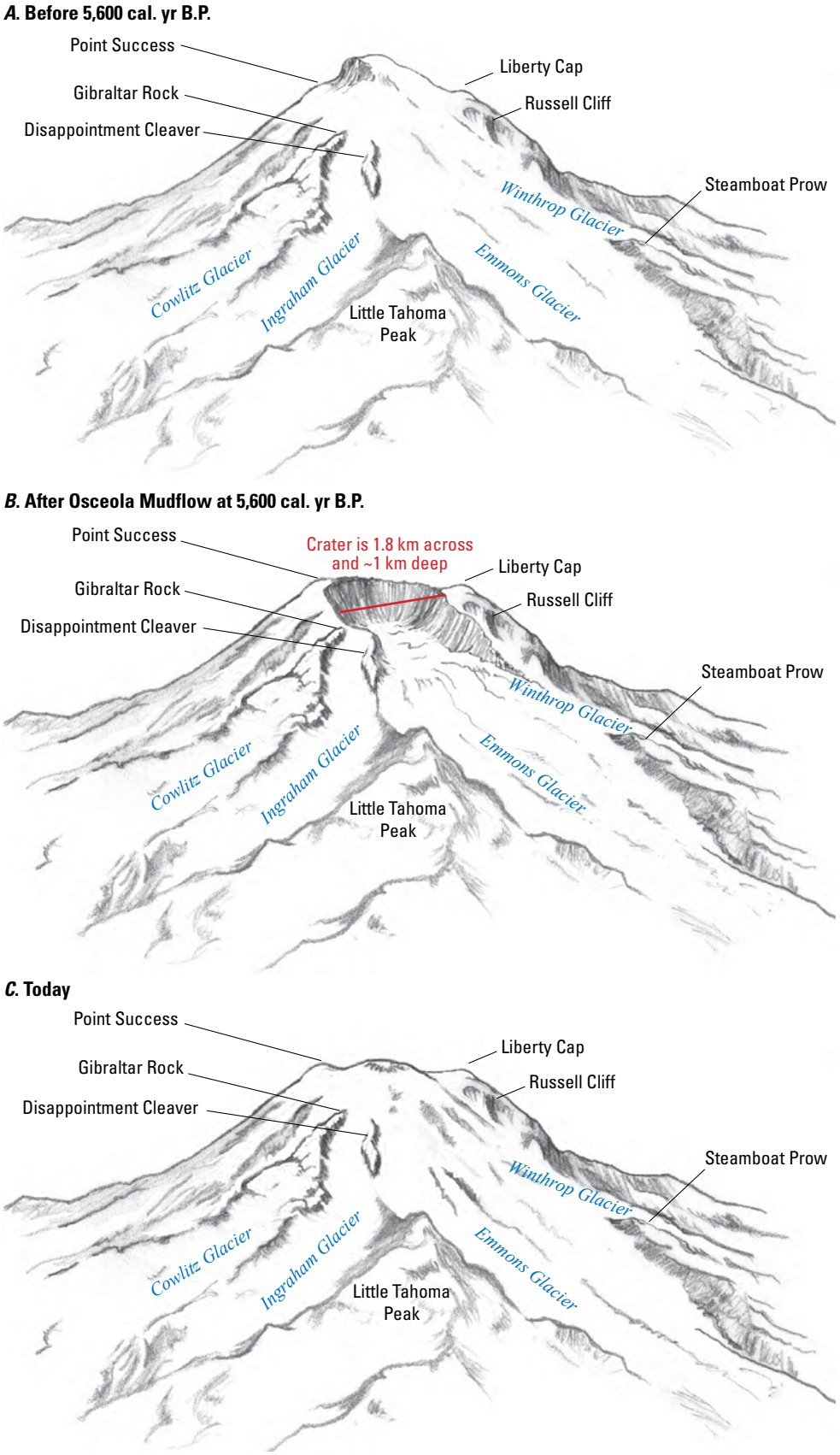

Figure 14. Schematic diagrams of Mount Rainier viewed from the east. *A*, Speculative perspective of Mount Rainier before the Osceola Mudflow. *B*, Perspective of Mount Rainier just after the Osceola edifice collapse 5,600 calendar years before present (cal. yr B.P.). *C*, Modern perspective of Mount Rainier. Landmarks like Disappointment Cleaver, Gibraltar Rock, Point Success, Liberty Cap, and Russell Cliff delineate the edifice collapse scarp and form the boundary between the pre- and post-Osceola Mudflow edifice. Bobbie Myers of the U.S. Geological Survey, now deceased, improved our original artwork. km, kilometer.

was at ~1,000 cal. yr B.P. This left a thin, fine-grained ash rich in chemically homogeneous glass in the valley of the White River (Sisson and Vallance, 2009), but spawned voluminous lahars that reached the Puget Lowland.

Petrogenesis at Mount Rainier (after Sisson and others, 2013)

Most of Mount Rainier's magmas ascended through an axial magmatic system underlying the main edifice and erupted from the summit or from upper and mid-flank vents fed by radial dikes. The axial products are predominantly (77 percent) calc-alkaline andesites (57–63 weight percent SiO_2), with lesser (23 percent) dacites (63–68 weight percent SiO_2), and a sole rhyodacite pumice fall deposit (<<1 percent) (fig. 15). No known flows or tephras of basaltic andesite (52–57 weight percent SiO_2) or basalt (<52 weight percent SiO_2) erupted through the axial magmatic system. Porphyritic andesites and dacites are the norm, dominated in decreasing abundance by phenocrysts of plagioclase, orthopyroxene, and clinopyroxene, with microphenocrysts of Fe-Ti oxides and apatite. Amphibole is absent to minor in most andesites, but abundant in relatively high-K_2O andesites, and also in the higher SiO_2 dacites and rhyodacite. Olivine is irregularly present in hand samples and thin sections of rocks that have SiO_2 as great as 59 weight percent, but sparse rounded olivine grains are routinely recovered in mineral separates from higher SiO_2 samples, probably as relicts from magma mingling. Other minor mineral phases include a Cu-Fe magmatic sulfide, typically preserved only where included in phenocrysts, minute zircon grains in the more evolved dacites and rhyodacite, biotite phenocrysts solely in the rhyodacitic pumice-fall rocks but as a trace groundmass phase in thick and well crystallized andesite-dacite lava flows, and traces of resorbed phenocrystic quartz in an evolved dacite.

Evidence for magma mingling, in the form of fine-grained quenched magmatic inclusions (enclaves; Bacon, 1986), is widespread in Mount Rainier's eruptive products. Quenched magmatic inclusions (QMIs) are commonly 4 to 8 cm across, fine-grained, sparsely vesicular in their interiors, and contain <10 percent phenocrysts of olivine (or orthopyroxene or amphibole in some higher SiO_2 QMIs), commonly accompanied by traces of resorbed phenocrysts entrained from the host magma. Compositions of QMIs overlap those of Mount Rainier's lavas and tephras, but extend the suite to lower SiO_2 concentrations, consisting of andesites (77 percent) and basaltic andesites (22 percent), with only one basaltic QMI having been found. Nearly all Mount Rainier products contain sieve-textured phenocrysts, and phenocrysts with overgrown internal resorption surfaces, as are commonplace in calc-alkaline andesitic magmas worldwide, recording magma mingling and mixing events. Accompanying the complex grains in variable proportions, however, are idiomorphic phenocrysts and microphenocrysts with few resorption features. At the extreme are rare lava flows of non-porphyritic andesite in which texturally simple non-sieved mineral grains range continuously from groundmass to as large as ~0.5 millimeters (mm). These flows result from infrequent eruptions of phenocryst-free andesitic liquids, as opposed to crystal-laden andesitic magmas whose phenocrysts betray their complex origins. Additional magmatic products are medium-grained inclusions of vuggy gabbronorite to quartz diorite, as large as 20 cm across, that characterize some lava flows; U-Pb ages of zircons from these inclusions indicate that they are Pleistocene plutonic products of Mount Rainier's magmatic system (Sisson and others, 2009). True xenoliths of pre-Quaternary rocks are exceptionally uncommon.

Vents on the north flank of Mount Rainier (fig. 11) erupted magmas distinct from those of the axial magmatic system, consisting of olivine basaltic andesites and amphibole-phenocrystic spessartite (spessartite is lamprophyric textured calc-alkaline andesite with phenocrysts of amphibole but not of plagioclase), as well as hybrids of basaltic andesite and spessartite. North flank basaltic andesite compositions overlap those of QMIs. These basaltic andesites result from eruptions of some types of mafic magmas that replenish Mount Rainier's axial magmatic system, but that bypassed it by ascending 6 to 7 km laterally to its side, whereas basaltic andesites ascending through the axial magmatic system only reach the surface as QMIs after having mingled with the andesites and dacites that dominate the axial system. The 6 to 7 km distance is therefore a maximum limiting estimate of the radius of the axial andesitic system. North flank basaltic andesite compositions also overlap the high-SiO_2 portion of the field of regional basalts and basaltic andesites of the southern Washington Cascade Range.

Trace element and isotopic variations indicate that the dominant process of magmatic evolution is a form of crystallization differentiation in which magma batches stall at various crustal levels and crystallize to advanced extents, commonly saturating with accessory minerals including apatite and zircon, as well as with relatively low temperature major minerals (such as amphibole). Subsequent magmas that ascend through these stalled intrusions entrain and mix with their evolved residual liquids and low-degree partial remelts. At times, the near-solidus liquids from stalled intrusions segregate in sufficient quantities to capture the axial conduit system, erupting as evolved dacite or rhyodacite. This process of in-place differentiation and mixing suppresses the systematically increasing then decreasing concentrations of elements such as Zr and Nb with increasing SiO_2 that is expected for progressive crystal fractionation. Assimilation also takes place, notably of continental-interior sedimentary rocks of the Puget Group that underlie the Oligocene and Miocene arc volcanic and plutonic rocks, upon which the volcano is built. The maximum amounts of assimilation are low, however—no more than 20 weight percent and typically less. Tertiary and Mesozoic mafic volcanic and mafic meta-plutonic rocks of the region are unsuitable as significant assimilates or magmatic sources as shown by their diverse $^{206}Pb/^{204}Pb$ signatures at consistently high $^{143}Nd/^{144}Nd$ that are not seen in other volcanic rocks from Mount Rainier.

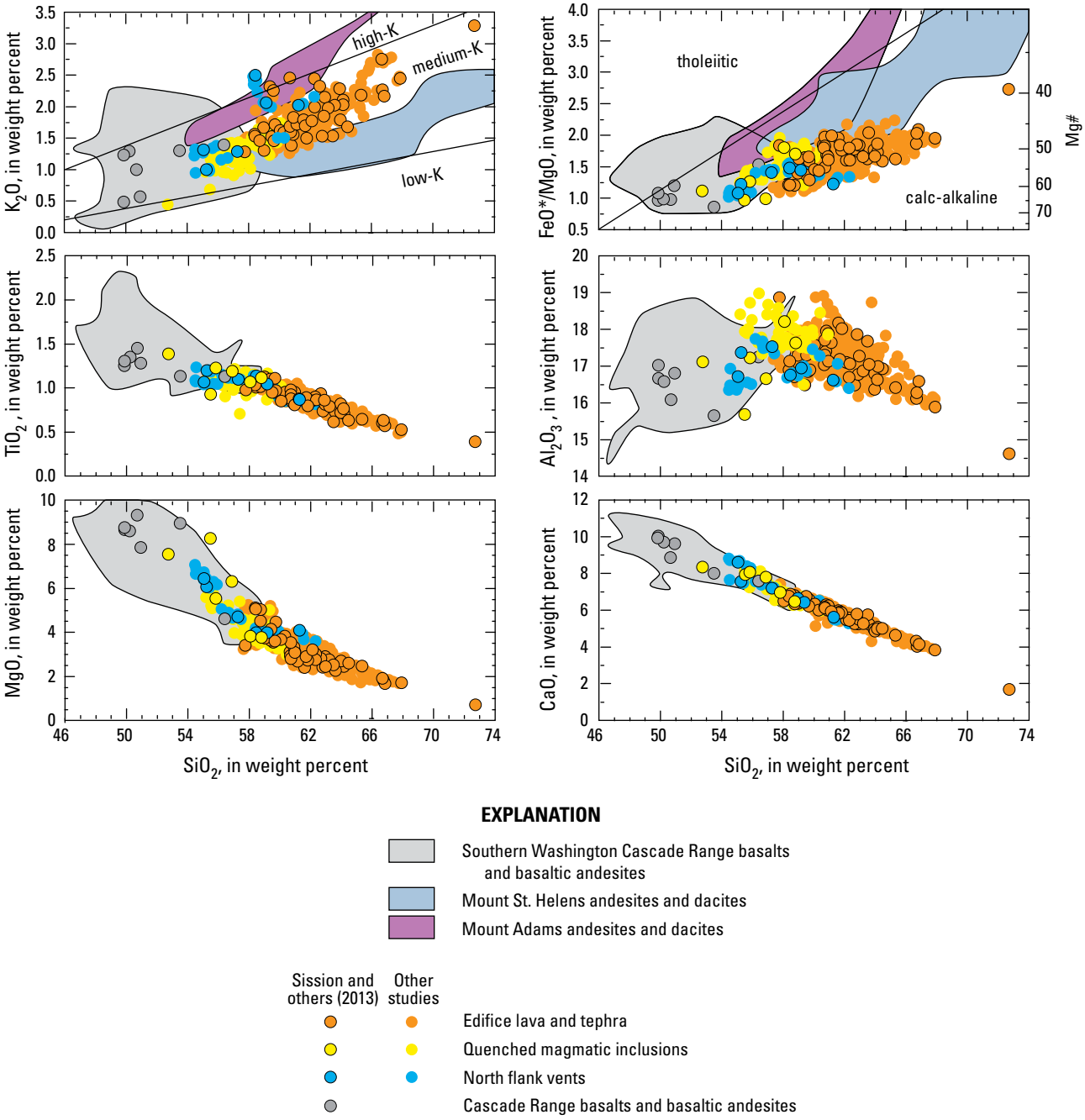

Figure 15. Major-oxide variation diagrams for magmas that erupted through Mount Rainier's axial magmatic system as lavas and tephras and as quenched magmatic inclusions, and from its north flank vents. For comparison, also shown are Quaternary andesites and dacites of Mount St. Helens and Mount Adams, and regional basalts and basaltic andesites of the southern Washington Cascade Range. High-, medium-, and low-potassium fields from Gill (1981) and tholeiitic and calc-alkaline fields from Miyashiro (1974) (magnesium number [Mg#] is 100 Mg/Fe+Mg, molar). FeO* is total iron as FeO. Black outlined symbols are analyses reported by Sisson and others (2013); other Mount Rainier compositions (without black outlines) are from Stockstill and others (2002), McKenna (1994), and Sisson and Vallance (2009). Quaternary southern Washington Cascade Range, Mount Adams, and Mount St. Helens volcanic rock compositions are from Halliday and others (1983), Hammond and Korosec (1983), Smith and Leeman (1987, 1993, 2005), Leeman and others (1990, 2004, 2005), Gardner and others (1995), Mullineaux (1996), Bacon and others (1997), Conrey and others (1997), Reiners and others (2000), Clynne and others (2008), and Jicha and others (2009). Mount St. Helens fields include some glass compositions. Figure modified from Sisson and others (2013).

Holocene Volcanism of Mount Rainier

Delineating History of Volcanism: Tephra, Pyroclastic Flows, and Lava

Tephra stratigraphy is the key to delineating Holocene volcanism at Mount Rainier. Early study of Holocene volcanism at Mount Rainier focused on ten distinctive pumiceous to scoriaceous fall deposits (tephras) (Mullineaux, 1974), one preserved pyroclastic-flow deposit (Crandell, 1971), and more than 50 lahars (Crandell, 1971), but omitted numerous volumetrically small, seemingly insignificant tephras and lava flows of uncertain age exposed locally on the upper edifice but otherwise obscured or destroyed by glaciers (fig. 16) (Sisson and Vallance, 2009). These results implied that Holocene volcanism at Mount Rainier chiefly comprised 10 moderately explosive eruptions (Hoblitt and others, 1998) and that many lahars were unrelated to eruptive activity (Scott and others, 1995).

Detailed stratigraphic studies of tephras and lahars, supported by accelerator mass spectrometer (AMS) ^{14}C age measurements, as well as paleomagnetic secular variation measurements of near-summit lava flows, yielded a more robust Holocene eruptive history for Mount Rainier. Important

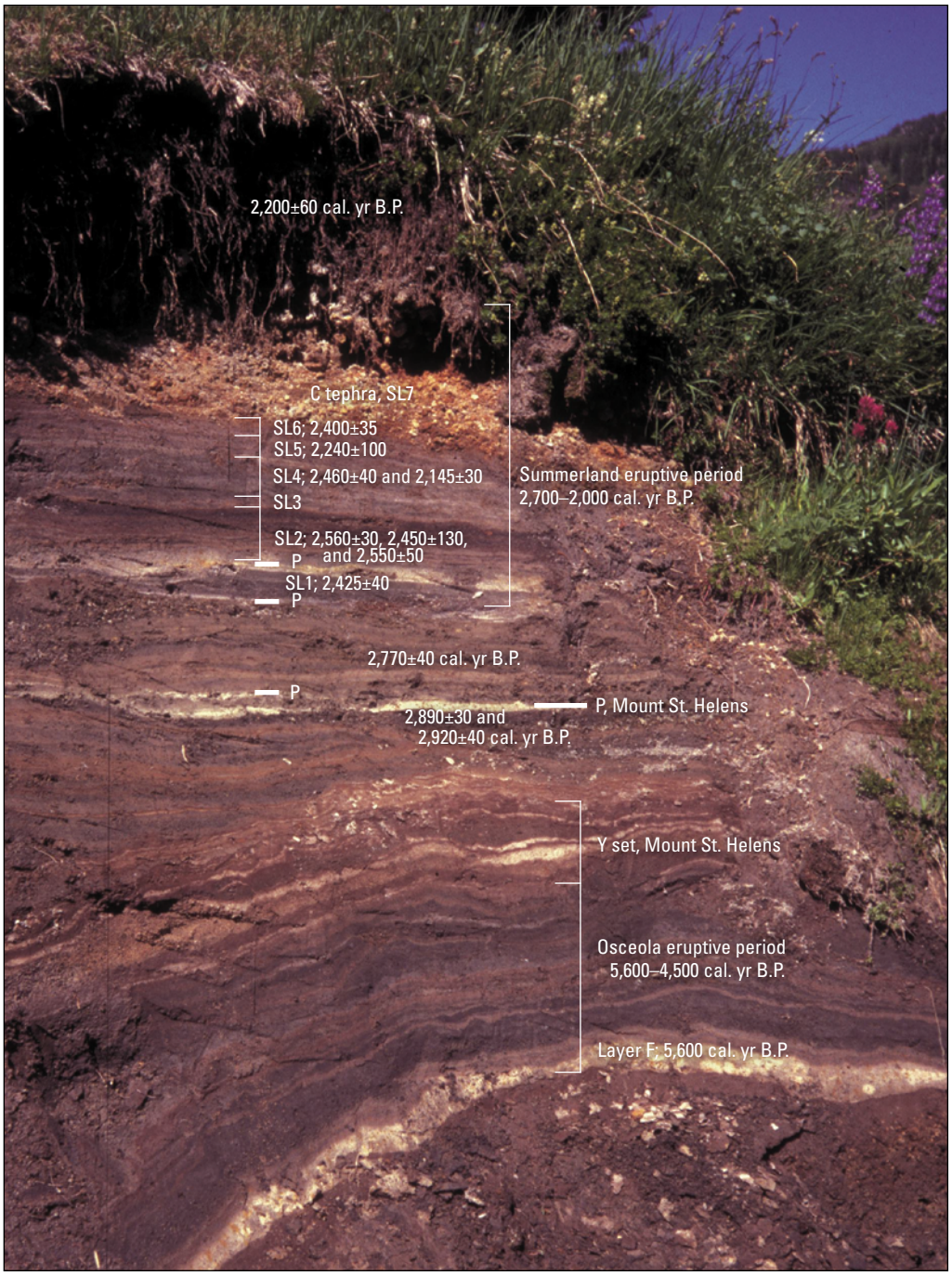

Figure 16. Photograph of a section showing Mount Rainier tephras of the past 5,600 years at Summerland, about 8 kilometers east-northeast of the summit. Brackets mark tephras of the last two eruptive periods (Osceola and Summerland). Field of view encompasses about 2 meters of section. Ages are in calendar years before present (cal. yr B.P.). SL, Summerland eruptive period tephra; P, Mount St. Helens Pine Creek tephra. Photograph by Jim Vallance, U.S. Geological Survey.

findings are that (1) 40 or more separate Holocene tephras can be identified, each representing the product of one or more explosive events, (2) eruptions clustered into periods of as many as several hundred years duration separated by apparent dormant periods as long as 2,000 years, and (3) the great majority of far-traveled lahars took place during periods of frequent eruptions (Sisson and Vallance, 2009; Vallance and Pringle, 2008). The newly discovered temporal association of lahars with eruptions reduces concern that future lahars will occur without warning, even though it does not preclude the possibility of unheralded lahars caused by edifice flank failure or rockfall-avalanche-induced lahars like that from Little Tahoma Peak in 1963 (Crandell and Fahnestock, 1965).

Holocene tephras near Mount Rainier are divisible into three general types: (1) widespread, fine-grained vesicular ashes of generally light color derived from eruptions of Mount St. Helens and Mount Mazama, (2) vesicular (pumice- and scoria-rich) ash, lapilli, and bombs derived from Plinian and sub-Plinian eruptions of Mount Rainier, and (3) thin, sparsely vesicular glassy (SVG) ash deposits (generally very fine to coarse ash, some with lithic and sparse pumice lapilli) that form multiple indistinctive layers between thicker and coarser vesicular tephras (fig. 16). The vesicular Mount Rainier tephras commonly contain multiple macroscopically distinguishable juvenile components, including andesite to dacite pumice, crystal-poor basaltic andesite scoria, and poorly inflated crystal-rich andesite and dacite. Multiple components and mingling textures result from magma mixing and mingling at magma-reservoir (~8–12 km) and conduit-level depths (Venezky and Rutherford, 1997; Sisson and others, 2013). SVG ashes comprise blocky andesitic lithic grains ranging from hydrothermally altered to fresh and glassy (fig. 17). Juvenile particles can range in vesicularity from dense and blocky to scoriaceous or pumiceous (Sisson and Vallance, 2009). Microlites are abundant in the blocky glassy grains, whereas the more vesicular glassy grains are generally poorer in microlites and commonly have partly to entirely fluidal shapes (fig. 17*A* and *B*). The range of particle shapes and widespread microlites probably result from shallow (edifice-level) fragmentation of largely degassed magma during modest magmatic to hydromagmatic explosions. Rare pumice lapilli and pumiceous ash codeposited with some SVG tephras result from small portions of magma that ascended rapidly from magma reservoir depths. Local distribution, and thickening relations between ridge tops and valley floors, suggests several SVG tephras are co-ignimbrite ashes, even though associated pyroclastic-flow deposits are not preserved.

Tephra stratigraphy, supported by ^{14}C age measurements as well as correlations with large lahars, shows that Holocene tephras from Mount Rainier cluster into four eruptive periods and several short, isolated episodes (figs. 18 and 19). These periods are named the Sunrise eruptive period (calendar age ~10,900 to ~9,600 cal. yr B.P.), the Cowlitz Park eruptive period (7,500 to 6,400 cal. yr B.P.), the Osceola eruptive period (5,600 to 4,500 cal. yr B.P.), and the Summerland eruptive period (~2,700 to 2,000 cal. yr B.P.) (table 1). Volumetrically small eruptions occurred during quieter intervals between eruptive

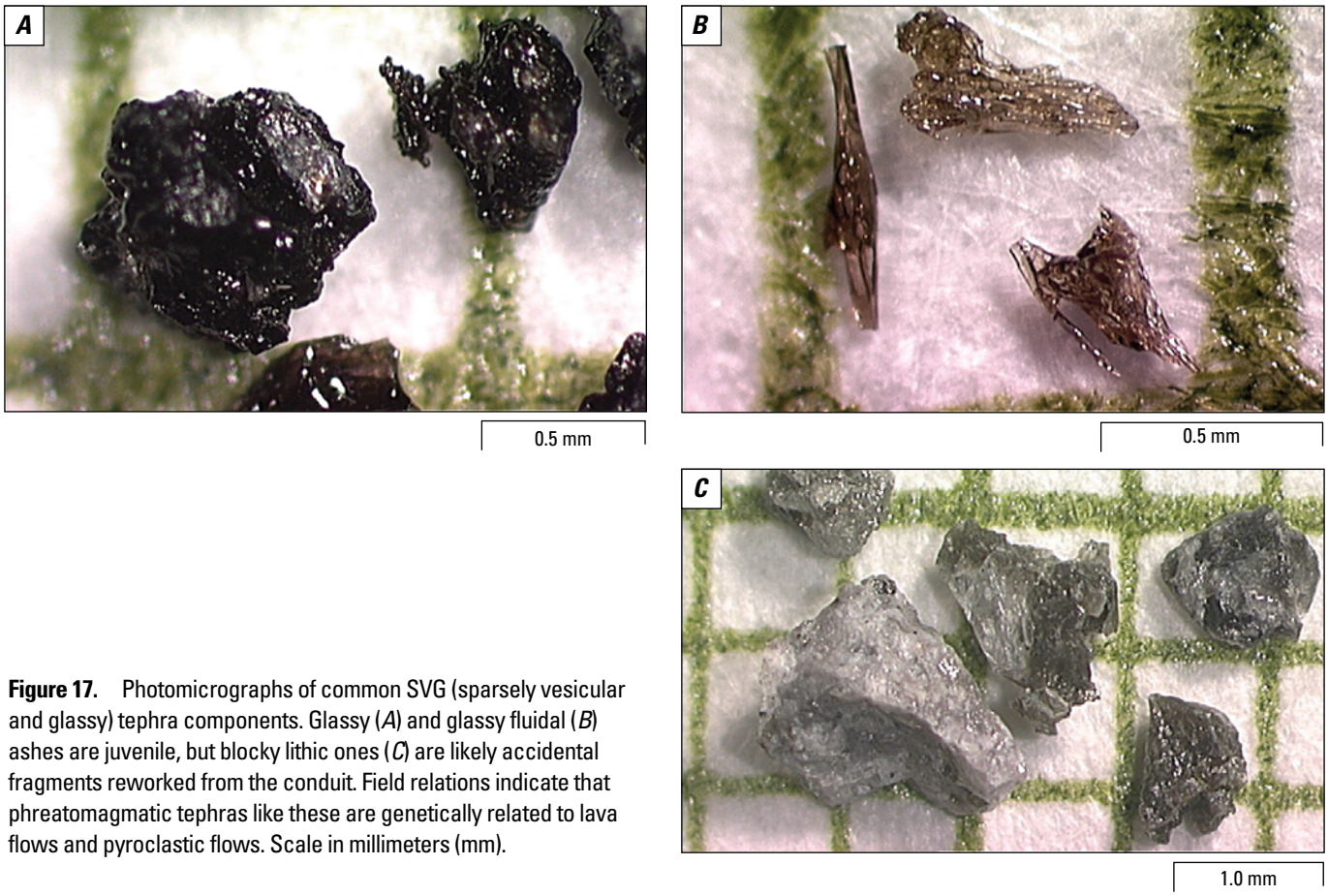

Figure 17. Photomicrographs of common SVG (sparsely vesicular and glassy) tephra components. Glassy (*A*) and glassy fluidal (*B*) ashes are juvenile, but blocky lithic ones (*C*) are likely accidental fragments reworked from the conduit. Field relations indicate that phreatomagmatic tephras like these are genetically related to lava flows and pyroclastic flows. Scale in millimeters (mm).

episodes. The most recent of these sporadic episodes are the Twin Creeks episode (~1,650 to ~1,360 cal. yr B.P.) and the Fryingpan Creek episode (~1,170 to ~900 cal. yr B.P.) (table 1 and Zehfuss and others, 2003). Though these two episodes were small in volume and modest in explosivity, large lahars accompanied them (figs. 16 and 19).

During the two most recent eruptive periods, 5,600–4,500 and 2,700–2,000 cal. yr B.P., the volcano extruded ~2.5 km^3 of lava flows, ~0.1 km^3 of tephra, and ~0.1 km^3 of pyroclastic flows. Since 2,000 cal. yr B.P., the volcano has produced large lahars (~10^8 cubic meters [m^3]), several small tephras (<10^6 m^3), and no lava flows. Thus, Mount Rainier's juvenile output during the past 5,600 years comprises about 90 percent lava and 10 percent pyroclastic deposits. In the Holocene, Mount Rainier's behavior has ranged from effusive, punctuated by small explosive eruptions, to sub-Plinian. Nonetheless, even volumetrically small explosive eruptions (<10^6 m^3) have produced large lahars (>10^8 m^3) that have swept more than 100 km downstream into areas now heavily populated. During the last three eruptions of the past 2,700 years, post-eruption aggradation buried areas, now including Seattle's southern suburbs, with several meters of sediment (Zehfuss and others, 2003).

Table 1. Postglacial eruptive periods and episodes at Mount Rainier, Washington.

Eruptive period or episode	Age, in calendar years before present	Vesicular layers	Sparsely vesicular glassy (SVG) layers
Sunrise period	10,900–9,600	2	5–6
Cowlitz Park period	7,500–6,400	4	5–6
Osceola period	5,600–4,500	4	8–12
Summerland period	2,700–2,000	1	10–18
Twin Creeks episode	~1,600	0	2
Fryingpan Creek episode	~1,000	0	1
White River (?) episode	500–400	0	0
Total		11	31–45

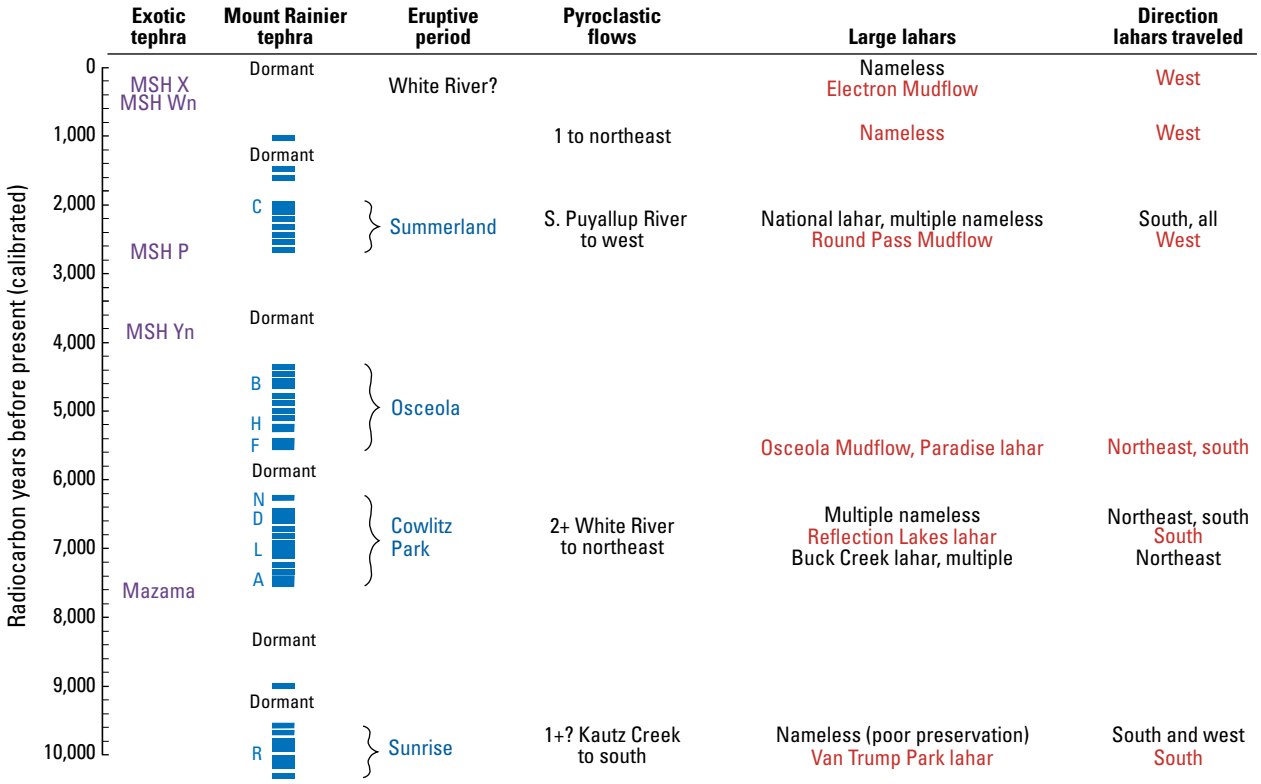

Figure 18. Age correlation diagram of Holocene eruptions and major lahars (>50 kilometers long) from Mount Rainier. Eruptive episodes (blue bars) and named ashes from Sisson and Vallance (2008) and Mullineaux (1974). Lahars indicated in red originated as avalanches of hydrothermally altered rock; those indicated in black originated as a result of hot pyroclastic rock interactions with ice and snow. Mount St. Helens is abbreviated MSH. Modified from Sisson and Vallance (2001).

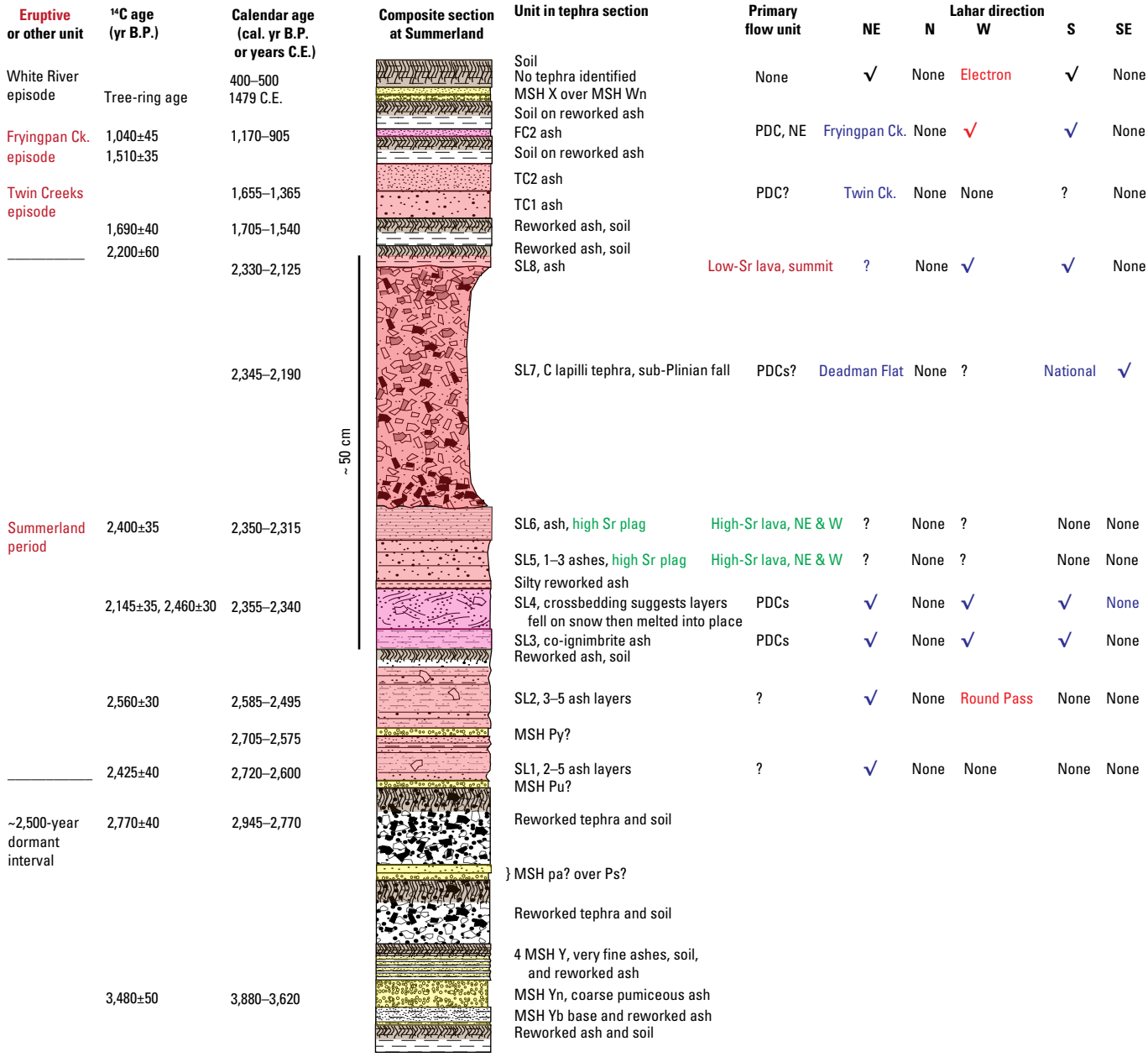

Figure 19. Detailed composite stratigraphic section of tephra sequence at Summerland, 8 kilometers east-northeast of the Mount Rainier summit, illustrating the relation of individual tephra units to voluminous lava flows, pyroclastic flows, and lahars. Of the Mount Rainier tephras, those colored pink originated as co-ignimbrite ashes; those colored salmon resulted from explosions at the vent. Ages given in years before present (yr B.P.), calendar years before present (cal. yr B.P.), and in the Common Era (C.E.). MSH, Mount St. Helens; PDC, pyroclastic density current (flow); plag, plagioclase.

Holocene Eruptive Episodes at Mount Rainier

Sunrise Eruptive Period, Between 10,900 and ~9,600 cal. yr B.P.

Because the Sunrise eruptive period is old enough that its deposits are poorly preserved or even absent in many places, our knowledge of eruption frequency, character, and consequences is fragmentary. The onset of this eruptive episode was shortly after the retreat of McNeeley age glaciers during the last glacial-interglacial transition. At least two vesicular tephras separated by fine ash (R layers) (Samolczyk and others, 2016) and five fine-grained SVG tephras erupted. Samolczyk and others (2016) dated the two vesicular R layers at 10,050±50 cal. yr B.P. The final two SVG tephras in this sequence may be as much as 500 years younger than the others.

An avalanche-induced lahar containing hydrothermally altered rock called the Van Trump Park lahar occurred at about this time on the south side of Mount Rainier. At Van Trump Park, at least one R layer overlies the avalanche-induced lahar. An avalanche-induced lahar deposit exposed in scattered localities in the Paradise area and downstream as far as Kautz Creek is probably the same unit. Scattered clay-poor lahar outcrops south and west of the volcano may be products of hot rock and ice interactions during this eruptive period.

Cowlitz Park Eruptive Period, Between 7,500 and 6,400 cal. yr B.P.

During the Cowlitz Park eruptive period, at least six eruptive episodes produced at least nine tephras and at least four lahars in the White River valley and three lahars in the Nisqually River valley.

Two of the tephras (L and D) were among the largest in the Holocene (30 and 50 $\times 10^6$ m^3). Other tephra layers are small volume, fine grained, and SVG.

In the White River valley, northeast of Mount Rainier, breadcrust blocks within one or two lahars have glass chemistry consistent with tephra layer L, the third eruptive episode, and suggest avalanches of hot rock flowing over snow and ice. At least one lahar underlying the breadcrust lahar is related to a previous eruptive episode and two others overlying it are related to subsequent eruptive episodes. One of these lahars flowed as far as the Puget Lowland, 70 km downstream (volume of the order 10^8 m^3). Well borings near Orting indicate black Mount Rainier sands in the same stratigraphic position as the lahars. We infer that the black sands are genetically related to at least one of the lahars.

The Reflection Lakes lahar is an avalanche-induced lahar that occurred ~7,000 cal. yr B.P. on the south side of Mount Rainier during this period and now crops out between tephra layers of the third (L) and fourth eruptive episodes of this period. The lahar contains abundant hydrothermally altered rock. At least two clay-poor lahars descended the south flank of Mount Rainier after the Reflection Lakes lahar, probably during the fifth eruptive episode (D).

Osceola Eruptive Period, Between 5,600 and 4,500 cal. yr B.P.

The first eruption of the Osceola period shortly before 5,600 cal. yr B.P. generated the Paradise lahar, which swept down the south flank of the volcano and the Nisqually River as far as National. It contains hydrothermally altered rock.

At about 5,600 cal. yr B.P., phreatic and phreatomagmatic eruptions produced tephra units containing hydrothermal clays plus fresh juvenile pumice and triggered an edifice collapse and debris avalanche that transformed to debris flow within a few kilometers of the summit and formed the Osceola Mudflow (Crandell, 1971; Mullineaux, 1974). The collapse of the edifice during the Osceola eruption removed 2–3 km^3 from Mount Rainier's summit and formed an amphitheater, 1.8 km across, as much as 1 km deep, and open to the northeast (fig. 14). Decompression of a hydrothermal system near its pressure boiling point and equilibrated to 1,000 m depth caused at least two laterally directed explosions that blew hydrothermal mud to the northeast while pumice fell in a broad arc to the east. The resulting tephra, layer F, contains an unusual assemblage of hydrothermal-alteration minerals including pyrite, jarosite, alunite, kaolinite, smectite, gypsum, and opal (John and others, 2008). John and his colleagues found mineral assemblages consistent with an acid-sulfate-leaching hydrothermal system equilibrated to as deep as about 1 km in both tephra layer F and in debris of the Osceola Mudflow.

After 5,600 cal. yr B.P., the vent area was confined by the open amphitheater and affected by the removal of a significant portion of Mount Rainier's ice volume. At least five subsequent tephra packages suggest a period of cone rebuilding that must have ended by 4,500 cal. yr B.P., but probably somewhat earlier, around 4,900 cal. yr B.P. These tephras are small in volume and not widely distributed, implying small explosions with explosivity indices of about VEI 2. A lack of even moderate size lahars during the post-Osceola interval is also consistent with minimal explosivity. Apparently, effusions of lava characterized early stages of cone rebuilding at Mount Rainier. Because some of the earliest products of the subsequent eruptive period (Summerland) spilled westward into the Puyallup River drainage, we infer that a significant proportion of the 2-to-3-km^3 edifice that underlies Columbia Crest must have extruded as lava flows during the Osceola eruptive period, but lavas of the Osceola period have not been identified and are probably buried by glacier ice and younger Summerland lava flows.

Downstream, a period of aggradation and channel adjustment followed the Osceola Mudflow emplacement. Within 10 to 20 km, the White River aggraded up to tens of meters then cut back through the resulting deposits. The small subsequent Osceola period eruptions produced no lahars large enough to be identified downstream from this aggradational reach.

Summerland Eruptive Period, Between 2,700 and 2,000 cal. yr B.P.

By about 2,700 cal. yr B.P., Mount Rainier began to erupt again, first producing SVG tephras (SL1) and a clay-poor lahar that flowed northeastward into White River valley (fig. 19) (Sisson and Vallance, 2009). Subsequently, another series of SVG tephras (SL2) generated clay-poor lahars that flowed northeastward into the White River valley.

Volcanism toward the end of SL2 time or at the outset of SL3 time (fig. 19) caused a large avalanche-induced lahar on the west flank of the volcano (Round Pass Mudflow, 2–3 $\times 10^8$ m^3), which contains abundant hydrothermally altered rock. After SL2, continued growth of the Holocene edifice and avalanche of the west rim of the Osceola amphitheater allowed pyroclastic density currents and lahars to escape the confines of the Osceola amphitheater and spill westward and southward into the Nisqually and Puyallup River drainages as well as flow northeastward into the White River drainage.

At about 2,500–2,400 cal. yr B.P., a sequence of SVG tephra units (SL3 and SL4), cogenetic clay-poor lahars, and at least one pyroclastic flow indicate continuing eruptions (fig. 19). Voluminous high-Sr lava flows, correlating to high-Sr SVG tephras, SL5 and SL6, then descended the northeast and west flanks of Mount Rainier (fig. 19). Remnants of the lava flows occur at Camp Schurman and protrude through ice of the Emmons, Winthrop, and Tahoma Glaciers. The source of the SVG tephras, pyroclastic flows, and lavas evidently is the partly truncated west crater of Mount Rainier. Sediment from these eruptions caused aggradation in the Green and Duwamish River drainages near Seattle.

At about 2,300 cal. yr B.P., a sub-Plinian eruption produced the largest Holocene tephra containing pumice, scoria, and juvenile lithics (layer C, 1×10^8 m^3). This eruption may have triggered a large clay-poor lahar (National lahar, volume ~1×10^8 m^3) that descended the Nisqually River south then west to Puget Sound. The presence of layer C pumice in lahars shows that additional clay-poor lahars descended the White (northeast), Cowlitz (southeast), and Nisqually (south) Rivers at this time. Columbia Crest lavas extruded about this time or shortly afterward; lahars and one tephra layer were also emplaced. All of this activity originated from the east crater of Mount Rainier. Sediment from lahars associated with the explosive C eruption caused aggradation in the Green and Duwamish River drainages.

Twin Creeks Eruptive Episode, Between 1,650 and 1,360 cal. yr B.P.

Mount Rainier erupted two small vesicle-poor tephra layers between 1,650 and 1,360 cal. yr B.P. A large lahar (~10^8 m^3) with radiocarbon ages of about 1,600 cal. yr B.P. descended the White River valley. In the Green River valley between Auburn and Seattle, several meters of aggradation resulted from post-lahar sedimentation owing to these lahars.

Fryingpan Creek Eruptive Episode, ~1,000 cal. yr B.P.

At about 1,000 cal. yr B.P., Mount Rainier erupted fine ash that contained charred twigs and needles and generated a clay poor lahar that descended the White River drainage as far as 100 km. The fine ash containing delicate charred fragments suggests pyroclastic density currents and co-ignimbrite ash fall, though no pyroclastic-flow deposits are preserved. If true, then the lack of vesicular particles in the ash suggests that the pyroclastic density currents derived from avalanches of hot rock from the vent. The interaction of hot rock and extensive snow and ice of the summit ice cap and the Emmons and Winthrop Glaciers caused large clay-poor lahars that descended the White River system to Auburn (volume is on the order of 10^8 m^3). Reworking of lahar sediment caused extensive aggradation in the Green and Duwamish River valleys as far as Puget Sound, including the southern Seattle suburbs near Boeing Field. At about this same time, an avalanche of hydrothermally altered rock and debris from the west side of Mount Rainier caused a moderate-size, clay-rich lahar in the Puyallup River system.

White River Episode, ~500 cal. yr B.P.; Did the Volcano Erupt?

A large edifice-collapse lahar (Electron Mudflow) and numerous small clay-poor lahars that inundated valleys west, northeast, and south of the volcano between ~500 and 400 cal. yr B.P. may suggest volcanism at that time, but no indisputable tephra deposits or other products of magmatism have been identified in this time interval, and the cause of these events is unknown (Sisson and Vallance, 2009). About 500 years ago, an avalanche of hydrothermally altered rock from the west side of Mount Rainier caused a lahar (Electron Mudflow) that swept down the Puyallup River drainage as far as Sumner (Crandell, 1971). An avalanche-induced lahar, previously named the Tahoma lahar that swept down Tahoma Creek (Scott and others, 1995) is now known to be part of the Electron Mudflow. By ~400 years ago, clay-poor lahars descended the Nisqually and White River drainages. The clay-poor lahars contain prisms and blocky particles that are glassy and suggest the possibility of eruptions, but no coeval tephra layers or other indicators of magmatism are known. The lahars occurred near the time of the Little Ice Age glacial maximum, suggesting the possibility that larger glaciers upstream somehow played a role in their origin.

Purported Historical Eruptions of Mount Rainier

Sisson and Vallance (2009) discredited a purported eruption of Mount Rainier between 1820 and 1854 C.E. (Mullineaux, 1974). Scattered pumiceous lapilli inferred to have been deposited between 1820 and 1854 C.E. (Mullineaux, 1974) are not a fall deposit from that time but rather are older tephra transported by snow avalanches downslope into misleading positions on top of young moraines (Sisson and Vallance, 2009). An entry in the account of the Fremont expedition of 1843 to 1844 reported

that Mount Rainier was erupting on November 13, 1843. Small clay-poor lahars occurred at about this time, but these could have originated from hydrologic or meteorologic events.

In 1894, newspaper accounts reported small light and dark clouds interpreted to be steam and ash emissions from the summit of Mount Rainier, but no deposits or other concrete evidence confirming such an eruption have been found. One account from an expedition to the volcano reports seeing a clear eruption plume from the summit on December 24, 1894, but a sharp photograph of the volcano from Tacoma dated December 29, 1894, shows neither summit plumes nor discoloration of near-summit snowfields (University of Washington Special Collection photograph WAT042). To summarize, no solid evidence has been found that would confirm magmatic eruptions during the 19th century at Mount Rainier, and the last well supported eruptions were during the 1,000 cal. yr B.P. Fryingpan Creek episode.

Origin and Distribution of Lahars at Mount Rainier

Mount Rainier readily generates lahars. It has an enormous volume of snow and ice available for melting during an eruption. It also stores water beneath its glaciers, which sometimes release outburst floods. Its huge mass of hydrothermally altered rock (especially prior to 5,600 years ago) weakens the edifice and stores additional water in the hydrothermal system of the volcano (Vallance and Scott, 1997). More than 50 Holocene lahars have been identified at Mount Rainier (Crandell, 1971; Scott and others, 1995). Many of these lahars are eruption related, but many are not. Lahars at Mount Rainier can be classified into three groups according to their genesis.

1. Lahars that form owing to flank collapse of hydrothermally altered, water-saturated rock. At Mount Rainier, these lahars are clay rich. The largest lahar of this type (Osceola Mudflow) resulted from an eruption. Other lahars of this type also occurred during eruptive episodes; however, one or more (notably the Electron Mudflow) occurred during periods for which definitive evidence of eruptive activity is not known. We note that preservation of very small tephra layers is unlikely and that lahars like the Electron Mudflow could be eruption related despite a lack of associated primary eruptive products.

2. Lahars that result from the interaction of pyroclastic flows or hot rock avalanches with glacial ice and snow. At Mount Rainier, such lahars are clay poor. Lahars of this type invariably occur during eruptions. Excepting the enormous Osceola Mudflow, lahars having this origin are among the largest in the Holocene record at Mount Rainier. Prismatic, monolithologic clasts of possible juvenile magmatic origin suggest eruptive origins for clay-poor lahars even during certain episodes lacking well preserved tephra layers, most notably about 500 cal. yr B.P.

3. Lahars caused by glacial outburst floods and torrential rains are generally differentiated as debris flows at Mount Rainier. These lahars are commonly smaller than those described in classes 1 and 2 above and are not related to eruptive activity. They are clay poor and have diverse clast types.

Geographic Distribution of Lahars in the Holocene

Avalanche-induced lahars and their associations with weakened hydrothermally altered rock are a particularly interesting result of studies at Mount Rainier (Crandell, 1971; Scott and others, 1995; John and others, 2008). The well-documented clay-rich lahars at Mount Rainier were not randomly distributed in time or space (John and others, 2008).

The three well-documented Holocene deposits containing abundant hydrothermally altered rock that were emplaced before the time of the Osceola collapse of 5,600 years ago are all on the south side of Mount Rainier (John and others, 2008). The oldest of these lahars crops out at Van Trump Park and all three crop out in the Paradise Park area. Each of these deposits was emplaced in time intervals during which Mount Rainier erupted. There presently are no voluminous outcrops of in-place hydrothermally altered rock on the south side of Mount Rainier's edifice. Presumably the last remnants of the hydrothermally altered rock mass that was the source of clay-rich lahars on the south side of Mount Rainier slid away during the Osceola eruption 5,600 years ago.

About 5,600 years ago, eruptions triggered collapse of the volcano's altered east-northeast flank, spawning the Osceola Mudflow. Deposits of both the Osceola Mudflow and its co-genetic tephra layer (layer F) contain abundant hydrothermal clays (Crandell, 1971). Tephra layer F also contains juvenile glass shards, crystals, and pumice (Mullineaux, 1974). The upper and lower clay-rich parts of the tephra are distributed as lobes to the east-northeast whose axes coincide with that of the U-shaped Osceola amphitheater (Mullineaux, 1974). The wind-blown, pumiceous, middle part of the tephra has a more southeasterly axis of distribution. Their distribution parallel to the failure axis rather than downwind suggests that the upper and lower parts of tephra layer F may have been deposited from laterally directed explosion clouds resulting from decompressive unloading of the edifice hydrothermal system during avalanching (Vallance and Scott, 1997; John and others, 2008). It seems likely that the Osceola Mudflow began as two or more slide blocks (Vallance and Scott, 1997). If so, then hummocky deposits and deposits now found at inundation limits may result from the initial slide block. Remnants of an outer, less altered carapace may have formed these parts of the deposit. Subsequent slide blocks eviscerated the more altered edifice interior, producing the volumetrically dominant, clay-rich, valley-bottom deposits.

After the Osceola Mudflow and beginning about 2,700 ago, avalanches of hydrothermally altered rock were solely from the western flank of Mount Rainier where the only sizeable exposures of altered rocks remain at high elevation (Crandell, 1971; John and others, 2008). The resulting lahars descended the Puyallup River and Tahoma Creek drainages. These lahars included the Round Pass mudflow at about 2,600 cal. yr B.P., a lahar at ~1,000 cal. yr B.P., and the Electron Mudflow at ~1500 C.E.

Clay-poor lahars that formed during eruptions descended all major drainages that head on Mount Rainier except the Carbon River drainage (Scott and others, 1995). The largest of these appear to be produced by avalanches of hot rock or pyroclastic flows that moved across snow and ice. Events of this type occurred at least a dozen times in the Holocene at Mount Rainier. They include four or more events between 7,300 and 6,800 cal. yr B.P.; several events between 2,700 and 2,400 cal. yr B.P.; at least one event at about 2,300 cal. yr B.P. that affected the White, Nisqually, Cowlitz, and possibly Puyallup River drainages. Such events also include lahars in the White River drainages at about 1,600 and 1,000 cal. yr B.P. The largest lahars (volumes ~10^8 m^3) of this type have magnitudes similar to those of large avalanche-induced lahars, excepting the Osceola Mudflow (total bulked volume of 3.8×10^9 m^3).

Lahars (debris flows) unrelated to avalanches of hydrothermally altered rock or eruptive episodes are typically the result of hydrologic or meteorologic events, such as glacial outburst floods or heavy precipitation (Walder and Driedger, 1995; Vallance and others, 2003). Such debris flows are typically small ($1–5\times10^5$ m^3) but can reach moderate sizes (for example, the Kautz Creek event of 1947, which according to Crandell [1971] had a volume of 40×10^6 m^3).

Downstream Lahar Behavior at Mount Rainier

Lahars Induced by Sudden Melting of Snow and Ice, Voluminous Floods, or Torrential Rains

Floods of water moving across the easily erodible loose clastic sediments common on the flanks and aprons of Mount Rainier easily erode and incorporate that debris to form lahars (fig. 20*A*, *B*) (Scott, 1988; Scott and others, 1995; Vallance, 2000). Erosional incorporation of sediment (bulking) is critical to forming all lahars that begin with sudden water releases. Lahar formation depends on the right mix of readily available sediment and water discharge. Because clay-rich sediment is uncommon on the flanks of Mount Rainier, lahars induced by sudden water release are typically clay poor (less than about 4 percent clay in matrix).

As they continued down active river channels, lahars, like the National, Deadman Flat, or Fryingpan Creek lahars, gradually incorporated water, became progressively more dilute, and underwent transformations to hyperconcentrated flows and muddy streamflows (fig. 20*C*, *D*). Such flow transformations begin at the flow front and migrate back through the lahar wave as it travels downstream (Scott, 1988). Once off the flanks of the volcano and confined in river channels, lahars, which typically move faster than normal streamflow, push river water ahead of them and gradually, with distance downstream, begin to mix with that water. As the flow front becomes progressively more water rich, it loses the capacity to transport larger clasts, and these clasts progressively lag behind the flow front and eventually are deposited. With time and distance downstream, a dilution front regresses from the front of the lahar to its middle, and eventually the entire lahar becomes more dilute.

Edifice- or Flank-Collapse-Induced Lahars

Although most edifice collapses behave as debris avalanches, those at Mount Rainier had sufficient, widely dispersed, pore and hydrothermal water in the pre-collapse rock to liquefy as the material deformed during collapse (Scott and others, 1995; Vallance and Scott, 1997). The process of hydrothermal alteration, especially at glaciated volcanoes like Mount Rainier, increases the probability of edifice-collapse lahars. Acid-sulfate leaching in hydrothermal systems removes soluble elements, adds sulfate and sulfide, and breaks down framework silicates to form silica phases, like cristobalite and opal, and clay minerals, like kaolinite and smectite (John and others, 2008). This process weakens the rock so that it more readily disintegrates during deformation after collapse. Thus, huge blocks (hummocks) typical of debris avalanches are less common in edifice-collapse lahars from Mount Rainier even though the lahars have the same origins. Abundant alteration minerals, especially clay minerals, increase porosity and decrease permeability of the rock, and thus, in combination with the hydrothermal system, trap a widely dispersed reservoir of water within the pre-collapse mass. Because of its water content and its tendency to disintegrate, hydrothermally altered rock, unlike fresh rock, readily liquefies as it deforms. Collapse-induced lahars are typically clay rich, and most are observed to have greater than 4 percent clay in their matrix. Because the clay-rich lahars consist of weak materials and abundant water, they can travel farther than debris avalanches that come to rest relatively short distances from their source volcanoes.

Depositional Processes

Emplacement of lahar deposits can occur en masse, by steady incremental accretion or, most likely, by some intermediate process in which accretion begins then accelerates, wanes, or does both alternately (Vallance and Scott, 1997; Vallance, 2000). Debris-flow deposits are poorly sorted, generally massive, and unstratified. It is common to infer that such massive deposits were emplaced en masse and preserve a frozen portion of the debris flow. In contrast, hyperconcentrated-flow deposits are better sorted, commonly show faint stratification, and hence are interpreted to have accreted during significant time intervals.

An increasing body of evidence suggests that deposits of both hyperconcentrated flows and debris flows accrete incrementally (Scott, 1988; Vallance and Scott, 1997). Such evidence includes (1) strong alignment of elongate clasts parallel to flow directions or imbrication of such clasts in upstream directions, (2) strong changes in the proportion of erosively incorporated (exotic) particles with vertical position in outcrops, especially those that are graded, (3) inundation limit deposits with exotic-particle proportions similar to those at the base of thick valley-bottom deposits, (4) marks of peak-flow levels in upland valleys that indicate flow depths 5 to 10 times greater than deposit thicknesses, (5) abundant evidence of cataclasis (breakage of clasts owing to collisions), and (6) stratification in deposits of transitional or hyperconcentrated flows.

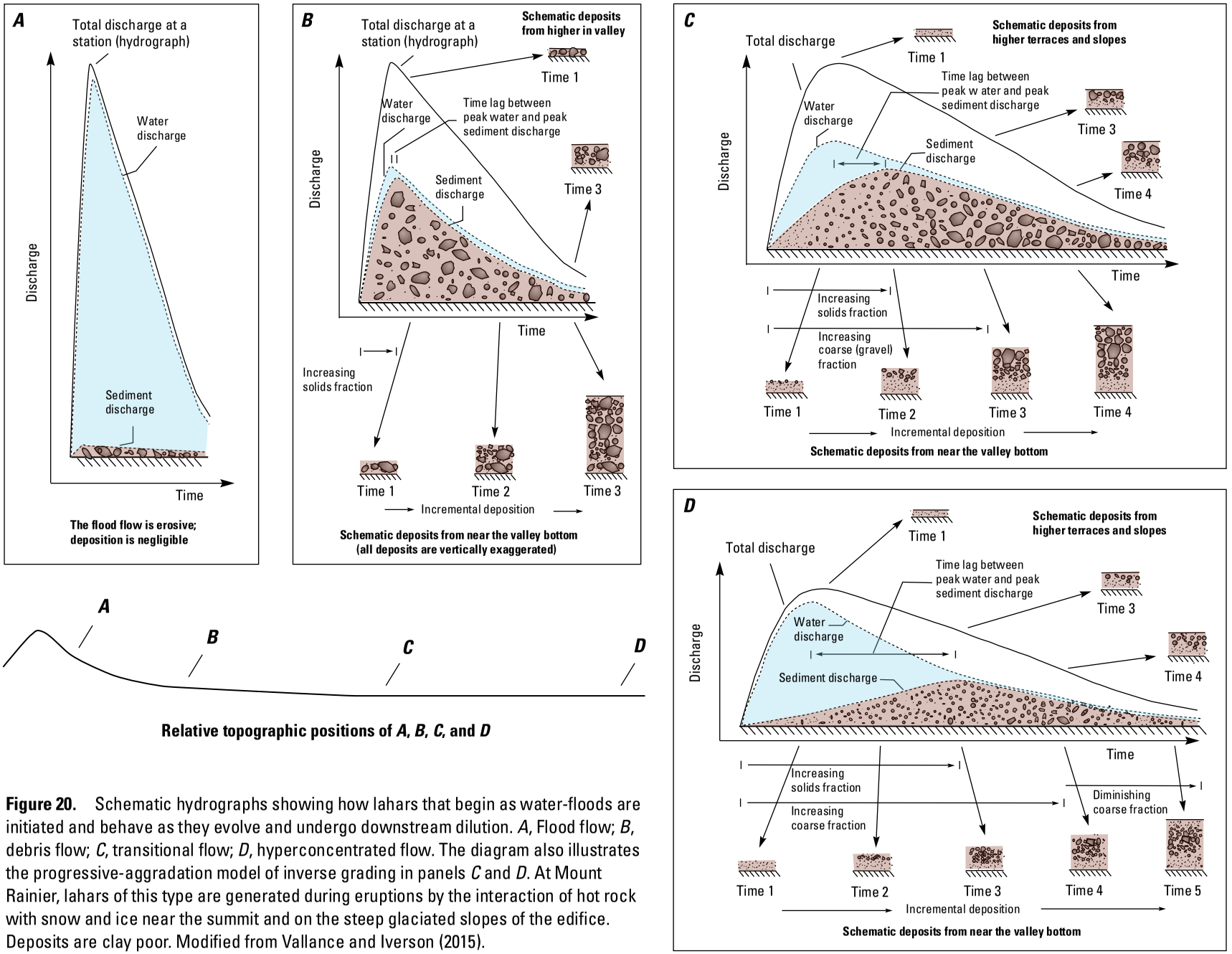

Figure 20. Schematic hydrographs showing how lahars that begin as water-floods are initiated and behave as they evolve and undergo downstream dilution. *A*, Flood flow; *B*, debris flow; *C*, transitional flow; *D*, hyperconcentrated flow. The diagram also illustrates the progressive-aggradation model of inverse grading in panels *C* and *D*. At Mount Rainier, lahars of this type are generated during eruptions by the interaction of hot rock with snow and ice near the summit and on the steep glaciated slopes of the edifice. Deposits are clay poor. Modified from Vallance and Iverson (2015).

Although rapid deposition of a vertically size-segregated flow can generate normally and inversely graded deposits, incremental accretion of longitudinally size-segregated flow can also be responsible (Vallance, 2000). Because lateral and longitudinal variations in both sizes and compositions of particles commonly develop in moving lahars, accretion from such laterally graded systems during significant time intervals can cause vertically graded deposits. Clay-poor lahars that migrate down river channels commonly push the river water in front of them and become more dilute downstream. Downstream, the flow front mixes with the water and forms a progressively more dilute flow. Figure 20 (parts *B*–*D*, times 1 to 5) illustrates schematically how accretion from a debris-flow wave with a concentration of large particles at its front can generate a normally graded deposit. Note that accretion occurs for a short time only near inundation limits where grading does not occur (times 1–2). The front of a lahar wave that flows down a river becomes progressively more dilute and less capable of carrying larger particles, which lag behind (fig. 20*C*, *D*). Therefore, accretion from a dilute debris flow that coarsens from head to tail produces inversely graded deposits (fig. 20*C*). Farther downstream, the entire lahar, and especially its flow front, becomes hyperconcentrated so that accretion produces finer grained beds that may be inversely graded or both inversely graded and normally graded (fig. 20*D*). Deposit facies from such clay-poor lahars show systematic changes downstream (fig. 21). At Mount Rainier, the large lahar deposits that best exhibit such facies changes are in the White and Nisqually River drainages.

At Mount Rainier, debris flows that do not undergo downstream dilution commonly form cobble- and boulder-rich perimeters owing to segregation of coarse grains to the surface. The surface of the flow, with its concentration of large particles, moves faster than the rest of the flow so that cobbles and boulders migrate to the flow front (Vallance and Iverson, 2015). Once the flow peak has passed at any particular cross section, boulders begin to accrete at flow margins to form coarse levees. Flow fronts, with concentrations of large angular particles, that move onto gentle slopes become progressively drier because water can more easily escape from more permeable coarse-grained flow perimeters than from fines-rich interior flows. The net result is a dry, frictional, resistant flow perimeter that surrounds a liquefied interior. When flows of this type reach sufficiently gentle slopes, the frictional perimeter slows to a stop and leaves behind a steep-fronted, fines-poor margin and a partly liquefied, fines-rich interior (Vallance and Iverson, 2015). Debris flows such as these are common on the south side of Mount Rainier and occur almost yearly. These debris flows are generally not big enough to escape the boundaries of Mount Rainier National Park.

Osceola Mudflow Downstream Behavior and Deposition (Summarized from Vallance and Scott, 1997)

The 3.8-km^3 Osceola Mudflow filled valleys of the White River system to depths of as much as 150 m, inundated more than 240 km^2 of the Puget Lowland, and flowed at least 20 km underwater to the present sites of Tacoma and the Seattle suburb of Kent (fig. 22). Near Mount Rainier, deposits of the Osceola Mudflow cap ridges high above the Winthrop and Emmons Glaciers. Remnants also are present on top of Steamboat Prow and throughout the Inter Fork of the White River drainage basin (geographic features are illustrated at discussion for day 2, stop 8; fig. 40). The homogeneity of these deposits, the lack of hummocky terrain within 10 km of the summit, and the apparent fluidity suggest the avalanches that initiated the Osceola Mudflow mixed thoroughly within 2 km of their source and abruptly began to behave like an enormous water-saturated debris flow.

Mapping the upper limits (inundation limit) of the Osceola Mudflow along the steep-sided White River valley between Mount Rainier and Mud Mountain, 75 km downstream, reveals that the peak-stage height of the mudflow attenuated sharply near the volcano then reached an equilibrium height downstream. In the

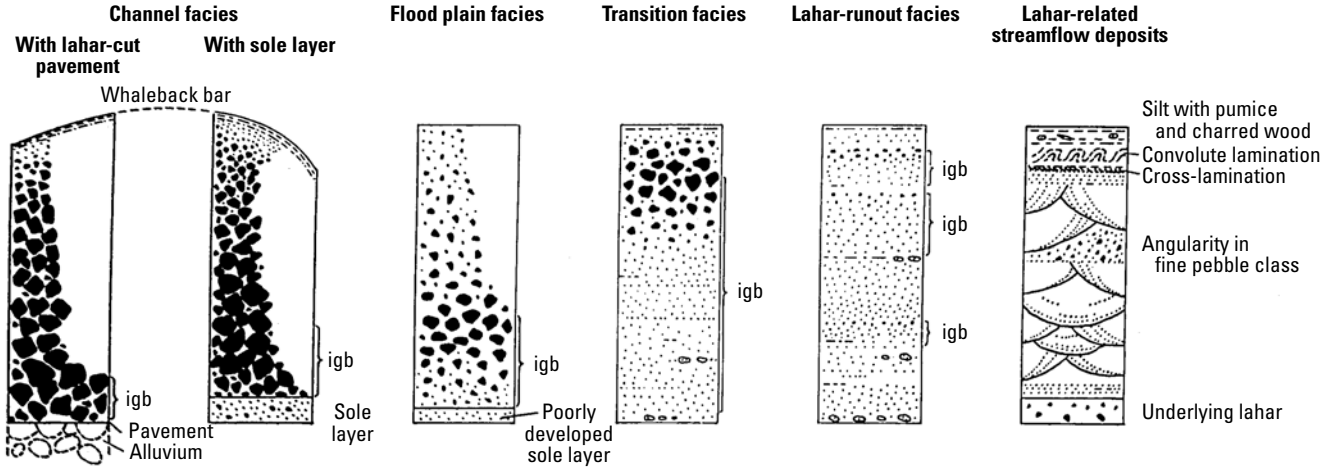

Figure 21. Schematic sections illustrating deposit characteristics of clay-poor lahars. Upstream facies are illustrated in sections to the left. Deposit facies from lahar flows that accrete particles as they move progressively downstream and overrun river water to become more dilute are in sections to the right. Inversely graded bedding in sections is abbreviated as igb. Modified from Scott (1988).

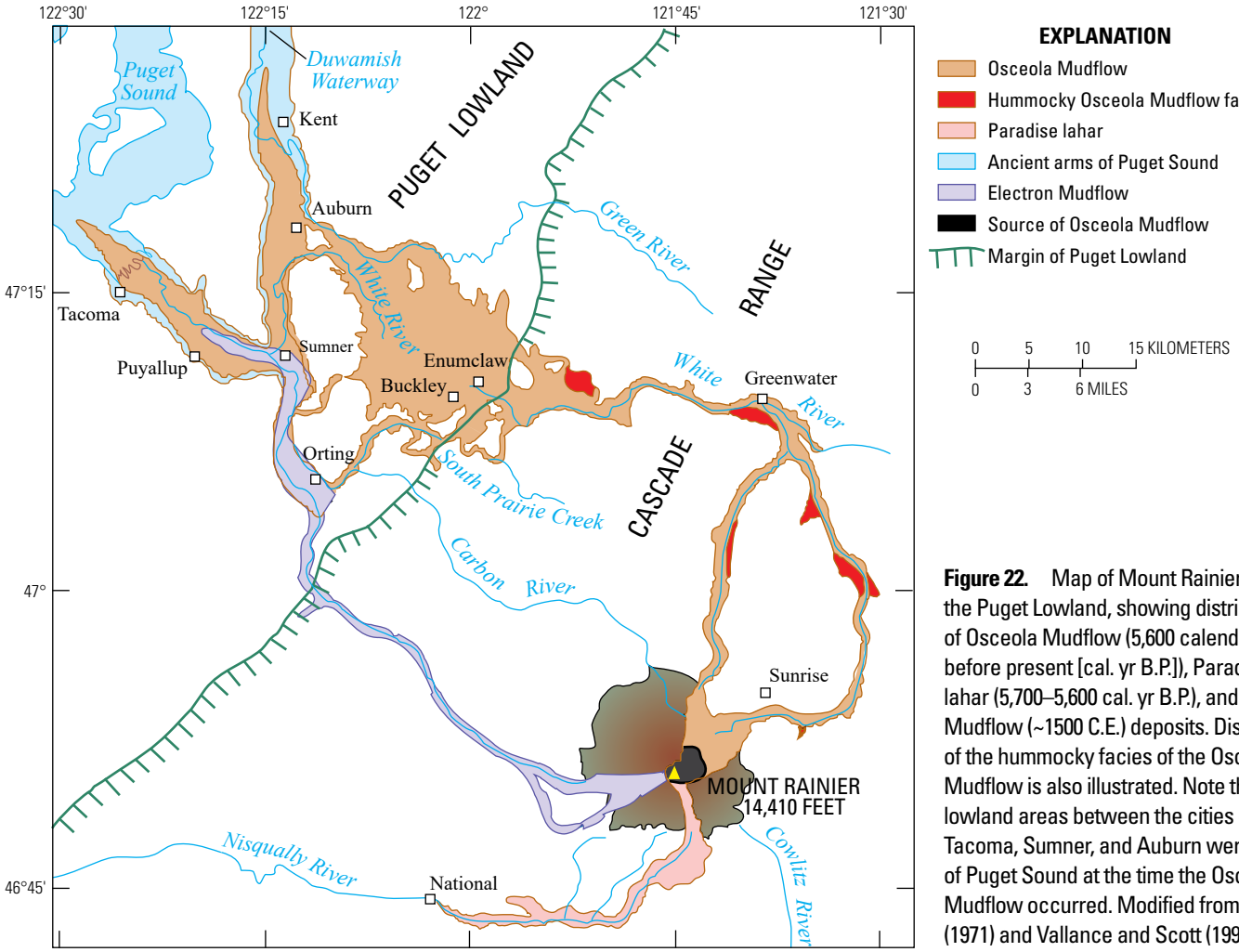

Figure 22. Map of Mount Rainier area and the Puget Lowland, showing distribution of Osceola Mudflow (5,600 calendar years before present [cal. yr B.P.]), Paradise lahar (5,700–5,600 cal. yr B.P.), and Electron Mudflow (~1500 C.E.) deposits. Distribution of the hummocky facies of the Osceola Mudflow is also illustrated. Note that lowland areas between the cities of Tacoma, Sumner, and Auburn were arms of Puget Sound at the time the Osceola Mudflow occurred. Modified from Crandell (1971) and Vallance and Scott (1997).

Inter Fork valley, deposits of the mudflow are present 400 m above the valley bottom. The deposit ran up more than 530 m above the valley bottom at Goat Island Mountain and an astonishing 670 m at Sunrise (see fig. 40). About 10 km downstream, the inundation limit is 200 m; farther downstream, it stabilizes, varies between 85 and 150 m, and averages about 100 m. The decrease of the maximum inundation depth downstream by longitudinal spreading and by deposition was counteracted by the additional discharge from the West Fork White River 45 km downstream and by bulking of the flow through the incorporation of eroded sediment.

Mud and debris of the Osceola Mudflow that ran up onto a mountain, about 10 km from Mount Rainier, and onto a ridge, about 45 km downstream from Mount Rainier, allow the maximum velocity and peak discharge of the flow to be estimated at these two places (Vallance and Scott, 1997). At 10 km the mudflow ran up 110 m, implying that the velocity of the flow must have been at least 46 meters per second (m/s). Similarly, downstream, the lahar ran up about 18 m onto the ridge allowing a maximum velocity of 19 m/s to be estimated. The total discharge of the Osceola Mudflow along the White River would have been about 2,600,000 cubic meters per second (m^3/s) (Vallance and Scott, 1997).

At the Cascade Range front, the Osceola Mudflow encountered a narrow gorge of the White River that is only 300 m wide then spread over glaciofluvial and drift terraces of Vashon age that are as much as 110 m above the White River (fig. 22; also see day 1, stops 1–3). In the lowland, the Osceola Mudflow completely choked the channel of the White River, which in pre-Osceola time followed the relatively confined valley of South Prairie Creek southwestward to join the Puyallup River at Orting, then flowed northwestward across the drift plain into the Green River drainage (fig. 22) (Crandell, 1963). When the White River reestablished normal flow, it flowed northwestward toward Auburn along a radically different course near the axis of the lahar lobe.

The Osceola Mudflow entered the Duwamish and Puyallup embayments of Puget Sound via deltas at the mouths of the Green and Puyallup Rivers (fig. 22). Low gradients on the deltas caused the debris flow to thicken to more than 20 m near Auburn and Sumner (Dragovich and others, 1994). Deposits are generally present only in the subsurface in the Green and Puyallup River valleys. Wood-bearing, clayey, gravel-rich deposits at depths of 20 to 100 m northwest of Puyallup and north of Auburn show that the Osceola Mudflow retained its coherence and flowed more than 20 km underwater.

Sedimentology

Osceola Mudflow deposits comprise three facies (Vallance and Scott, 1997). The axial facies forms normally graded deposits 1.5 to 25 m thick in lowlands and valley bottoms and ungraded deposits in lowlands where it thins to a feather edge; the valley-side facies forms ungraded deposits 0.3 to 2 m thick that drape valley slopes; and the hummocky facies, interpreted before as a separate (Greenwater) lahar, forms 2-to-10-m-thick deposits dotted with scattered hummocks as much as 20 m high and 60 m in plan that crop out along deposit margins as far as 70 km downstream (fig. 22). The hummocky facies contain coherent fragments of Mount Rainier andesite surrounded by greater proportions of matrix rich in scoured bedrock, alluvium, and glacial drift.

Near their source, Osceola Mudflow deposits contain only fresh and hydrothermally altered rock from the volcano. The proportion of hydrothermally altered rock in the deposit is high. One proximal deposit contains 15 percent clay (37 percent of its matrix), all of which is the product of hydrothermal alteration. In addition, inspection of recognizable Mount Rainier andesite clasts shows that about a third are moderately to highly affected by hydrothermal alteration. Deposits are typically massive and have small proportions of gravel incorporated by erosion.

Downstream, Osceola Mudflow deposits contain significant proportions of exotic alluvial and colluvial grains that can only have been incorporated through erosion as the flow moved as far as 120 km down valley (Vallance and Scott, 1997). Overall, as a function of both distance downstream and height above the valley bottom at any particular distance downstream, the Osceola Mudflow deposit increases systematically in its proportion of exotic gravel and sand in its matrix (sand/[sand+silt+clay]), as well as decreases in its proportion of clay-size grains (Vallance and Scott, 1997). Similar changes in proportions of the same characteristics are observed with position from top to bottom of individual, normally graded, axial-facies deposits. Abundant exotic clasts (as much as 80 percent in some deposits) suggest that the Osceola Mudflow wave eroded and entrained abundant sand and gravel at its front and during its peak inundation at any place within the valley (fig. 23, also see day 1, stops 4–5). As

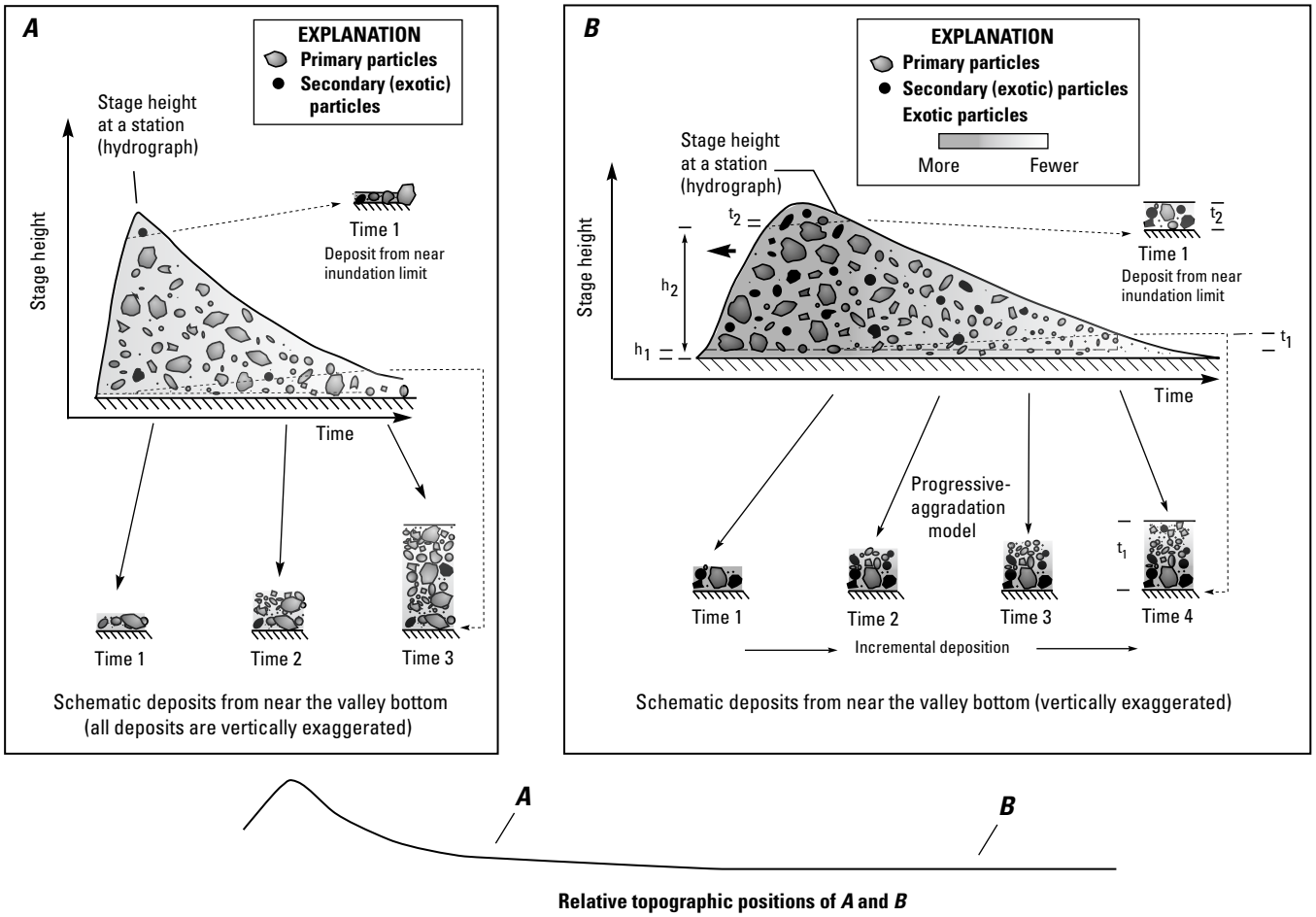

Figure 23. Schematic hydrographs showing the behavior and downstream changes of the Osceola Mudflow, a lahar that began with avalanche of debris and became water-saturated upon deformation. With increasing distance downstream (*A* to *B*) the lahar incorporates exotic particles, especially near its flow front. Panel *B* also illustrates how a flow, coarser grained at its head than at its tail, can accrete incrementally to form a normally graded deposit. In *B*, exotic particles are most common at the base of normally graded deposits and at inundation limits. Modified from Vallance and Scott (1997) by Vallance and Iverson (2015).

the flow stage fell, the Osceola Mudflow transitioned from erosive to depositional and therefore contained progressively fewer exotic gravel and sand grains. As there is no significant source of clay in the White River valley, nearly all clay grains came from the source avalanche at the volcano. Clay proportion is greater in deposits that have fewer exotic grains and less in deposits that have more exotic grains. Overall, 2–2.5 km^3 of the total volume of the deposit is from source and the remainder of the total 3.8 km^3 is exotic.

Progressive Aggradation from a Longitudinally Segregated Flow

Systematic variation of grain size and composition within and among deposits suggests that the Osceola Mudflow was longitudinally segregated such that it was coarser grained, better sorted, and contained more exotic particles at its front than at its tail (fig. 23*B*) (Vallance and Scott, 1997). Although little can be inferred about the rising stage of the Osceola Mudflow, deposition began following passage of its peak flow wave and continued as its flow stage receded. Deposits near peak-flow limits contain large proportions of exotic clasts, particularly gravel-size alluvium. The presence of gravel-size alluvium indicates thorough vertical mixing of exotic particles by the time of peak flow because alluvium is not present on valley sides and must have been transported about 100 m upward from valley bottoms. At any position downstream, deposits decrease in exotic fraction from peak-flow limit to valley floor, indicating changes in the composition of the lahar as flow level fell. The large to moderate proportion of alluvial particles at progressively falling stages (fig. 23*B*) suggests continued vertical mixing at successive times because these particles also were carried upward tens of meters from valley bottoms. We infer that peak-flow-limit deposits, hummocky facies deposits, and the basal parts of thick normally graded axial facies came from the same part of the flow wave because they are similarly rich in exotic sand and gravel and poor in clay. These parts of the Osceola Mudflow were apparently emplaced first, probably at or shortly after peak flow. Similarly, deposits progressively closer to valley floors and higher in normally graded valley-bottom deposits have diminished exotic fractions and increased clay fractions. We infer that these parts of the Osceola Mudflow came from falling stages of the flow and were emplaced at successively later times. A schematic hydrograph of a debris flow (fig. 23) shows how incremental deposition of a longitudinally segregated flow could produce normally graded deposits in valley bottoms because aggradation occurs over a significant time during which the flow contains progressively less coarse exotic debris (Vallance and Scott, 1997). At a site near the inundation limit, deposition would occur very rapidly because the inundation limit is only a little higher than remnants of the deposit, and the deposit is ungraded because the flow is at or above this stage only briefly.

Volcano Hazard Assessments and Mount Rainier

Evolution of Volcano Stratigraphic Studies and Hazard Assessments

That volcanoes are hazardous is obvious from their observed eruptions, and those hazards motivated governmental responses at least as long ago as Roman Emperor Titus sending officials to assess the devastation from the 79 C.E. eruption of Vesuvius and to report on the prospects for reestablishing the destroyed cities of Pompeii and Herculaneum. The idea, however, of systematically investigating the geologic record of a quiescent volcano to assess its hazards was pioneered at Mount Rainier by Dwight R. “Rocky” Crandell (1923–2009). Crandell is best known for his studies of volcanic debris flows (lahars), especially of the Osceola Mudflow, and for conceiving, initiating, and supervising the Volcano Hazards Project during his years with the U.S. Geological Survey (USGS) (fig. 24).

Figure 24. Photograph of Dwight R. “Rocky” Crandell examining sediment from a lahar. In the background are the Electron Mudflow (next to Rocky’s hat) and an older lahar below. Photograph by Pat Pringle, Washington State Department of Natural Resources, 1991.

While sitting in a hospital after falling into a crevasse on Mount Rainier, Crandell conceived the groundbreaking idea of using a volcano's stratigraphic record as a guide to its future behavior and hence as a means of assessing its hazards. He had been at work that year (1964) examining the rockfall avalanche of Little Tahoma Peak. In idle time enforced by his leg injury, he began cogitating about the implications of his mapping and stratigraphic studies when he thought, "What if something like that were to happen now?" Eventually he came to the idea that the stratigraphy of Mount Rainier, particularly its Holocene eruptive and lahar record, would not only tell its history of recent volcanism but also indicate the volcano's potential future hazards. This approach is commonplace now, and it is hard to conceive that in 1964 nobody had previously attempted such a systematic approach. Crandell's bright idea was enabled, in part, by the recent development and proven utility (since 1949) of the ^{14}C radiometric dating method and its maturation and promulgation in the 1950s, including establishment in 1953 of a USGS radiocarbon dating laboratory. In 1954, Crandell received some of the first ages from the new USGS laboratory and used these data to date the Osceola Mudflow (Crandell and Waldron, 1956), so he was aware of the potential to quantify the geologic histories of young volcanoes. Crandell proposed his insightful idea to the USGS as a project and initially pursued it at Mount Rainier. Similar studies soon followed at Lassen Peak, Mount St. Helens, and other Cascade Range volcanoes.

Volcanic Hazards at Mount Rainier

Chief among hazards at Mount Rainier are lahars (fig. 25) (Scott and others, 1995; Hoblitt and others, 1998). Most of the many geologic phenomena common to volcanoes could affect the immediate vicinity of Mount Rainier. Such phenomena include lava flows, pyroclastic flows, landslides, ballistic fallout, and debris flows resulting from hydrologic and meteorological events. In the past, such events at Mount Rainier affected areas within current national park boundaries but have extended no farther than about 20 km from the summit. In contrast, tephra falls and voluminous lahars have also been common at Mount Rainier, and these are the volcanic processes that could affect the greatest number of people far from the volcano. Mount Rainier tephra is most commonly dispersed eastward by winds, but more than half of the volcano's tephra falls have not extended over broad areas. Nonetheless, Holocene tephras have been as voluminous as 0.2 km^3 and future such ashfalls could extend far downwind. In distal areas, tephra effects can be quite disruptive but not lethal. In contrast, lahars, though confined to valleys that originate at the volcano, can threaten areas 100 km or more downstream. In terms of their potential threat, lahars from Mount Rainier constitute the greatest volcanic hazard in the Cascade Range.

Field Trip Itinerary and Field Stop Descriptions

Travel Day—Gather Mid-Morning in Portland and Depart for Crystal Mountain

After gathering in the Portland-Vancouver area, our group will travel in vans to the Mount Rainier area. Lodging is typically arranged for the first three nights at an appropriate lodging facility northeast of Mount Rainier, near Greenwater, Washington. Lodging for the last two nights is typically arranged on the south side of Mount Rainier, near Paradise, inside or just outside Mount Rainier National Park.

All field trip stops are indicated by both latitude and longitude and Universal Transverse Mercator (UTM) coordinates. Maps in the field guide show stop locations. Access to stops 2, 6, and 7 of day 1 require permission for access. For stop 2 of day 1, one can obtain permission at the Corliss quarry entry station. Stops 6 and 7 require advance permission, key, and liability waivers for each participant from Hancock Forest Management, North Cascades Region, 317 Camp 1 Road, Orting, WA 98360, or at phone number (253) 271-3136. Ask for the area manager. Large groups may also require permission from Mount Rainier National Park. Groups of more than 12 proposing to hike together in Mount Rainier National Park need to make special arrangements and may need permits from the National Park Service.

Day 1 will focus on lahars in the White River valley. We will drive to Enumclaw, Washington, to begin the day then work our way back upvalley toward Mount Rainier. Day 2 concentrates on geology of the Sunrise-Glacier Basin area within Mount Rainier National Park. As part of day 2 activities, we will hike about 10 miles from Sunrise to the top of Burroughs Mountain, down into Glacier Basin, and be picked up at White River Campground. On day 3 we will pack up and move to Paradise, stopping to examine geology along Stevens Canyon Road. We will hike from Paradise along the Golden Gate Trail and eventually eastward to the former Paradise Ice Caves area (the ice caves have melted out). Day 4 involves hiking from Comet Falls trailhead to Mildred Point and return (~7 miles; 11 km), examining geology along the way. During the first half of day 5, we will visit sites on the south side of Mount Rainier to study lahar deposits, then return to the tour origin.

Day 1. White River Traverse: Holocene Lahars, Especially Osceola Mudflow

Stop 1, Enumclaw (47°11.958' N., 121°58.45' W.; UTM 10T, 5227822N, 577699E)

Stop at the east end of Enumclaw at the Forest Service office near milepost 25 of State Route (SR) 410. The Forest Service office is on the south side of the highway.

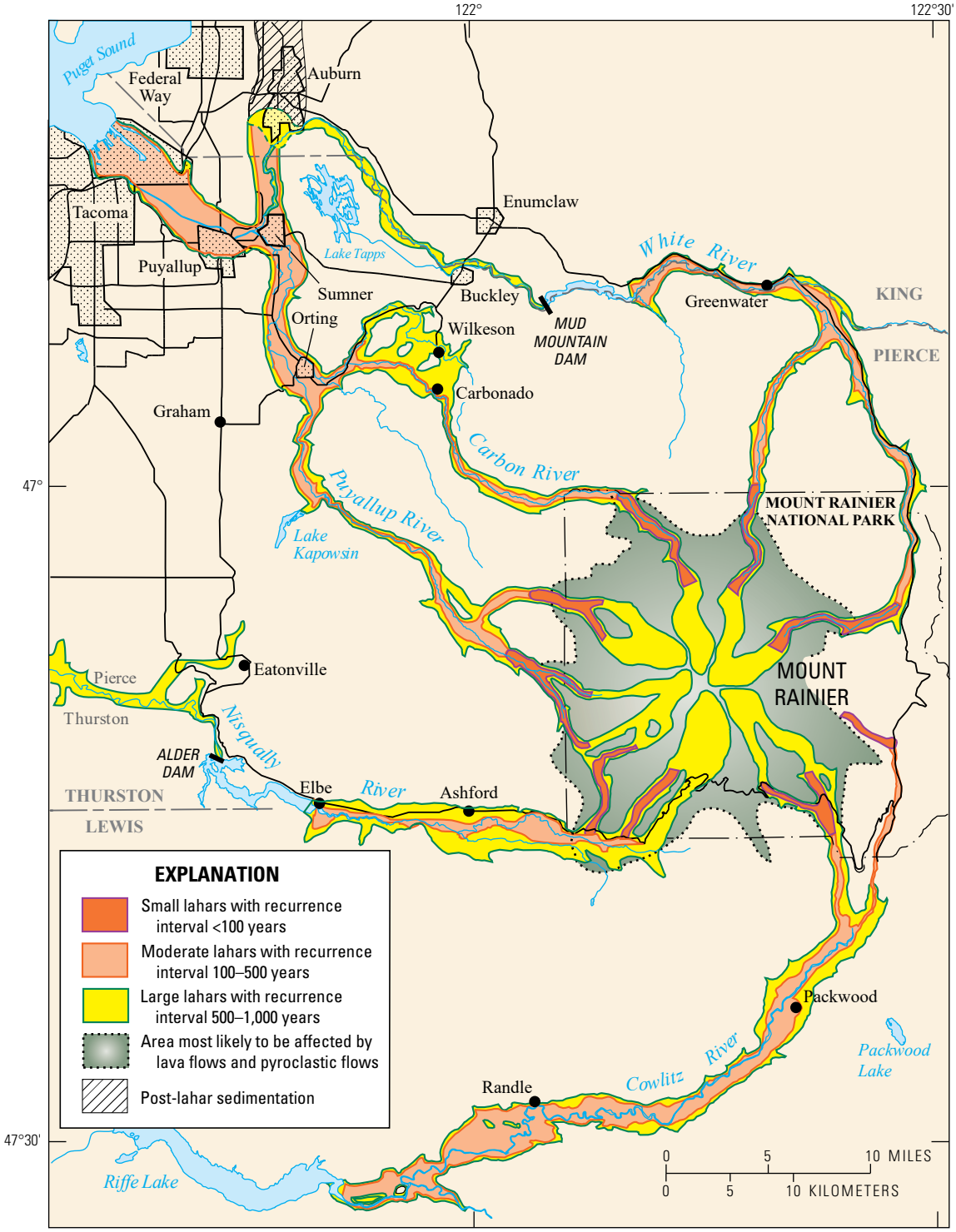

Figure 25. Map showing hazard zones for lahars, lava flows, and pyroclastic flows from Mount Rainier. Small, moderate, and large refer to hazardous events of decreasing volume and increasing frequency. The affected zone for large lahars is generalized from geologic events with recurrence intervals of 500–1,000 years, that typically were sufficiently voluminous to reach the Puget Lowland, and that commonly reached Puget Sound along at least one drainage; the zone for moderate lahars is based on events with recurrence intervals of 100–500 years, that were sufficiently voluminous to reach beyond the foot of the volcano, and that in some cases reached the Puget Lowland; the zone for small lahars depicts events that recurred at intervals of 1–100 years and that are restricted to the immediate area of the volcano. Nearly all moderate and large lahars in the geologic record can be shown to have been during periods of volcanic unrest, whereas small historical events were associated with high rainfall or high degrees of melting of snow and ice. Dotted pattern shows urban areas. Modified from Hoblitt and others (1998).

Water-well logs show that the flat surfaces of Enumclaw and Buckley (fig. 26) are underlain by as much as 20 m of Osceola Mudflow, which in turn overlies Vashon age glacial drift. The Osceola Mudflow, a clay-rich lahar derived from edifice collapse of Mount Rainier's hydrothermal system 5,600 cal. yr B.P., thins gradually to the west and northwest, and glacial features increasingly poke through the lahar deposit as it thins. After spreading across the drift plain, the Osceola Mudflow funneled into several channels (South Prairie Creek, Fennel Creek, and Green River), crossed deltas, then entered deep water (>60 m) of what used to be the Duwamish and Puyallup arms of Puget Sound (these are both now completely filled with sediment) (fig. 22). The lahar flowed as far as 20 km underwater to the present sites of the Port of Tacoma and the Port of Seattle.

The adjacent foothills to the east are mostly Tertiary volcanic rocks, with small uplifts exposing the underlying Eocene sandstones and shales of the Puget Group (Schuster, 2005). Several meltwater channels formed in this bedrock when the Vashon glacier banked up against the Cascade Range foothills, forcing water to erode through now abandoned channels. The 100–150 m deep Osceola Mudflow flowed into and through several of the meltwater channels as it descended from the confines of the White River valley to the Vashon drift plain of the Puget Lowland.

Stop 2, Corliss Quarry (47°11.784′ N., 121°56.550′ W.; UTM 10T, 5227532N, 580101E) (optional stop; depends on present state of quarrying)

Drive east 1.4 miles along SR 410 and turn left into Corliss quarry. Drive quarry roads to the upper southeast corner of the quarry. This is an active quarry so cautious navigation is important. Quarry managers at the entry station can give advice concerning the best route to the outcrop, which may eventually be quarried out.

The Corliss quarry produces sand from fluvial gravels and glacial kame terraces that banked along the west side of the Cascades Range during late Pleistocene Vashon glaciation that covered the Puget Lowland (John and others, 2003). The Osceola Mudflow is exposed locally in the quarry as a 4- to 5-m-thick deposit overlying the fluvial-glacial deposits (fig. 27). In this stop, we will compare characteristics of the Osceola Mudflow exposed here to those exposed elsewhere upvalley (especially at stops 4, 5, and 9).

The Osceola Mudflow deposit in the Corliss quarry consists mostly of rounded cobbles and small boulders as much as about 50 cm across. Quaternary andesites from Mount Rainier are the most common clasts, but rounded alluvium, Tertiary andesites, welded tuffs and granites also are common. The ratio of rocks from Quaternary Mount Rainier to older rocks is much lower here than the average at the Greenwater (stop 5) locality, an indication of bulking of the mudflow by erosion and incorporation of surface materials that it passed over. Hydrothermally altered clasts are much less common than at sites upstream or lower in valley bottoms (as at the Greenwater stop 5), probably indicating both dilution by incorporation of surface materials (bulking) and mechanical abrasion of the softer, hydrothermally altered rocks during transport. The Osceola Mudflow here also contains small trees and tree branches that were incorporated during flow (fig. 27).

The matrix of the Osceola Mudflow in the Corliss quarry is gray, sandy, and noticeably richer in clay than the underlying fluvial and glacial deposits, but it is much poorer in clay than the matrix of the Osceola Mudflow at Greenwater, closer to the volcano (stop 5). A 1- to 2-cm-thick, Fe-rich hardpan, present locally at the base of the Osceola Mudflow deposit, forms when reduced fluids from the lahar react with oxygen in pores of the underlying deposits, precipitating water-insoluble ferric iron.

Stop 3, Mud Mountain Dam (47°8.670′ N., 121°55.884′ W.; UTM 10T, 5221776N, 581021E)

From Corliss quarry, drive east 3.2 miles (5.1 km) to the junction of SR 410 and Southeast Mud Mountain Road (at 0.7 miles [1.1 km], past mile post 29, there is a large sign at the intersection for the Mud Mountain Dam Recreation Area), turn right, drive 2.2 miles (3.5 km) on the access road and then 0.1 miles (160 m) left to the dam viewpoint. A trail winds down to the lower viewpoint (20-minute round-trip walk); however, the upper viewpoint is impressive.

A landslide in 1996 exposed glacial deposits beneath several meters of the Osceola Mudflow deposit on the valley wall to the north. Behind the outcrop is the fairly flat surface of the Osceola Mudflow, draped over thick Vashon deposits and dotted sparsely with bus- to house-size hummocks.

The path of the Osceola Mudflow as it cascaded across the Puget Lowland east of Enumclaw must have been spectacular. When the mudflow encountered the narrow gorge of the White River at Mud Mountain that is only 300 m wide, it spread out over terraces formed of glaciofluvial and till deposits of Vashon age that are up to 110 m above the White River. Although we are about 110 m above the river here, the Osceola Mudflow was deeper in this area, with its peak-flow surface as much as 40 m higher than this site. As the lahar continued westward, it poured over terrace scarps to form a spectacular pair of falls. The upper fall would have formed an arc more than 6 km wide and more than 80 m high, and the second would have been more than 3 km wide and more than 110 m high.

Mud Mountain Dam was built by the U.S. Army Corps of Engineers solely for flood control in the lower White River basin. The earth-fill embankment dam was constructed between 1939 and 1942, and its floodgates were constructed in 1948.

Stop 4, Slippery Creek near Osceola Mudflow Inundation Limit (47°10.554′ N., 121°39.978′ W.; UTM 10T, 5225574N, 601061E)

From the Mud Mountain junction, drive east 12.6 miles (20.3 km) on SR 410 and turn left at Slippery Creek. Drive straight up the dirt road 1.2 miles (1.9 km), avoiding spur roads

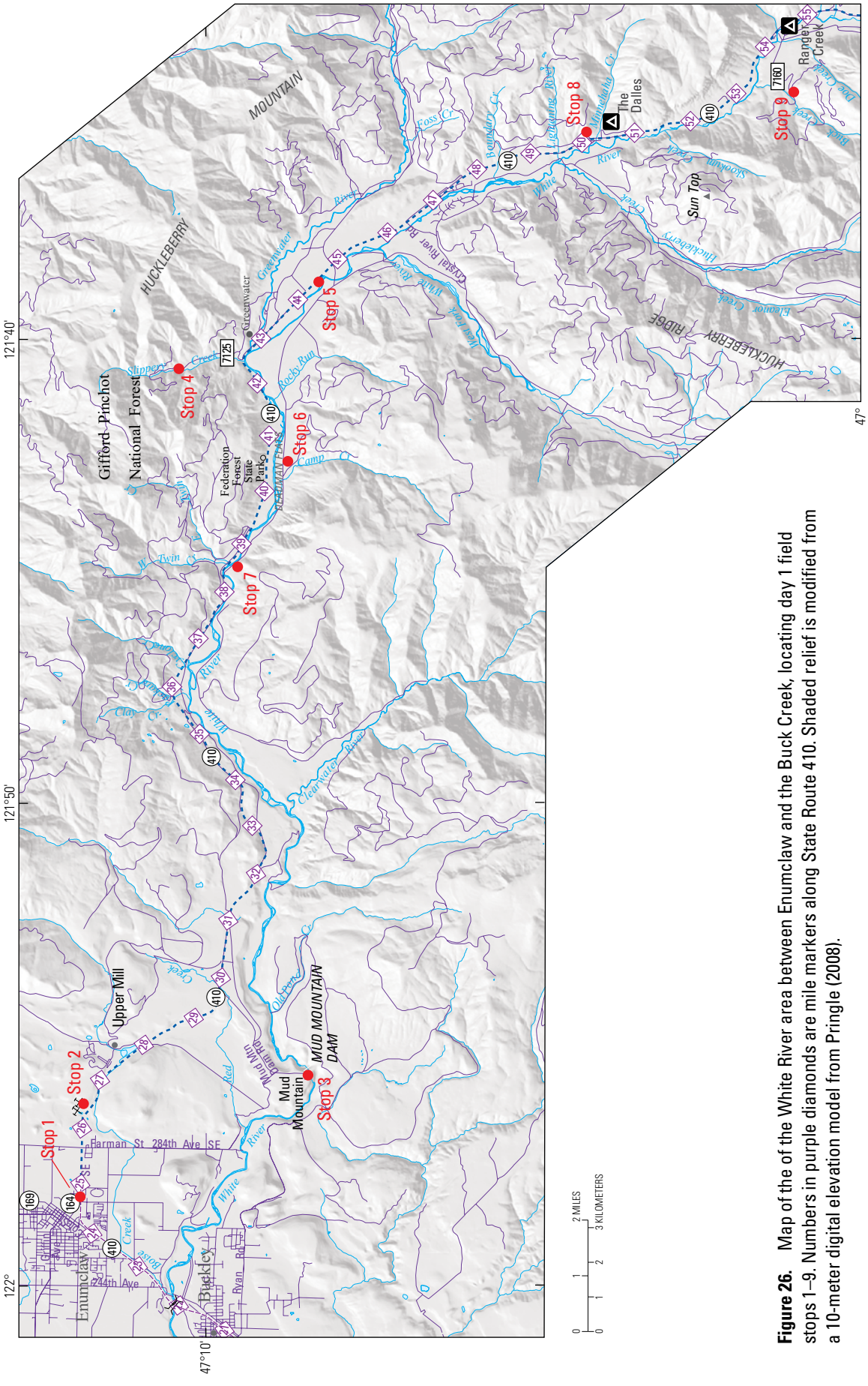

Figure 26. Map of the of the White River area between Enumclaw and the Buck Creek, locating day 1 field stops 1–9. Numbers in purple diamonds are mile markers along State Route 410. Shaded relief is modified from a 10-meter digital elevation model from Pringle (2008).

Figure 27. Photograph of Osceola Mudflow deposits at Corliss quarry (day 1, stop 2). The Osceola Mudlfow deposit, 2.5–3 meters thick, overlies terrace gravels deposited here by the Puget lobe of the Cordilleran ice sheet during Vashon time. Note pack in foreground for scale. Age of Osceola Mudflow given in calendar years before present (cal. yr B.P.). Photograph by David John, U.S. Geological Survey.

to the right or left. The outcrop will be on the right. It may be revegetated and require some searching around and digging.

The valley-side veneer facies of the Osceola Mudflow is exposed here near its inundation limit about 90 m above the valley bottom (Vallance and Scott, 1997). The outcrop exposes soil atop 20–30 cm thick Osceola Mudflow, which overlies paleosol and hillslope talus. Locally, the Mazama ash (7,600 cal. yr B.P.) is visible beneath the Osceola Mudflow as discontinuous orange-brown patches of fine ash. Valley-side veneer deposits are rarely more than a meter thick and are commonly so thin that the deposit can only be recognized by out-of-place gravels in the section between the surface soil and paleosol beneath—these commonly appear as one soil. Gravels comprise Mount Rainier andesites, some of which are hydrothermally altered, and exotic particles. Exotic gravels include Tertiary volcanic rocks, Tertiary intrusive rocks, and rounded alluvial clasts. Especially obvious in even the poorest valley-side-veneer-facies outcrops (>90 percent of them are nondescript zones in the soil) are stream-rounded gravel clasts. There is no local source of such particles on these hillsides, and the rounded particles can only derive from the river bottom and its terraces more than 70 m below this position in the valley. Vallance and Scott (1997) concluded that such exotic grains must have been incorporated through erosion (bulked) by the lahar as it passed over unconsolidated valley-floor sediments.

The sedimentology of the deposit represents the character of the lahar at peak inundation. The thin deposit is massive and ungraded. Relative to Osceola Mudflow deposits lower on valley sides or in valley bottoms (axial facies), this deposit contains greater proportions of exotic particles, greater proportions of sand in its matrix, and smaller proportions of clay in its matrix.

Stop 5, SR 410 (47°8.034′ N., 121°37.357′ W.; UTM 10T, 5220964N, 604454E)

From Slippery Creek, drive east on SR 410 past Greenwater to 0.5–0.6 miles (0.8–1.0 km) past mile post 44 and pull off on the right (there is not much room along the edge of the highway, so be cautious). Access the outcrop using a fisherman's path to the bank of the White River and then walk downstream less than 0.1 mile (160 m).

Many features of the Osceola Mudflow are exposed in outcrop along the right (northeast) bank of the White River near Greenwater. Note that, whereas axial facies deposits like this range from a few meters to 20 m thick, the Osceola Mudflow filled the valley in this area to the much greater depth of 90–100 m. Erosion by the White River has exposed 8 m of Osceola Mudflow deposits at this location (fig. 28). Underlying the Osceola Mudflow are runout facies of clay-poor lahars derived from the Cowlitz Park eruptive episode of Mount Rainier, dated between 7,200 and

Figure 28. Photograph of Osceola Mudflow deposit along the White River near Greenwater (day 1, stop 5). The deposit is 8 meters thick and overlies 50–60-centimeter-thick lahar deposits of the Cowlitz Park eruptive period and older alluvial gravel. One can observe normal grading in the gravel fraction of the Osceola Mudflow deposit. Ages given in calendar years before present (cal. yr B.P.). Photograph by David John, U.S. Geological Survey.

6,800 cal. yr B.P., and rusty brown, cobble-boulder alluvium. Just downstream, but not accessible or visible from here, lahars younger than 2,500 cal. yr B.P. unconformably overlie the Osceola Mudflow deposit. These younger deposits may be accessed with permission of the landowner.

The exposure here provides excellent views of the sedimentologic characteristics of a clay-rich lahar deposit. The outcrop is normally graded, not only with respect to the coarse gravel-size fraction, but also with respect to the fraction of sand within the matrix (sand versus sand+silt+clay) (fig. 29). Conversely, clay (chiefly of hydrothermal origin in the pre-collapse edifice) and other particles affected by hydrothermal alteration increase upsection within the outcrop.

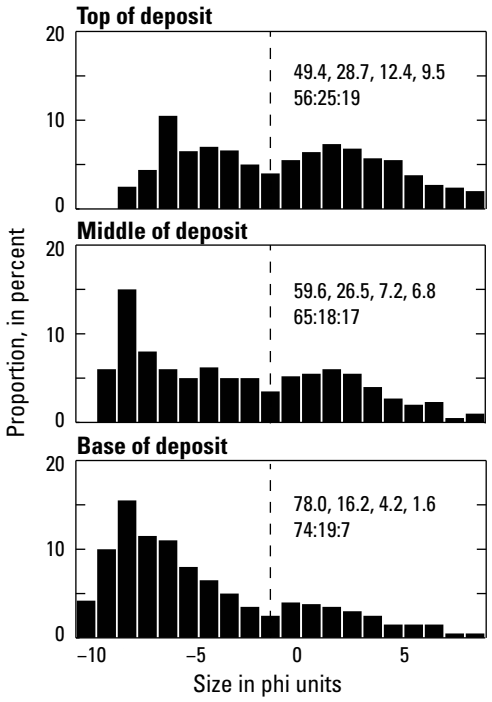

Figure 29. Plots of grain size distribution of the Osceola Mudflow at the Greenwater site (day 1, stop 5), located 50 kilometers downstream from Mount Rainier. The deposit is 8 meters thick here. Dashed line indicates phi size –1 to –2 or granules. Upper groups of numbers are relative proportions of gravel, sand, silt, and clay. The lower groups of numbers are the proportions of sand, silt, and clay in the matrix (sand+silt+clay). The increase in gravel fraction (first of the upper quartet of numbers at the top of each plot) downsection and the increase in clay (last of the quartet of numbers) upsection indicate increased bulking of gravel downsection. Also note that the proportion of matrix sand (the first of the lower trio of numbers at the top of each plot) increases from top to bottom (56 to 65 to 74 percent) and suggests increased bulking of the sand fraction downsection. The lack of grains in granule size fraction (dashed line) is an indication of bulking of alluvium because alluvium contains gravel and sand but lacks granules and because the Osceola Mudflow deposits farthest upstream do not lack granules. Modified from Vallance and Scott (1997).

Osceola Mudflow deposits show a progressive downstream improvement in sorting, increase in sand and gravel, and decrease in clay. These downstream progressions were caused by incorporation (bulking) of well-sorted gravel and sand. Normally graded axial deposits, like those in this outcrop, show similar trends from top to bottom because of bulking (fig. 30). The coarse-grained basal deposits in valley bottoms are similar to deposits near inundation limits. Normal grading in deposits is best explained by incremental aggradation of a flow wave, which is coarser grained and contains more exotic particles at its front than at its tail (fig. 23).

A wide variety of hydrothermally altered rocks and hydrothermal minerals from Mount Rainier are present as clasts and matrix in the mudflow here (John and others, 2003). The larger clasts, as large as 1 m in width, are mostly fresh or weakly altered to a smectite-pyrite assemblage. More strongly altered clasts, notably advanced argillic assemblages (kaolinite+pyrite+opal± alunite), tend to form much smaller, well-rounded clasts. Much of the mudflow matrix here is clay rich. The clay size fraction of the matrix contains smectite, kaolinite, alunite, hydrothermal quartz, and minor pyrophyllite. Unoxidized parts of the clay matrix are dark gray owing to the presence of abundant fine-grained pyrite.

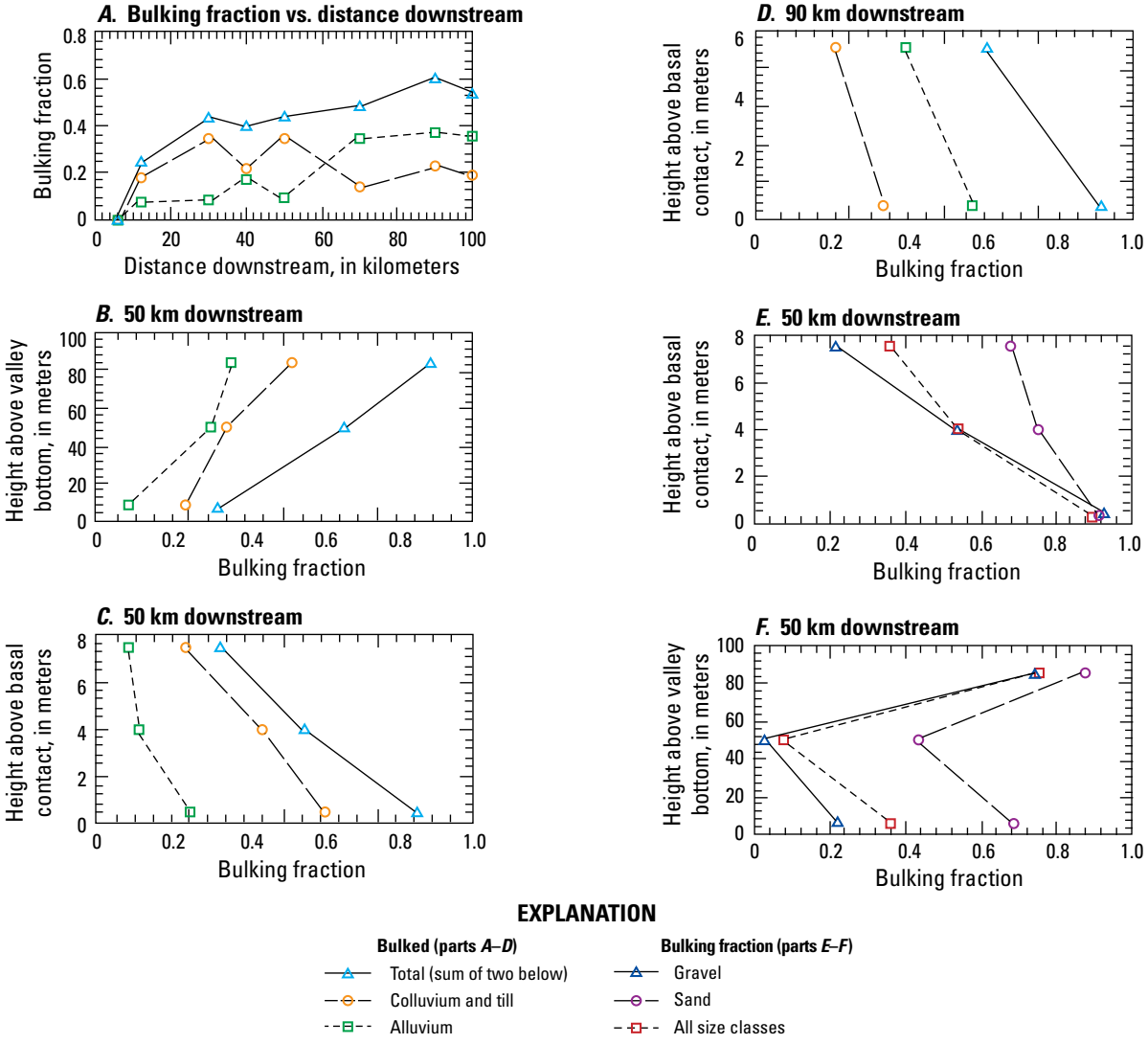

Figure 30. Plots of bulking fraction (proportion of exotic particles incorporated by erosion) in the 16–32 millimeter size class of the Osceola Mudflow deposit versus (vs.) distance downstream from lahar source (*A*); position of deposit in White River valley, 50 kilometers (km) downstream from source (*B*); position in 8-meter (m)-thick valley-bottom deposit along White River, 50 km downstream from source (shown in fig. 28) (*C*); and position in 6-m-thick deposit, 90 km downstream from source (*D*); and two plots of calculated bulking fractions 50 km downstream from source versus position in valley (*E*) and position in same 8-m-thick valley-bottom deposit (*F*). Note that bulking fraction can visually be assessed separately for angular gravels (colluvium and till) and rounded gravels (alluvium). Calculations of total bulking fraction, bulking fraction of gravel, and bulking fraction of sand are done by comparison to clay fraction, which is assumed not to be available for incorporation through erosion (see Vallance and Scott, 1997, for details). Bulking fraction increases systematically toward the inundation limit, downsection in individual valley-fill outcrop, and with distance downstream. Sites designated 50 km downstream are from outcrops at stops 4 and 5. Modified from Vallance and Scott (1997).

Stop 6, Osceola Mudflow Hummocks, Greenwater Area along Tree Farm Road (47°8.974′ N., 121°40.311′ W.; UTM 10T, 5222641N, 600690E)

Note that advanced permission and a key are required to access private timberland for stops 6 and 7. Turn right off SR 410 at mile 44.8; turn right on private timber road at 0.4 miles (0.6 km), then left at 2.5 miles (4.0 km).

On the south (left) side of the private road is a patch of clear-cut land exposing about a dozen mounds, or hummocks (fig. 31). The surface here is underlain by deposits of the Osceola Mudflow, which flowed through this part of the White River valley at a width of ~3 km and maximum depth of 100 m (Scott and Vallance, 1995; Vallance and Scott, 1997). Most hummocks of the Osceola Mudflow consist of car- to house-sized pieces of the volcanic edifice that survived collapse and transport but became stranded and deposited along the margins of the flow as it waned (Scott and others, 1995; Vallance and Scott, 1997). A hummock core is exposed ~0.1 mile (~160 m) to the left (upstream). It consists of fractured Mount Rainier andesite.

Stop 7, Twin Creeks Lahar in Quarry off Tree Farm Road, Opposite Deadman Flat (47°9.665′ N., 121°44.553′ W.; UTM 10T, 5223832N, 595310E)

Turn right off SR 410 at mile 44.8; turn right on private timber road at 0.4 mile (0.6 km), then left at 6.0 miles (9.7 km) from SR 410 and continue 0.2 miles (0.3 km) to quarry. From stop 6, the entry to this site is 3.5 miles (5.6 km) west along private forest road.

As of August 2016, the walls of this active quarry formed a large (30 m diameter) horseshoe-shaped exposure made up entirely of a single lahar deposit, locally at least 3 m thick. The White River flows 300 m to the north and 13 m below, meandering around the deposit site. The stop is 4.3 miles (7 km) downstream from the town of Greenwater and 50 km from the summit of Mount Rainier, as measured down the main-stem White River.

The exposure provides excellent views of clay-poor lahar deposits. In grain size and sedimentary structures, the deposits closely resemble those of the lahar floodplain facies described

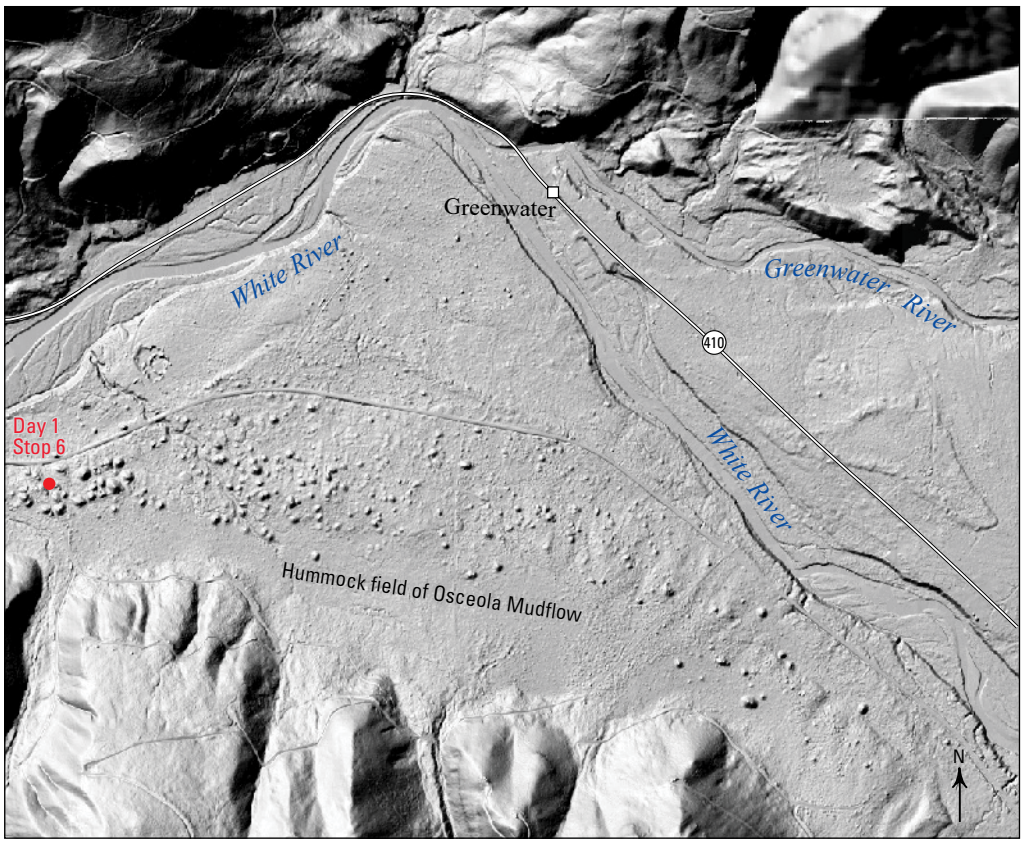

Figure 31. Light detection and ranging (lidar) digital elevation model image of the White River valley and the terrace south of the White River near Greenwater showing the hummocky topography of the surface of the Osceola Mudflow (day 1, stop 6). Individual hummocks are as large as 50 meters (160 feet) across and 15 meters (50 feet) high. Hummocks are mostly composed of shattered fragments of lava or breccia from Mount Rainier's old edifice. They were deposited here after the more fluid part of the flow drained downstream and left them stranded here.

by Scott (1988) for modern lahars in the Toutle-Cowlitz River system of Mount St. Helens. Overall, the portion of the deposit in view is normally graded and composed of sand- and pebble-sized material. The upper meter of the exposure contains more pumice lapilli (layer C) than does the rest of the section.

Especially striking are dish and pillar structures. These form chains of concave-upward silt partings commonly broken from one another at their ends (fig. 32). The partings themselves are millimeters thick and are spaced tens of centimeters apart vertically. Although typically associated with subaqueous sediment gravity flows, these structures also occur in hyperconcentrated-flow deposits (Scott and others, 1995). They apparently begin to form soon after deposition as water is expelled upward out of the deposit. Continued translocation of clay and silt enhances the structures (Scott and others, 1995).

Charcoal collected from within the deposit gave ages of 1,520–1,350 and 1,610–1,410 cal. yr B.P. (Zehfuss and others, 2003). The dates are similar to that of a lahar deposit near the confluence of the White River with Buck Creek (1,560–1,320 cal. yr B.P.). The ages are also similar to those of logs in fluvial deposits near Kent (1,560–1,320 cal. yr B.P.; Pringle, 2000). Eruptive products that correlate with this lahar episode (Twin Creeks eruptive episode) have been identified on Mount Rainier volcano itself as two thin SVG tephras.

Stop 8, Young Lahars at The Dalles Campground (47°4.217′ N., 121°34.725′ W.; UTM 10T, 5213955N, 607909E).

Turn right off SR 410 at the road sign for The Dalles Campground (mile 50.3) then turn right again and park near campsite 44. Walk down to river level beyond fencing (fig. 26).

Lahar runout deposits crop out along the eroded right bank of the White River. The deposits appear to be less than 530 years old, as tephra layer Wn (1479 C.E.) is not present in poorly developed soils at the top of the section. We do not know whether these deposits were caused by eruptive activity or some other event, such as torrential rain or a glacial outburst flood. These deposits are typical of lahars that have undergone transition to hyperconcentration. Lahar transitions develop by overrunning and pushing river or stream water ahead of them, becoming progressively diluted (water rich) through mixing as they advance downstream. Once the flows become sufficiently dilute, coarse cobbles and boulders lag behind and are confined to channel thalwegs; hence, marginal flood-plain facies like these may lack coarse pebbles, cobbles, and boulders. Deposits from such flows may be massive or low-angle crossbedded. Sorting is characteristically intermediate between that of debris-flow deposits and fluvial deposits.

Eruption-generated lahars of the past 2,500 years and the upper part of the Osceola Mudflow crop out at campsites 37, 39, and 41 downstream.

Figure 32. Photograph illustrating dish structure in a hyperconcentrated-flow deposit (day 1, stop 7). Dish structure develops as a result of escaping fluid during compaction after deposition. Photograph by Jim Vallance, U.S. Geological Survey.

Stop 9, Osceola Mudflow Inundation Limit at Buck Creek (optional stop; 47°1.165′ N., 121°33.473′ W.; UTM 10T, 5208331N, 609597E)

Continue southeast on SR 410 and at mile 54.3 turn right on Forest Service Road 7160. Proceed 1.6 miles (2.6 km) along the winding road (hairpin turn is at 1.2 miles [1.9 km]) and park where a spur road runs off to right (fig. 26). The outcrop is the roadcut to the left. Scramble upslope about 10 m to near the top of the outcrop.

This is the inundation limit of the Osceola Mudflow where it drapes the Evans Creek age (last glacial maximum) lateral moraine. About 20–40 cm of Osceola Mudflow is interbedded among soils and tephra layers from three volcanoes. From outcrop top downward, the sequence is:

- 5 cm soil,
- 2 cm light-brown medium pumiceous ash from Mount St. Helens (Wn) erupted in 1479 C.E.,
- Soil,
- 5 cm brown lapilli pumice erupted from Mount Rainier, 2,300 cal. yr B.P.,
- Soil and duff,
- 3–5 cm yellow-brown, coarse pumiceous ash erupted from Mount St. Helens (Yn), 3,700 cal. yr B.P.,
- Soil and duff,
- 20–40 cm Osceola Mudflow,
- Soil and duff,

- 2 cm orange-brown Mazama ash, erupted 7,600 cal. yr B.P.,
- Soil and duff containing scattered, soft brown pumice lapilli from Mount Rainier (R), 10,050 cal. yr B.P., and
- 10 m glacial drift of the last glacial maximum (Evans Creek age).

Stop 10, White River at Fryingpan Creek Confluence (46°53.494′ N., 121°35.861′ W.; UTM 10T, 5194069N, 606827E)

Take SR 410 to Mount Rainier National Park (mile 57.6) and continue for 4.6 more miles (7.4 km) to White River entrance road (at mile 62.2). Proceed past the entrance station at mile 1.3 to a car park at mile 3.6. Walk 100 m down the private road on the right (fig. 33). Be careful here, as the White River has severely undercut the ~15-m lahar terrace you are overlooking! It is usually possible to scramble down to river level to the left.

A series of seven lahar deposits vary in age; from youngest to oldest, they are: ~1,000 cal. yr B.P. (Fryingpan Creek episode), ~1,500 cal. yr B.P. (Twin Creeks episode), and five in the interval from 2,600 to 2,200 cal. yr B.P. (Summerland period). These lahars unconformably overlie the Osceola Mudflow at this site. The upper four lahars are easily visible from the top of the terrace (figs. 34 and 35). All seven lahars were generated by hot rock and ice interaction during eruptions at or near the summit of Mount Rainier. At least four of them moved as far as 100 km from Mount Rainier along the White River valley to Auburn in the Puget Lowland.

Depending on the position of the braided river, it may be possible to traverse downstream to a terrace remnant about 40 m high (46°53.533’ N., 121°35.783’ W.; UTM 10T, 5194143N, 606925E). This higher terrace is chiefly formed of post-Osceola (5,600–4,500 cal. yr B.P.) alluvium and lahars and is bounded to the south by an abandoned river channel. The deposits were mostly emplaced during post-Osceola aggradation, which was followed by a period of channel readjustment and incision that was probably complete by the end of Osceola time. The youngest deposit of the upstream sequence, a Fryingpan Creek age lahar, drapes the terrace remnant unconformably; older deposits from the previous outcrop are not present in this section.

Stop 11, Inundation Limit of Fryingpan Creek Lahar (1,000 cal. yr B.P.) (46°53.172′ N., 121°36.710′ W.; UTM 10T, 5193453N, 605759E)

Drive White River Road to the Fryingpan Creek trailhead (at mile 4.2 [km 6.8] from the White River junction and 0.6 miles [1.0 km] from stop 10). Walk along the trail, past the Wonderland Trail junction about a quarter of a mile, then drop down to the left (east) following a faint path onto a low terrace, cross it, and scramble down to Fryingpan Creek flood plain (46°53.172’ N., 121°36.710’ W.).

Streamcuts in the 4-m terrace expose the ~1,000 cal. yr B.P. Fryingpan Creek lahar where it flowed upstream from the White River at its inundation limit. The lahar deposit is overlain by soil with interbedded coarse pumiceous ash of Mount St. Helens layer Wn (1479 C.E.) and underlain by alluvium. The lahar deposit pinches out about 30 m upstream. The lahar chiefly contains fresh Mount Rainier andesite clasts and abundant brown pumice lapilli that were incorporated by erosion.

Across Fryingpan Creek, yellowish-brown Osceola Mudflow deposits crop out along higher terraces. One can return to the trail and walk up another quarter mile along it to the south to where scattered hummocks from the Osceola Mudflow, up to 10 m high and 50 m in plan, are visible in the forest on the left. The hummocks were carried up Fryingpan Creek from the White River during peak inundation of the ~100-m-deep Osceola Mudflow, then were stranded as it drained away during its recessional phase. The first of these hummocks was cut in half by floods in 2006. The incised hummock (46°53.046’ N., 121°36.741’ W.; UTM 10T, 5193219N, 605724E) exposes relatively fresh but broken up andesite of Mount Rainier.

Stop 12, Outcrop of Breadcrust Lahar of Cowlitz Park Age (7,500–6,400 cal. yr B.P.) from North Side of White River (optional stop; 46°54.175′ N., 121°37.752′ W.; UTM 10T, 5195287N, 604404E)

Drive along White River Road, cross its bridge across the White River, turn left toward White River Campground (mile 5.3), then go 0.6 miles (1.0 km) up the road toward the campground. Park on the left at a gravel pullout.

Across the White River, at least three Cowlitz Park age lahars crop out, with the Osceola Mudflow upsection but concealed by forest. The lowest of the three contains prismatically jointed blocks and breadcrust blocks whose chemistry is consistent with the chemistry of Cowlitz Park age tephra layer L (7,300–7,200 cal. yr B.P.). This sequence of lahars correlates with the 1-m sequence of lahars at the base of the Osceola Mudflow at the Greenwater site (stop 5). Because of downstream dilution by overrun river water and attenuation, the lahars underwent a facies change from debris flow to hyperconcentrated flow between here and 40 km downstream at the Greenwater site.

Day 2. Sunrise Area, Plus Hike over Burroughs Mountain and through Glacier Basin: Lava-Ice Interaction, Burroughs Mountain Flow, and Holocene Tephras and Lava Flows

This day involves several hours and about 10 miles (15.5 km) of trail hiking from Sunrise (6,400 ft; 1,950 m) on the volcano’s northeast flank, over Burroughs Mountain (7,410 ft; 2,260 m), down to Glacier Basin (5,960 ft; 1,815 m), and out to the White River Campground (4,290 ft; 1,310 m). As presented, the trip involves a car shuttle, but it can be made into a loop by

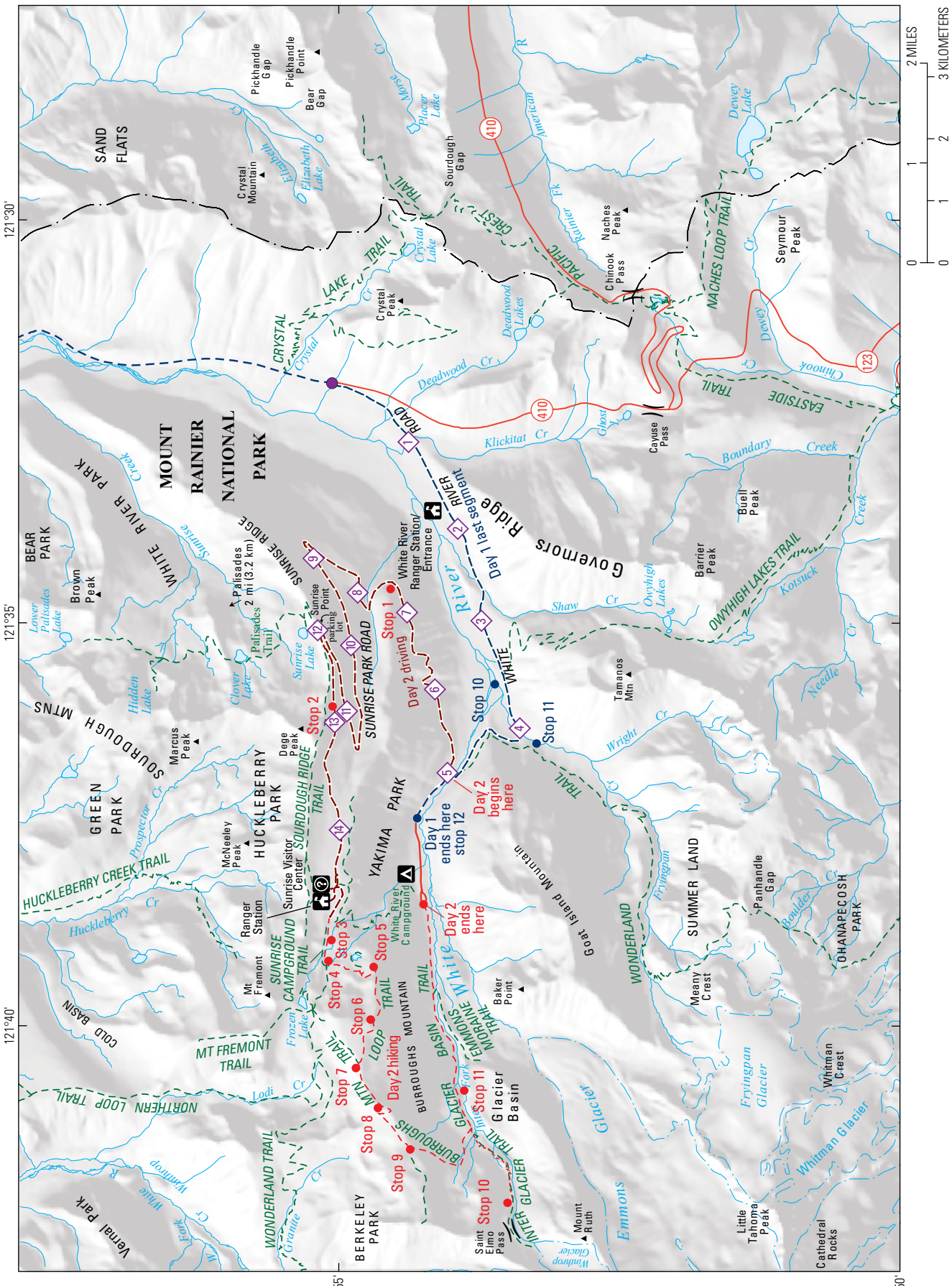

Figure 33. Map of the upper main-stem White River drainage and Sunrise areas showing the last three field stops of day 1 (stops 10–12; blue) and the 11 stops of day 2 (red). Numbers in diamonds indicate road mileages. Modified from Pringle (2008).

Figure 34. Photograph showing the youngest three lahar deposits at stop 10 of day 1 near the confluence of Fryingpan Creek and the main-stem White River. The brown lahar, which is the oldest of these three deposits, contains abundant C tephra throughout, as well as rafts of C tephra at its top; this lahar is the same age as layer C and is apparently the product of the same eruption as layer C. Ages given in calendar years before present (cal. yr B.P.). Photograph by Jim Vallance, U.S. Geological Survey.

Figure 35. Photograph illustrating older lahars in section at the site for day 1, stop 10. These lahars unconformably overlie the Osceola Mudflow and are all products of the Summerland eruptive period. This part of the outcrop, at the confluence of Fryingpan Creek and the White River, is periodically cleaned off when the White River shifts to the base of the scarp and begins undercutting it. At other times the lower part of the outcrop is covered with talus. Mount St. Helens is abbreviated MSH. Photograph by Jim Vallance, U.S. Geological Survey.

adding a short (2.5 mile; 4 km) but stiff climb (2,110 ft; 640 m) back to Sunrise from the White River Campground via the Wonderland Trail. The first half of the hike is at and above tree line and can be windy even if the weather is clear, so carry appropriate clothing, food, and water. The area between Sunrise and Burroughs Mountain is heavily visited, so please stay on the trails. The top of Burroughs Mountain is also featureless, so if visibility is poor, it's especially important to keep to the trail, and remember, no sampling without a permit from the National Park Service. In the summer months, Sunrise hosts a National Park Service visitor's center and restrooms, but check ahead for hours of operation.

This hike traverses part of the oldest large-volume flank lava flow of the modern edifice (the andesite of Burroughs Mountain, 506 ka) and provides views of the underlying fragmental deposits that support Steamboat Prow, as well as views of the massive upper Emmons and Winthrop Glaciers, which conceal the young summit cone that fills the Osceola collapse amphitheater. On a clear day this is one of the most spectacular easy trail hikes in the park. Consult the day 2 geologic map (fig. 36) for a summary of the geology.

The day begins on the National Park Service road to Sunrise off SR 410. From the White River entrance station

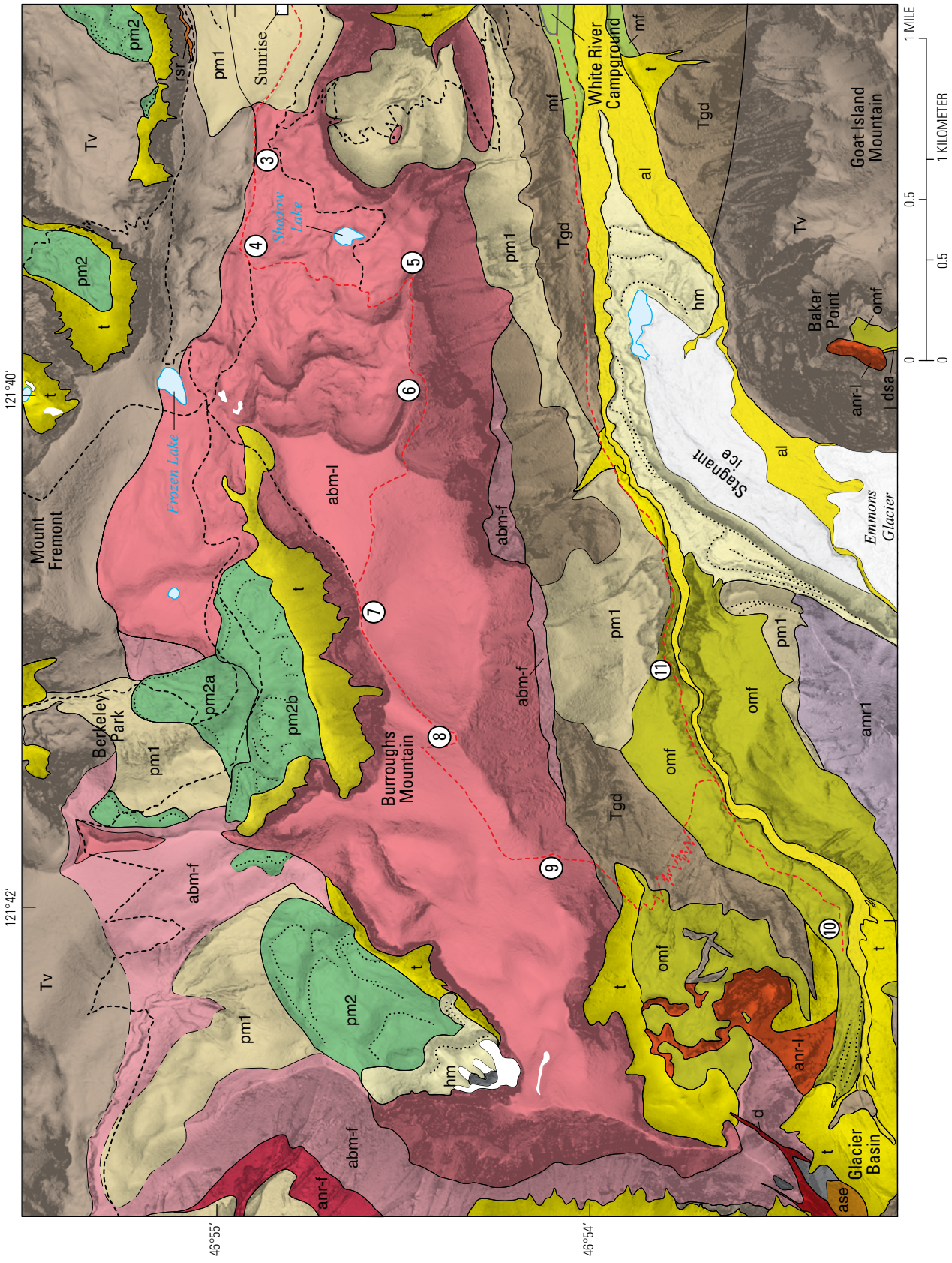

(46°54.139' N., 121°33.210' W.; UTM 10T, 5195324N, 610170E), the road continues along the south side of the White River through Quaternary cover and scattered small outcrops of Miocene plutonic rocks, crossing the bridge over Fryingpan Creek, and then over the White River. If making the trip with two cars, turn left toward the White River Campground to leave a car at the hiker's parking lot, then return in the other car to drive up the road to Sunrise. The road now climbs the hillside on the north side of the river, first in Miocene plutonic rocks (U-Pb zircon age of 14 Ma; Mattinson, 1977), then in till and slope wash. Eventually a 1.5-m-thick band of yellowish-white pumice appears on the left side of the road near the top of the till exposures (46°54.210' N., 121°35.455' W.; UTM 10T, 5195404N, 607319E; 1.65 miles from junction with White River Campground road). This is the 85-ka dacite pumice of Sunset Amphitheater that can be seen as a prominent white band crossing Sunset Amphitheater headwall on the volcano's upper west face (Sisson and others, 2019). The correlation with Sunset Amphitheater tephra is made on the basis of whole rock, glass, and Fe-Ti oxide compositions, as well as an identical phenocryst assemblage. Because of traffic hazards, it is inadvisable for large groups to stop here and examine the pumice.

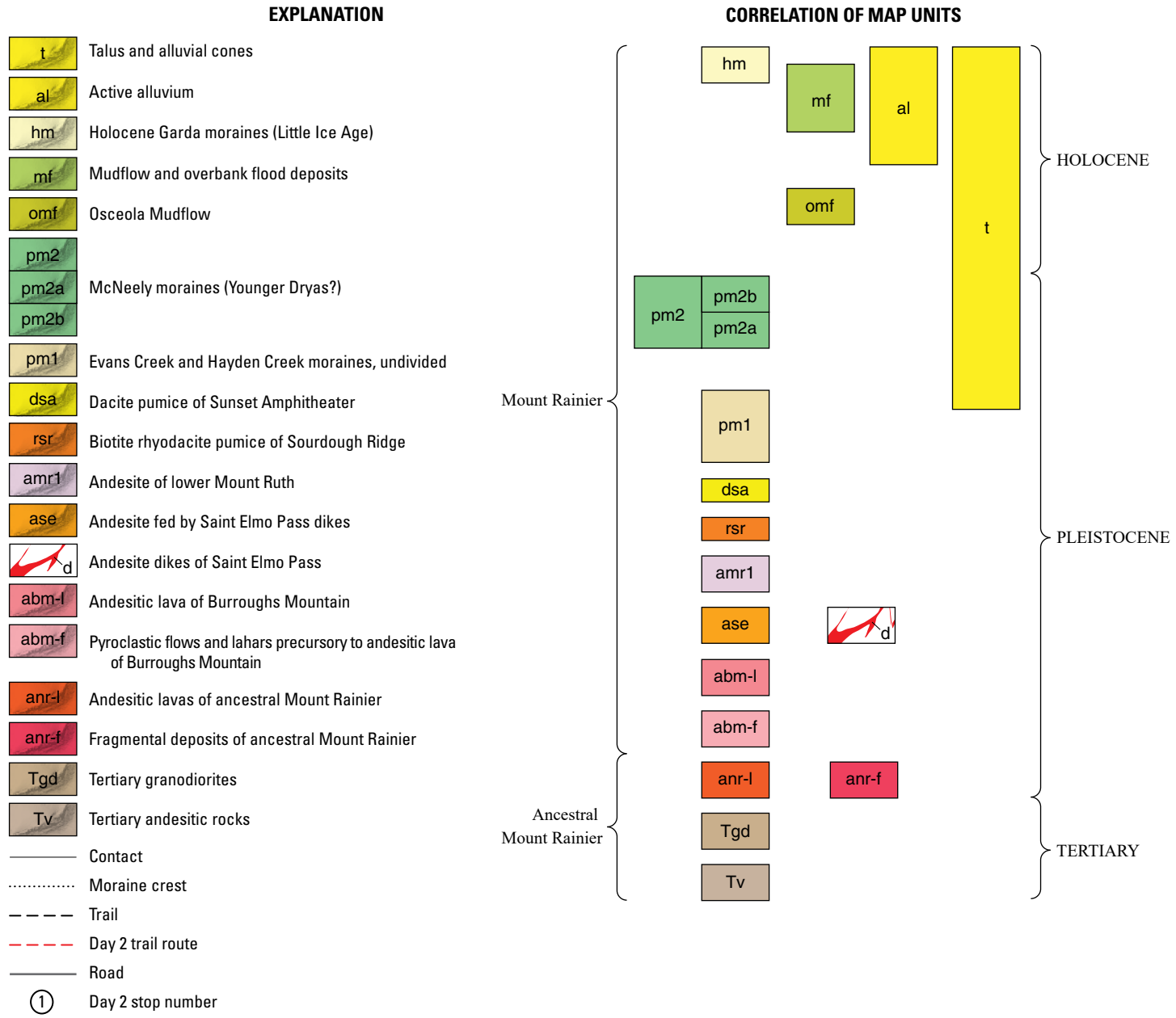

Figure 36. Geologic map of the area around Sunrise, Burroughs Mountain, and Glacier Basin showing day 2 stops 3–11. Geologic mapping by T.W. Sisson and from Stockstill and others (2002). Base topography is a slope map (darker is steeper) created from the light detection and ranging (lidar) digital topography of the Mount Rainier area of Robinson and others (2010).

Outcrops of jointed gray andesite appear on the uphill side of the road (46°54.337' N., 121°34.853' W.; UTM 10T, 5195654N, 608078E), developing columns that assume a horizontal orientation as the road bends to the left. This is the nose of the andesite of Burroughs Mountain (506 ka), which is the first voluminous lava flow from modern Mount Rainier.

Stop 1, Lava-Ice Contact Surface (46°54.452' N., 121°34.666' W.; UTM 10T, 5195870N, 608312E)

Drive Sunrise Park Road toward Sunrise Visitor Center. At 2.4 miles (3.9 km) from the turnoff to White River Campground, the road bends to the left, and a pullout is located on the right just as the road reenters the forest. Park here in the pullout. Just across the road from the pullout is a lava outcrop with a small overhang defined by horizontal columns. A National Park Service display at the pullout illustrates the origin of the horizontal columns and the position of the lava flow high above the canyon floor. Such columns result from contraction during cooling of the lava and point in the direction of heat loss (perpendicular to surfaces of uniform temperature), with the diameter of the columns being inversely proportional to the cooling rate (narrower columns result from faster cooling, other factors being the same). As described elsewhere in this guide, the narrow, horizontal columns are evidence that the lavas abutted glacial ice that filled the great canyons surrounding Mount Rainier. Emptying of the canyons of ice during the major interglacial periods, such as today, stranded the lava flows on the crests and sides of ridges high above deep open valleys. This interpretation of ice-confined lava flows is important because the heights of the tops of such lava flows are approximate measures of the ice surface elevation at the time of eruption. Ice thickness is approximated by the elevation difference between the top of the lava flow and the valley floor, with estimates of absolute thickness limited by poorly known rates of glacial downcutting. The horizontal columns at this stop lie at 4,665 ft (1,422 m) elevation whereas the closest floor of the adjacent White River valley is at 3,515 ft (1,071 m), so the ice may have been as much as 1,150 ft (350 m) thick in this area at 506 ka when the lava erupted. Besides horizontal columns, the outcrop exposes two ~20-cm-wide blocks of porous gabbronorite contained in the lava that from other localities in the andesite of Burroughs Mountain yield U-Pb zircon ages similar to the eruption age of the lava.

Stop 2, Enigmatic Block Layer from Osceola Mudflow (46°54.940' N., 121°37.272' W.; UTM 10T, 5196716N, 604988E)

Continue driving up the road toward Sunrise, passing the hairpin turn and the viewpoint of Sunrise Point (optional scenery stop). Just after the road levels out, about 1.65 miles (2.66 km) beyond Sunrise Point, watch for a sloping cutbank on the right with single-lane parking directly across on the left hand (south) side of the road. Park here.

In the roadcut to the north and in streamcuts below and to the south, a lithic block-and-lapilli layer crops out in the tephra section between the Mazama ash (7,600 cal. yr B.P.) and Mount St. Helens tephra layer Yn (~3,700 cal. yr B.P.) (fig. 37). Lithic blocks as much as 45 cm across and lapilli are in a deposit that is as thick as 1 m. Recognizable blocks and lapilli are a diverse mixture of Mount Rainier lavas. Because Miocene volcanic rock underlies this area and hillslopes to the north, and because no Mount Rainier lavas crop out above it, hillslope processes cannot have emplaced this deposit. As a result of these relations, Mullineaux (1974) interpreted it as a ballistic deposit from Mount Rainier, which is 11 km to the southwest, and named it layer S.

Crandell (1971) and Mullineaux (1974) further speculated that the deposit was emplaced by a directed blast from Mount Rainier during the Osceola collapse, prescient of the 1980 directed blast at Mount St. Helens, but we disagree and suggest instead that the deposit is actually a marginal facies of the Osceola Mudflow. Simple ballistic calculations (L. Mastin, USGS, oral commun., 2015) suggest implausible exit velocities and negligible drag coefficients would be required for 20–45 cm blocks to have travelled as far as 11 km. Recent excavations at the Sunrise Visitor Center exposed 1–2 m of Osceola Mudflow deposits that were unknown to Mullineaux (1974) and Crandell (1971). A simpler explanation for these large blocks is that the momentum of the Osceola Mudflow carried the blocks into position at this inundation limit. The receding flow then drained down the shallow valley south and east of this site, leaving the blocks stranded high above the White River.

Continue driving west to the large parking area at Sunrise (6,405 ft; 1,952 m). Sunrise sits atop the andesite of Burroughs Mountain, but the nearly flat top of the lava flow is concealed beneath Pleistocene till and Holocene tephras, notably, brown pumice lapilli from the 2,300 cal. yr B.P. tephra C eruption. This area is known as Yakima Park. The ridge to the north (Sourdough Mountains) exposes Miocene volcanic rocks interpreted to be a dome complex (Murphy and Marsh, 1993), and to the south is the prodigious valley of the White River that was filled with ice to about this level when the andesite of Burroughs Mountain erupted at 506 ka.

Optional Stop, Sourdough Mountains

From Sunrise, walk north up the short trail to a low point along the crest of the Sourdough Mountains. The trail starts just east of the restroom building and is initially paved, with a right turn onto dirt and gravel at 175 yards (160 m), and a left fork at 340 yards (310 m), attaining the crest of the Sourdough Mountains at 650 yards (595 m). Walk right (east) about 80 yards (75 m) along the trail running along the crest of the ridge, and look east along the north brink of the ridge to see ~2 m thickness of yellowish-white pumice lapilli and ash—this is a Plinian fall deposit of the biotite rhyodacite of Sourdough ridge (~200 ka), which is both the most evolved bulk magma composition known to have erupted from Mount Rainier, as well as the sole product known to have phenocrystic biotite (many thick Mount Rainier lava flows have traces of late-grown groundmass biotite, likely fluorine rich). Talus mantles the top of the pumice deposit at about the level of the bushes, accounting for its local preservation. The rhyodacite pumice deposit has only been observed intermittently

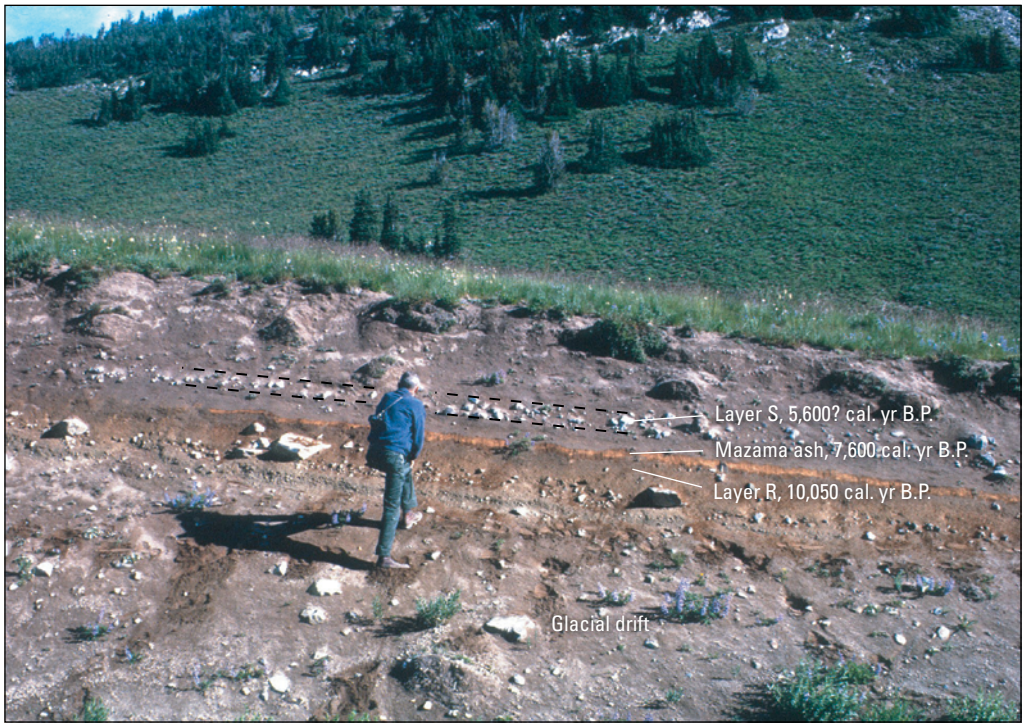

Figure 37. Photograph of rubble of layer S in a roadcut 3 kilometers (km) east of the ranger station at Yakima Park (day 2, stop 2). Layer S overlies ash from the Mazama eruption (Crater Lake) at 7,600 calendar years before present (cal. yr B.P.) and underlies Mount St. Helens layer Yn (3,700 cal. yr B.P.), which is present beneath clumps of vegetation but not visible in the photograph. Crandell (1971) and Mullineaux (1974) concluded that layer S must be a ballistic deposit because it consists exclusively of Mount Rainier andesite and there is no local source of andesite upslope from here. However, Crandell and Mullineaux did not realize that the Osceola Mudflow ran up as high as Yakima Park, and it seems likely that it may have washed up as high as this site too. Furthermore, it is physically implausible that a ballistic as large as 40 centimeters could have been propelled this far (11 km) (Larry Mastin, U.S. Geological Survey, oral commun., 2015). Person in photograph is Rocky Crandell; photograph by Don Mullineaux, U.S. Geological Survey, 1964.

along the crest of Sourdough ridge here and to the east. Accessing the pumice involves walking off trail, which is discouraged at Sunrise because of the heavy visitation. After viewing the pumice, either retrace the path to Sunrise to commence the hike at its beginning, or hike west along the Sourdough Ridge Trail that lies on the south side of the ridge past Frozen Lake and onto Burroughs Mountain via its northeast shoulder, rejoining the field-trip route near stop 4.

Stop 3, Sunrise Ranger Station

Several years ago, a trench dug behind the ranger station revealed 30–40 cm of Osceola Mudflow. Because of its incredible kinetic energy, the lahar ran up 2,100 ft (650 m) here. Inside the ranger station, a peel of the tephra section from Summerland (2.5 miles or 4 km south of Sunrise) is displayed. The tephra section near Sunrise differs from that at Summerland chiefly in exposing 15–30 cm of clayey ash of layer F, coeval with the Osceola Mudflow. In contrast, only 2–5 cm of pumiceous layer F ash crop out at Summerland.

Numerous, ash-size, SVG tephras are in section below Mount Rainier layer C and above Mazama ash that are respectively elements of the Summerland, Osceola, and Cowlitz Park eruptive periods. The SVG ash layers are the products of mildly explosive summit eruptions with VEI ~2 that may have accompanied lava flows and pyroclastic flows. Though thin and nondescript, the ash layers are important because they document about three-fourths of Mount Rainier's Holocene volcanic history and because many of them are genetically related to voluminous (0.05–0.2 km^3) lahars that swept 30–60 miles (50–100 km) down valleys.

Optional Stop, Alpine Meadow Outcrop of Holocene Tephra

A gravel road heads west from the southwest corner of the Sunrise parking lot; this road is known as the Sunrise Campground Trail in National Park Service literature and is closed to public vehicles. Walk this road about 0.4 miles (0.7 km) west to view tephra exposed in stream banks of an alpine meadow (south of 46°54.928' N., 121°39.257' W.; UTM 10T, 5196650N, 602470E).

Tephras from the Cowlitz Park, Osceola, and Summerland eruptive periods are present in the section. Three exotic and two Mount Rainier tephras are most prominent from grass roots to stream level:

- 2 cm white medium pumiceous ash from Mount St. Helens layer Wn (1489 C.E.),
- 15 cm of brown pumice and black scoria lapilli from Mount Rainier layer C (2,300 cal. yr B.P.),
- 6–7 cm pale yellow, coarse pumiceous ash from Mount St. Helens layer Yn (~3,700 cal. yr B.P.),
- ~20 cm beige to rusty orange clay and fine pumiceous ash from Mount Rainier layer F (5,600 cal. yr B.P.), and
- ~5 cm orange fine pumiceous ash from Mount Mazama (Crater Lake) (7,600 cal. yr B.P.).

Tephra layer F erupted simultaneously with formation of the Osceola Mudflow at 5,600 cal. yr B.P. (Mullineaux, 1974; Vallance and Scott, 1997). The tephra is much thicker here than it is elsewhere on the flanks of the volcano primarily because explosions of the hydrothermal system blasted clay and mud to the northeast when the Osceola edifice collapse suddenly decompressed hydrothermal water at the pressure boiling point at depths of 1–1.5 km. The deposit comprises three layers here, only one of which is primarily magmatic in origin (fig. 38). Layer F is unlike the lateral blast deposit of Mount St. Helens in 1980 because it contains a high abundance of hydrothermal clay minerals and very little magmatic ash (Mullineaux, 1974). Mullineaux ascribed the clay minerals to hydrothermal alteration of rocks within Mount Rainier prior to eruption of the tephra. Samples of the F tephra from this site and the head of Granite Creek, about 3 km west of here, examined by John and others (2008), contain the same hydrothermal phases as the matrix of the Osceola Mudflow. Various forms of opaline silica are abundant in both deposits, but clay minerals and quartz are more abundant in the F tephra than in the Osceola Mudflow matrix. Pyrite is abundant in one sample of the tephra that was deposited on a water-saturated peat layer (fig. 38). Clay minerals in the tephra include smectite, kaolinite, pyrophyllite, and trace amounts of illite.

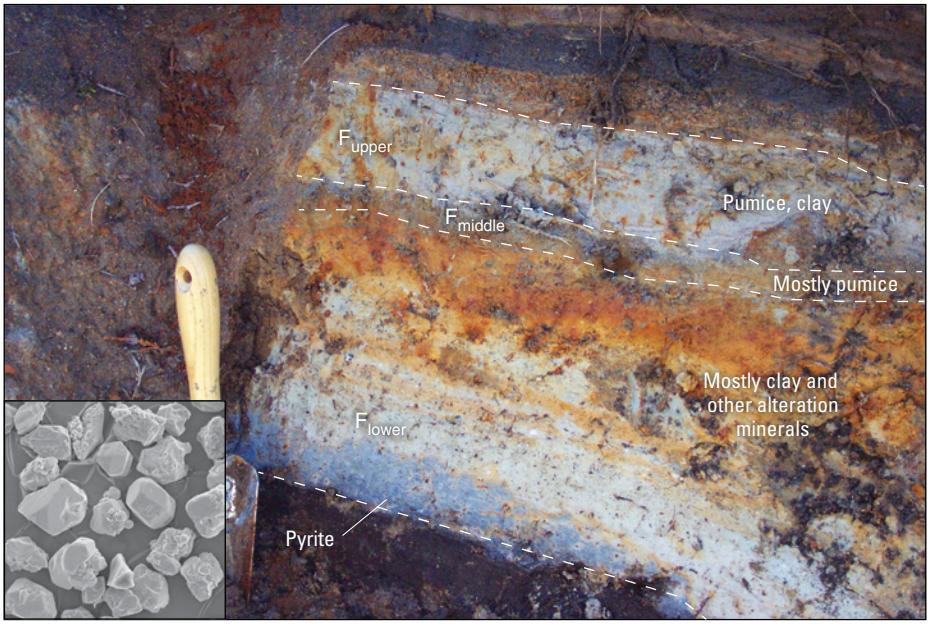

Figure 38. Photograph of clay-rich layer F from near the headwaters of Granite Creek, about 3 kilometers west of Yakima Park. Layer F and the Osceola Mudflow are cogenetic. Elsewhere around Mount Rainier, layer F consists chiefly of pumice, but in the Yakima Park and upper Granite Creek areas it is much thicker and contains distinctive hydrothermal clay minerals. The clay-rich facies of layer F crops out at stop 3 of day 2. Its distribution, mineral composition, and association with the Osceola Mudflow suggest that it is the result of laterally directed explosions of the pressurized hydrothermal system when the Osceola avalanche unloaded it. Inset is a scanning electron microscope image of pyrite extracted from the gray area at the base of the unit. Modified from John and others (2008). Photograph by David John, U.S. Geological Survey.

Stop 4, Andesite of Burroughs Mountain (46°54.970′ N., 121°39.473′ W.; UTM 10T, 5196723N, 602194E; 0.9 miles [1.4 km] from Sunrise)

Continue west along the Sunrise Campground Trail to where the gravel road makes a slight bend to the left; directly ahead is an exposure of columnar jointed lava above the right side of the road that forms the east end of a short east-trending (toward you) ridge. This is close to the base of the andesite of Burroughs Mountain. The lava flow was confined on the north (right) by the southeast ridge of Mount Fremont, which consists of texturally diverse Miocene arc volcanic rocks (Fiske and others, 1963; Murphy and Marsh, 1993). The lava's columns point down to the north (right), consistent with a south-dipping base to the lava flow in this area. The andesite of Burroughs Mountain is one of a group of voluminous lava flows whose eruptions constitute the first or Old Desolate stage of the growth of modern Mount Rainier. The andesite of Burroughs Mountain is ~3.4 km^3 in volume but is divisible into upper and lower emplacement units separated by a zone of oxidation. No evidence for erosion has been recognized between the two units, consistent with their emplacement as two phases of lava during the same eruption (Stockstill and others, 2002). Although the mean composition of the lava is silicic andesite (60.6 weight percent SiO_2), lava samples span from 56.6 to 64.3 weight percent SiO_2, encompassing much of the compositional spectrum of the modern volcano. The lava flow overlies unconsolidated volcanic breccias dominated by prismatically jointed juvenile clasts of similar compositional range (56.4–64.1 weight percent SiO_2) in apparent conformable contact, although

at this location the volcaniclastic deposits are absent or are no more than a few meters thick and fail to crop out.

Continue along the gravel road past its junction with the Wonderland Trail (46°54.920' N., 121°39.764' W.; UTM 10T, 5196624N, 601826E). The fork on the right (west) ascends toward Frozen Lake; early in the season or in heavy snow years, consider taking this right-hand trail past Frozen Lake and up onto the northeast shoulder of Burroughs Mountain via the Burroughs Mountain Trail to avoid a steep snowbank on the south face. In normal snow years, continue straight (south) a short distance along the Wonderland Trail to Sunrise Camp and turn right to join the Burroughs Mountain Loop Trail (46°54.625' N., 121°39.649' W.; UTM 10T, 5196080N, 601981E) that initially heads west, then bends sharply to the left and ascends southeast to the ridge crest.

Stop 5, White River and Emmons Glacier Scenic Overlook (46°54.506' N., 121°39.589' W.; UTM 10T, 5195860N, 602061E; 1.6 miles [2.5 km] from Sunrise)

Upon attaining the ridge crest, you will find a stone wall overlooking the valley of the White River and the Emmons Glacier. The view east down the White River gives a sense of the magnitude of ice during most of the growth of Mount Rainier. The flat bench of Yakima Park lies on the left above the north side of the valley and marks the top of the andesite of Burroughs Mountain. Shortly after emplacement of the lava at 506 ka, Pleistocene animals could have walked across the top of then greatly expanded Emmons Glacier between Yakima Park on the north and Goat Island Mountain on the south. Pleistocene lava is also perched at Baker Point about 1.4 miles (2.3 km) south of the viewpoint along bearing 188°.

Prominent in the valley floor are sharp-crested, sparsely treed moraines at the foot of and flanking the Emmons Glacier. These sharp-crested moraines are products of the advance and retreat of the Emmons Glacier during the late Holocene Little Ice Age. Ages of these moraine crests have been estimated by dendrochronology (Sigafoos and Hendricks, 1972), with the outermost poorly preserved lateral moraine on the north side yielding 1550–1600 C.E., the lowest elevation end moraine giving 1745 C.E., and the innermost moraine flanking a small pond dated to 1900 C.E. More broadly around Mount Rainier, the small moraine crests below and flanking active glaciers most commonly have ages more recent than 1820 C.E. (Sigafoos and Hendricks, 1972; Burbank, 1981), recording the retreat of glaciers since the end of the Little Ice Age, but crests have been identified as old as 1217 C.E., near the Little Ice Age's beginning, and scattered logs exposed in horizons along the inner walls of some lateral moraines yield ^{14}C ages as great as 350–130 C.E. (Samolczyk and others, 2010), recording Holocene glacial advances prior to the Little Ice Age.

Also prominent from this location is the steep, shaded, north face of Little Tahoma Peak overlooking the south edge of the Emmons Glacier. In December 1963 great masses of rock, estimated at about 10,000,000 m^3, fell from the east side (left, as viewed) of Little Tahoma Peak's north face, forming a rock avalanche that traveled about 4 miles (6.4 km) down the Emmons Glacier and beyond onto the Little Ice Age moraines, with most of the debris reaching no farther than the small pond impounded behind the 1900 C.E. moraine crests (Crandell and Fahnestock, 1965). A portion of the avalanche continued another 0.5 miles (0.8 km) down the main channel of the White River, generating a small lahar. Subsequent geologic mapping reveals an east-west striking system of near-vertical joints that passes through Little Tahoma Peak, associated with east-west striking andesitic dikes. The 1963 collapse from the north face can be attributed to failure of one or more of these joints owing to undermining by glacial erosion or (and) to glacial debuttressing after the end of the Little Ice Age. Rock debris from the 1963 failure covered and insulated the lower Emmons Glacier, which then advanced modestly (Driedger, 1986). Light detection and ranging (lidar) measurements from 2007–2008 show that the active terminus of the Emmons Glacier remained thicker and reached farther downvalley than it did in 1970, which was probably a residual effect of insulation by the 1963 rock avalanche. The terminus of the nearby Winthrop Glacier also thickened between 1970 and 2007–2008, probably owing to insulation by smaller rockfalls from Russell Cliff in 1989 (Sisson and others, 2011).

Continue hiking up the trail to the west as it ascends near the ridge crest, noting a small section of Pleistocene moraine on the right. Shortly, the trail rises above the tree line and bends to the left. The route for the next couple of hours lacks protection from the wind, so if conditions are poor at this point, consider returning another day.

Stop 6, Inclusions in Andesite of Burroughs Mountain (46°54.474' N., 121°39.972' W.; UTM 10T, 5195793N, 601577E; about 2 miles [3 km] from Sunrise)

This stop is more of a walk-by than a true stop. The trail makes a rightward bend with some rough steps—look in this area for comparatively coarse-grained, seemingly plutonic-textured inclusions in the andesite of Burroughs Mountain. Such inclusions are commonly angular, 5–20 cm across, and have a distinctive speckled light-and-dark or salt-and-pepper appearance. Look in the talus for pieces that can be examined by hand lens without use of a hammer. Unlike ordinary plutonic rocks, most of these inclusions are distinctively porous and vuggy with miarolitic cavities as large as about 4 mm across and abundant pores (too fine to distinguish by eye) within a sugary fine-grained groundmass. The coarser crystals are plagioclase, orthopyroxene, clinopyroxene, and Fe-Ti oxides similar in size and habit to the phenocrysts in the host lava. Some of the inclusions contain traces of olivine variably rimmed by orthopyroxene or by magnetite symplectite, and some contain amphibole, typically broken down to fine-grained Fe-Ti oxides and anhydrous silicates. These coarser crystals are set in a matrix that consists of alkali feldspar, tridymite, and about 50 volume percent pore space. Needle-shaped zircon grains poke into the pores, and these prove to have sufficiently high uranium concentrations to date by ion microprobe. Weighted mean U-Pb ages of zircons (T.W. Sisson, unpublished results, 2009) from two such plutonic-textured inclusions from the

506-ka andesite of Burroughs Mountain yield 560±60 ka and 463±10 ka (2-sigma uncertainty; note, ages can be brought to match more closely the host lava by assuming different Th/U for the ^{230}Th corrections). Similar correspondence of ages between host lava flows and vuggy, plutonic-textured inclusions has been found for three additional Mount Rainier lava flows as young as 250 ka, leading to the interpretation that the inclusions are cognate complements to the lavas that brought them to the surface, rather than either unrelated country rocks or distinctly older intrusive products of the Mount Rainier magmatic system. Compositions of such plutonic-textured inclusions overlap broadly with the Mount Rainier lava and pyroclast suite, but most lie toward the low-SiO_2, high-MgO end, similar to the compositions of fine-grained basaltic andesitic through andesitic quenched magmatic inclusions. Possibly, the porous plutonic-textured inclusions formed as comagmatic injections of basaltic andesite and andesite larger than, but otherwise similar in composition to, the injections that produce nearly aphyric quenched magmatic inclusions that are abundant in some Mount Rainier volcanic rocks, with the larger sizes of the injections allowing for slower cooling and growth of coarser crystals.

Continue up the trail across a steep, talus-filled basin and onto the broad upper surface of the andesite of Burroughs Mountain; dedicated Mount Rainier hikers refer to this plateau as "First Burroughs." Mountain goats commonly congregate here and to the west and north, so keep an eye out.

Stop 7, View from the North Precipice of Burroughs Mountain (46°54.639′ N., 121°40.806′ W.; UTM 10T, 5196081N, 600513E; 2.6 miles [4.2 km] from Sunrise)

The Burroughs Mountain Trail ascends from Frozen Lake and is an alternate approach to avoid the steep snowbank that persists in some heavy snow years just beyond stop 6. Halt at the trail intersection or shortly to the west (left) and look north and west to see the geology depicted in figure 39.

Unconsolidated volcaniclastic breccias that underlie the andesite of Burroughs Mountain are visible to the northwest, capped by an isolated erosional remnant of the lava flow. Clasts in these breccias appear to be juvenile based on common prismatic joints, moderate inflation, and similarity between clasts over restricted stratigraphic levels. Closer to the volcano, juvenile-appearing clasts in these breccias have shared normal magnetizations indicating hot deposition from repeated small-volume pyroclastic flows or from derivative hot lahars. Magnetic directions are random with greater distance from the volcano, and the breccias in view were probably deposited from lahars or from pyroclastic flows that had cooled below their Curie temperatures. Indistinct horizontal stratification can be seen in the breccias parallel to the contact with the overlying lava. Lack of incision on the contact between lava and volcaniclastic rocks, and its concordance with underlying stratification, are evidence that the pyroclastic debris and the lava erupted in rapid succession as part of the same volcanic event (Stockstill and others, 2002).

Beyond Berkeley Park, the peaks of Sluiskin Mountain, Skyscraper Mountain, and Mount Fremont consist of various largely Miocene volcanic and fine-grained subvolcanic rocks. On a clear day, look directly north to see Quaternary Mount Baker volcano, 130 miles (207 km) away; Glacier Peak volcano lies to the right but is concealed from view by the intervening Mount Fremont massif. Other distant high peaks are Mount Daniel (bearing 26°, 50 miles [80 km]), consisting of Oligocene andesites, and Mount Stuart (43°, 53 miles [86 km]), made up of Late Cretaceous quartz diorite and tonalite of the Mount Stuart batholith.

Also visible from this location are other members of modern Mount Rainier's initial Old Desolate growth stage: the andesite of Old Desolate (455 ka) to the west-northwest and the andesite of Grand Park (445 ka) to the north. Like the andesite of Burroughs Mountain, the andesite of Old Desolate is a thick, probably ice-marginal lava flow that overlies unconsolidated, indistinctly horizontally stratified volcaniclastic breccias. The andesite of Grand Park is visible from this site only as a distant, indistinct outcrop in the forest, but that lava flow ends 13.5 miles (22 km) from the summit, the farthest distance attained by any preserved lava flow from Mount Rainier. As with the andesites of Burroughs Mountain and Old Desolate, its ridge crest location is indicative of ice-marginal volcanism. All three of the visible Old Desolate stage lava flows are deeply incised and have been beheaded by glacial erosion from their likely source vents on the flank of Mount Rainier.

The far west skyline is defined by the eroded cinder cones of Echo and Observation Rocks (right and left, respectively) that fed the olivine basaltic andesite lava flow field of Spray Park at about 97 ka. Echo and Observation Rocks lie 4 miles (6–7 km) north-northwest of Mount Rainier's summit and are the closest vents to have erupted basaltic andesite as bulk lava and pyroclasts. Small-volume basalt and basaltic andesite vents and flows are scattered regionally to the north, east, and southeast of Mount Rainier, but no basalts or basaltic andesites erupted as bulk lava or pyroclasts through Mount Rainier's axial magmatic system, including from summit vents or from dike-fed flank vents. Rather, basaltic andesites only appear as quenched magmatic inclusions (enclaves) in the andesites and dacites of Mount Rainier's axial magmatic system.

Visible shortly below and toward the viewer from Echo and Observation Rocks is a low lava flow labeled on figure 39 as the spessartite of the Russell Glacier. Spessartite is a calc-alkaline andesite or basaltic andesite composition rock with a lamprophyric texture defined by phenocrysts of calcic amphibole but not plagioclase. Phenocrystic amphibole can be accompanied by subordinate phenocrysts of clinopyroxene and (or) olivine. Spessartites have geochemical affinities with shoshonites and absarokites; spessartite of the Russell Glacier has the greatest concentrations of K and Sr for its SiO_2 concentration and has the steepest rare earth element pattern known for any Mount Rainier magma (Sisson and others, 2013). The spessartite lava erupted at 57 ka from a vent now concealed by the Russell Glacier shortly south (left) of Echo and Observation Rocks, about 3.5 miles (5.5 km) from the

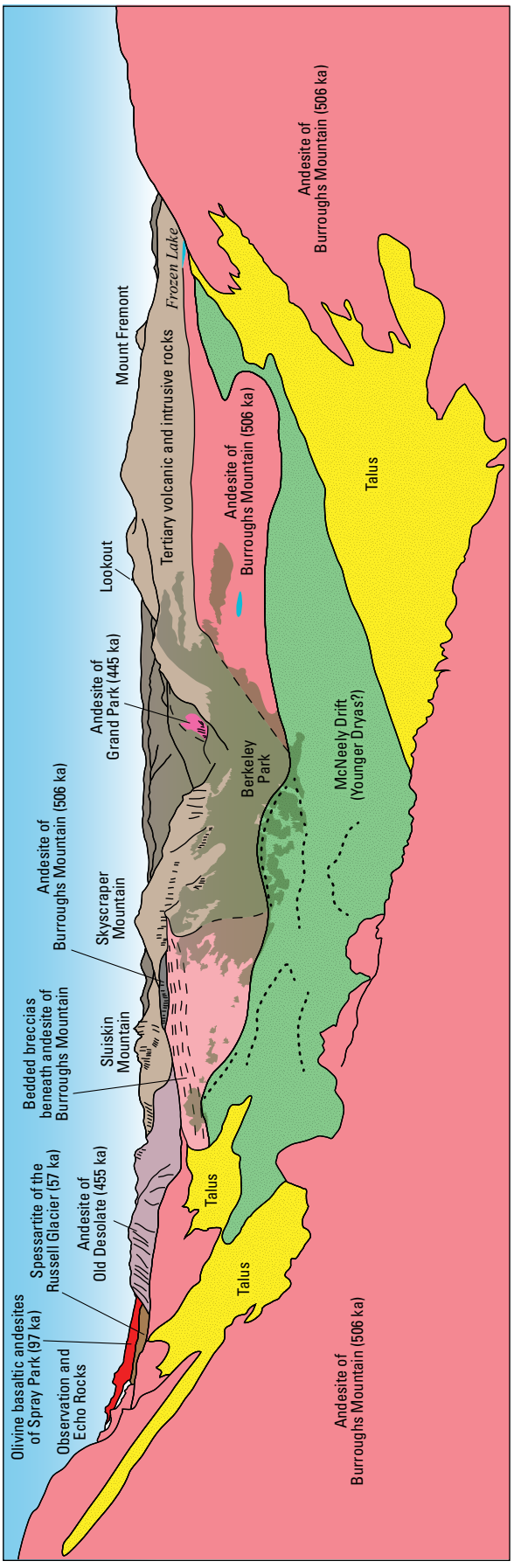

Figure 39. Overview perspective drawing of the view looking north and west from the flank of Burroughs Mountain and illustrating local geologic relations visible at stop 7 of day 2. Several lavas of the earliest Old Desolate stage are visible, including andesite of Burroughs Mountain overlying bedded breccias, andesite of Old Desolate, and andesite of Grand Park. In the foreground is the ~12 thousand year old (ka) McNeely Drift.

summit. Another small spessartite-basaltic andesite hybrid lava (spessartite of the Flett Glacier) erupted at 9±3 ka from a vent just out of view to the right of Echo Rock, about 4.5 miles (7.5 km) from the summit. As with basaltic andesite, no spessartite has erupted as bulk magma through Mount Rainier's axial magmatic system, but influxes of spessartite into axial magmas can be inferred from occasional otherwise ordinary plagioclase-porphyritic andesites and dacites distinguished by abundant amphibole and atypically high concentrations of K, Sr, and other trace elements characteristic of spessartite. The ability of basaltic andesites and spessartites to reach the surface near Echo and Observation Rocks without transiting andesitic and dacitic magmas provides a limiting radius to the magmatic axial system of less than about 4 miles (6 km) in a north-northwest direction.

The lumpy ground in the foreground at the foot of the north precipice, beyond the talus, is the McNeely Drift of probable Younger Dryas age. Poorly developed moraine crests are denoted on figure 39 with dotted lines.

Continue west along the trail to the summit of Burroughs Mountain.

Stop 8, Burroughs Mountain Summit (46°54.370′ N., 121°41.403′ W.; UTM 10T, 5195569N, 599763E, 3.2 miles [5.2 km] from Sunrise).

Local hikers refer to this as "Second Burroughs Mountain," with "Third Burroughs Mountain" being the higher skyline ridge a little more than 1.25 miles (2 km) to the west-southwest. Find a comfortable spot near the brink of the south precipice and view the geology to the south depicted in figure 40. This is the best place for lunch on the hike but beware of bold chipmunks and ground squirrels that will persistently try to steal food from unguarded packs and lunch bags.

Mount Rainier's summit, Columbia Crest (14,410 ft; 4,392 m), lies about 5 miles (8 km) to the southwest (bearing 222°), and 6,580 ft (2,006 m) higher, but the summit area is flattish and the exact high point is slightly out of view from here. Two overlapping craters cap the volcano's summit, each about 0.25 mile (0.4 km) across and filled with ice, with the east crater being younger and bisecting the west crater. The southern and eastern rim of the east crater exposes a dark, radially outward dipping andesite lava flow mantled discontinuously on its outer surface with rubble—this lava flow forms the narrow, nearly horizontal strip of rock visible at the highest point above the conjoined Emmons and Winthrop Glaciers. Paleomagnetic measurements on the lava are consistent with an age of about 2,000 cal. yr B.P., but it was probably emplaced shortly after the eruption of the 2,300 cal. yr B.P. C tephra, which has not been found at the summit. The 2,000 cal. yr B.P. lava flow is covered along the west through northwest rim of the east summit crater by an accumulation of faintly bedded, hydrothermally altered rock rubble. The exposed rim of the older west summit crater is also hydrothermally altered rock rubble, but lava is exposed in patches on the crater's outer west and northwest slopes.

The true summit of the volcano is a small, rounded dome of snow and ice at the north junction of the two craters. Because the true summit is snow and ice, its elevation can vary depending on degrees of ablation and snow accumulation, leading to discussions, chiefly of local but heated interest, as to the exact height of the volcano. Warm fumaroles vent along the inner walls of the craters and have melted a network of caves in the crater-filling ice, including having produced one or more sub-ice ponds. Benighted climbers have sheltered in these caves, at the cost of being saturated with tepid mist on one side and frozen on the other, as early as the first well-documented successful ascent in 1870 by Hazard Stevens and Philemon Van Trump. A party in 1857 led by Lt. August Kautz, U.S. Army, attained an elevation within 500 ft (150 m) of the summit but turned back because of approaching darkness and deteriorating weather. There are also reports of a possible successful ascent in 1855 and a near-successful ascent in 1852, although few specifics are known.

Below and toward you from the visible rim of the east summit crater spreads the broad expanse of the conjoined Emmons and Winthrop Glaciers. The glaciers separate below Steamboat Prow, which is the pointed rock peak in the middle distance in a direct line with the summit crater, with the Emmons Glacier on the left and the Winthrop Glacier on the right (fig. 40). Small windows through the ice, exposing dark rock, interrupt the surface of the conjoined glaciers. These are exposures of andesitic lava flows on the surface of the young, non-incised volcanic cone that grew within and filled the 5,600 cal. yr B.P. Osceola collapse amphitheater. The exposed lavas are andesites, but they are not the same as those forming the rim of the east summit crater, differing in having distinctly high concentrations of Sr for Mount Rainier's products. Their high-Sr character is matched in late Holocene tephra sections in sub-alpine meadows, and based on ^{14}C and paleomagnetic measurements, the high-Sr andesites are known to have erupted about 2,400 cal. yr B.P., shortly after eruption of an andesitic pyroclastic flow and tephra with ordinary Sr concentration for Mount Rainier (fig. 19; Sisson and Vallance, 2009). The high-Sr lavas were then followed by the 2,300 cal. yr B.P. C tephra that contains mingled normal- and high-Sr components; the C tephra was then followed by the ~2,000 cal. yr B.P. normal-Sr andesitic lava of the east summit crater, which is the most recent lava flow to have erupted from Mount Rainier.

The sides of the Osceola collapse amphitheater are marked by topographic breaks where the continuous glacier surface gives way laterally to the prominent bedded lava flows of Russell Cliff and Curtis Ridge on the right (north) and of Little Tahoma Peak and Disappointment Cleaver (with Gibraltar Rock behind on the skyline) on the left (fig. 40). The collapse amphitheater was about 1.1 mile (1.8 km) across at the top, widening with lower elevation and increasing distance from the axis of the volcano to about 2 miles (3 km) across just above the elevation of Steamboat Prow. For comparison, the 1980 Mount St. Helens collapse amphitheater is about 1.25 miles (2 km) across at the top, broadening to about 1.5 miles (2.4 km) at the amphitheater's mouth, but only about 1 mile (1.75 km) across the amphitheater's interior floor.

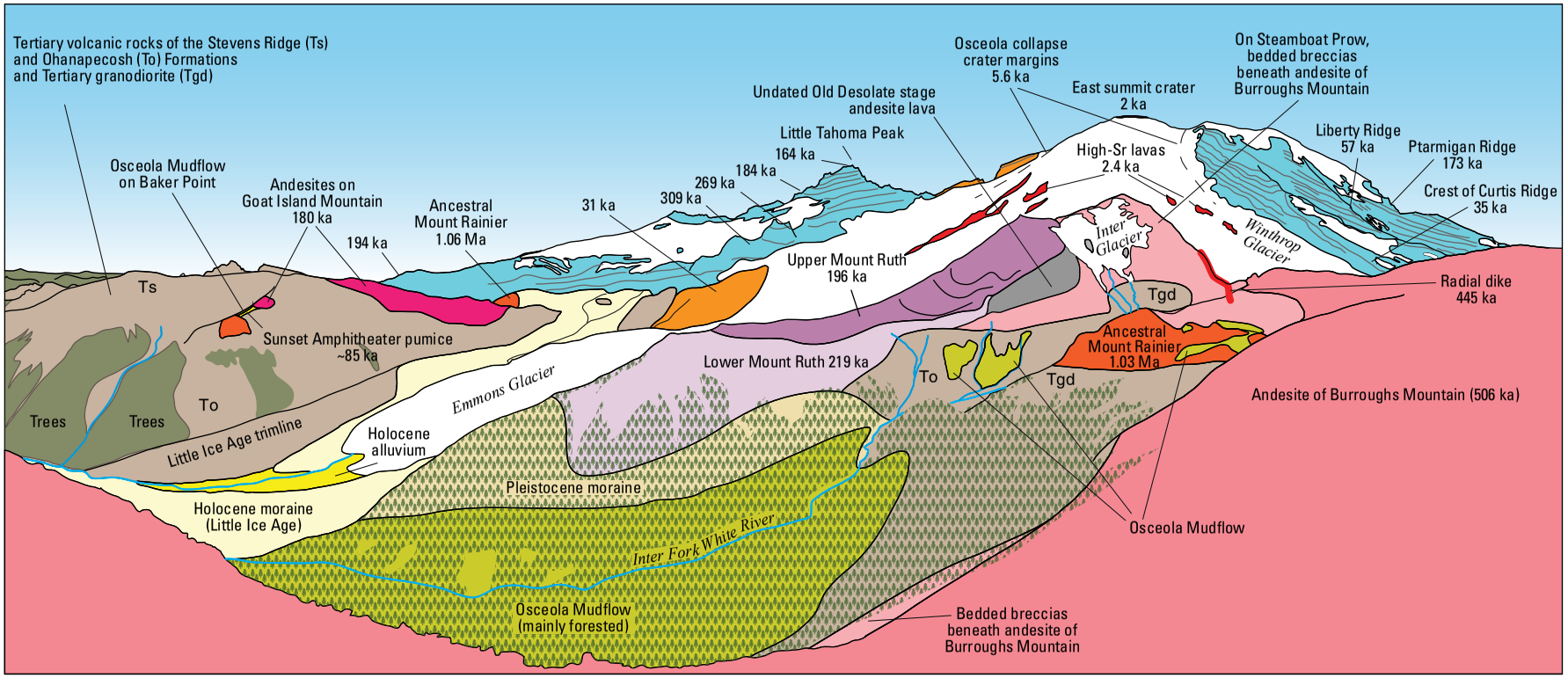

Figure 40. Overview perspective drawing of the view from the summit of what is locally known as "Second Burroughs Mountain" looking south and southwest toward the summit of Mount Rainier illustrating geologic relations visible at stop 8 of day 2. The oldest visible lavas are those of ancestral Mount Rainier (about 1 million years old [Ma]). Andesite of Burroughs Mountain and underlying bedded breccias exposed on Steamboat Prow are the oldest rocks of modern Mount Rainier. Little Tahoma Peak and pre-Osceola Mount Rainier expose andesite lavas that range in age from more than 300 thousand years old (ka) to less than 30 ka. The 5.6-ka Osceola collapse crater frames the youngest lavas that form the summit cone. Lavas that poke through the Emmons and Winthrop Glaciers are about 2.4 ka and predate the C tephra that is scattered on top of Burroughs Mountain. The ~2-ka lavas that crop out around the east summit crater are younger than the C tephra. Both these lavas and the C tephra are elements of the last major eruptive period at Mount Rainier, the Summerland period. Osceola Mudflow deposits, recognizable owing to their orange tint, drape parts of Mount Ruth and are found high on the opposing ridge that leads to Point Baker. Forested slopes in the low-lying parts of Glacier Basin conceal Osceola Mudflow deposits that are tens of meters thick. Unit labels and colors as in figure 36.

The rocks of Steamboat Prow are chiefly bedded breccias that map out as continuous with those that conformably underlie the andesite of Burroughs Mountain. The breccias high on Steamboat Prow dip toward you and away from the present summit at 15–20°, with dips shallowing to near horizontal with greater distance from the volcano. These breccias are the oldest known products of the modern volcano. Projecting updip, the 2-mile (3 km) map distance from Steamboat Prow toward the summit indicates a potential edifice height of 12,400–13,300 ft (3,770–4,060 m); no great significance attaches to these elevations except for showing that modern Mount Rainier grew rapidly, attaining great heights early in its history. The breccias of Steamboat Prow unconformably overlie Miocene granodiorite and Oligocene Ohanapecosh Formation andesites at about the level of the foot of the small glacier perched on the northeast face of Steamboat Prow (the Inter Glacier). The Tertiary-Quaternary contact is largely concealed by talus and till, but its location is marked locally by water seeps that darken the rocks and talus. The breccias also unconformably overlie a prominently columnar-jointed knob of ~1 Ma andesite from ancestral Mount Rainier, which is visible in the middle distance on the right side of the valley directly in line with the summit and the crest of Steamboat Prow. Andesitic dikes cut the breccias along the northwest ridge of Steamboat Prow (right side, as viewed). These dikes strike northeast, radially away from the summit, and have near-vertical dips. One of the larger dikes is dated at 445 ka, placing it as a member of the Old Desolate stage and a possible source for the similarly aged andesite of Grand Park. The breccias are hydrothermally altered, yellowish, and pyritic within about 10 m of the dike system, whereas light-colored bands that cross breccia cliffs approximately concordant with bedding are smectite-rich intervals that may mark former aquifers.

The southeast ridge of Streamboat Prow (left side, as viewed) is crowned by a spur peak known as Mount Ruth. Mount Ruth and the ridge down to the east-southeast (left) consist of younger lava flows that unconformably overlie the Old Desolate stage breccias. The lava flows of Mount Ruth erupted during the Mowich stage, which was Mount Rainier's most vigorous phase of growth. The lava flows of Mount Ruth are divided by an unconformity with local and modest angular discordance. Ages of the lower (219 ka) and upper (195 ka) andesites of Mount Ruth are within MIS 7 (modest interglacial) and the transition into MIS 6 (strong glacial). Ice contact features on the east-southeast edges of some upper Mount Ruth lava flows document that at about 195 ka, the surface of the Emmons Glacier was at least 1,020 ft (310 m) higher than today. Most other aspects of Mount Rainier's Pleistocene geology visible from this location are too distant to resolve and discuss in detail, but worth commenting is that the growth of Little Tahoma Peak also took place during the Mowich stage, mainly during MIS 6. Little Tahoma Peak's lava flows probably erupted from flank vents fed by east-striking radial dikes, accounting for its anomalous height on the volcano's east flank.

The flat valley floor in the immediate foreground is filled with the Osceola Mudflow from the 5,600 cal. yr B.P. collapse event, but most of the deposit is concealed by thick forest. A few areas on the north-facing, south side of the Inter Fork of the White River are too steep for trees to hold fast, and these areas expose the mudflow deposit as yellowish slopes (fig. 40). The mudflow also drapes the high bench on the right side of the valley, above the exposure of andesite from ancestral Mount Rainier, and patches of yellowish mudflow are scattered up to the apex of Steamboat Prow. The mudflow is also present across the valley of the White River on Baker Point. The distribution of deposits shows that the mudflow overtopped Steamboat Prow and Mount Ruth, crossed Glacier Basin (the head of the Inter Fork of the White River), and overran the spur ridge supported by the ancestral Mount Rainier lava flow. The mudflow also rode up over Baker Point on the southeast side of the Emmons Glacier.

After finishing lunch, pack up and resume walking down the trail on the west slope of the so-called Second Burroughs Mountain. This area is thickly carpeted with 2,300 cal. yr B.P. C tephra. Keep an eye open for dark scoria lumps containing pumiceous white blebs and streaks. The white blebs and streaks are distinctly high-Sr dacite mingled with the dominant normal-Sr andesite. Also present are brown, more homogeneous-looking andesitic pumice, as well as large lapilli and small bombs of light-colored, moderately inflated andesite, somewhat resembling pieces of cinderblock or kiln brick. These moderately inflated pyroclasts are high-Sr andesites and are interpreted as conduit linings residual from the 2,400 cal. yr B.P. high-Sr andesite eruptions, whereas the more fluid high-Sr dacite blebs and streaks are interpreted as residual liquids extracted from these conduit linings and intermingled with the newly arrived normal-Sr andesite that dominated the eruption (Venezky and Rutherford, 1997; Sisson and Vallance, 2009). Approaching the saddle between the so-called Second and Third Burroughs Mountains, an informal hikers' trail branches off to the right, crosses the saddle, and ascends to the summit of Third Burroughs Mountain, which offers a spectacular vista of the Winthrop Glacier, Curtis Ridge, the Willis Wall, and Liberty Ridge. This path is just under a mile in each direction (1.5 km) and involves an elevation gain of 800 ft (240 m). Our route stays on the maintained trail and begins to drop into the valley of the Inter Fork of the White River.

Stop 9, Near Saddle Between Second and Third Burroughs Mountains (46°54.100′ N., 121°41.827′ W.; UTM 10T, 5195061N, 599233E; 4 miles [6.4 km] from Sunrise)

Upon leaving the saddle, the trail descends gently south across talus and then begins to switchback down. After about four switchbacks, the trail approaches small bushes and crosses small rock outcrops. Look in these outcrops and in associated loose rocks for ovoid quenched magmatic inclusions (enclaves) that result from magma mingling. Though such inclusions are abundant in some Mount Rainier lava flows, they are uncommon in the andesite of Burroughs Mountain, having been found only in the lower (older) first phase of the lava flow. These quenched magmatic inclusions record an influx of basaltic andesite (54–57 weight percent SiO_2) that might have assisted or triggered the lava eruption (Stockstill and others, 2002). From this area, one can

also look east-northeast (bearing ~70°) to see the unconsolidated blocky fragmental deposits below the lava flow, though these are difficult to distinguish from the slope-mantling talus.

The trail now cuts south, gently down and across the slope, and enters small trees. Look while passing through the first trees for the first outcrops of granodiorite, which is the basement over which the lava erupted. Soon, the trail begins a long series of switchbacks down through the forest until joining the trail from the White River Campground to Glacier Basin. Upon reaching the trail junction (46°53.650' N., 121°41.626' W.; UTM 10T, 5194231N, 599503E, 5.2 miles [8.3 km] from Sunrise), turn right and walk up the trail just under a mile (about 1.3 km) to Glacier Basin, stopping at the meadow just past the camping area (6 miles [9.6 km] from Sunrise).

Stop 10, Glacier Basin (46°53.336' N., 121°42.096' W.; UTM 10T, 5193640N, 598915E)

Glacier Basin was a site of attempted copper mining, commenced by the discovery of potential deposits in 1897 and 1898, followed by the staking of claims in 1902 by Peter Storbo and B.P. Korssjoen, who then founded the Mount Rainier Mining Company in 1905 along with W.C. Berg. Mount Rainier National Park had been established in 1899, but a provision in the enacting legislation allowed mining (the U.S. Congress prohibited new mining claims in Mount Rainier National Park in 1908). In 1905, roads on the northeast side of the park ended at the village of Greenwater where the White and Greenwater Rivers join, but in 1906 the park's administration permitted the mining company to improve the pack trail into Glacier Basin, and then in 1914–1916 the mining company constructed a road, at times passable by automobile. That road originally crossed the White River by bridge about 1.5 miles north (2.4 km) of the present junction of SR 410 and the White River Road, ascended the west and north bank of the river, and then climbed into Glacier Basin. At the peak of attempted mining activity, Glacier Basin hosted a sawmill, electric generator, a blacksmith shop, various small cabins, an aerial tram to bring ore to the road, and even a building intended to serve as a hotel but that only ever lodged miners and road builders. The mining company relinquished the majority of its claims in 1913, following disputes with the park, and the last ore is reported to have left Glacier Basin in 1927 (Ripp, 1999). Peter Storbo and a colleague were convicted of mail fraud in 1930 related to selling of fraudulent mining claims, but in 1933 President Roosevelt commuted Storbo's sentence under petition of the residents of Enumclaw, and it later transpired that Storbo's signature had been forged on mining stock certificates. The would-be hotel was situated in the last stand of tall trees before the meadow, the blacksmith's shop and "TarPebble" cabin were on the south edge of the meadow overlooking the Inter Fork, and the sawmill and generator were about a third of a mile (0.5 km) down the Inter Fork on its west bank. The principal mines were directly south from the meadow across the Inter Fork in Ohanapecosh Formation andesites (Reven, Snowflake, Peach, and Orinda claims totaled ~200 ft [60 m] of tunnel), and in granodiorite, up the unmaintained path from the meadow that can be seen crossing distant talus slopes (Gate, Stronghold, and Washington claims totaled ~1,000 ft [300 m] of tunnel).

Geology visible from this location includes the spectacular columnar joints in ancestral Mount Rainier andesite (northwest, bearing 330°), overlain unconformably on the left by breccias from the beginning of modern Mount Rainier. Little Ice Age moraines are visible in the foreground, due west on the north (right) side of the Inter Fork, constructed of yellowish Osceola Mudflow deposits. Above these and to the right are cliffs that are the sidewall of a radial dike dated at 445 ka. This dike mostly cuts breccias, but the low-relief slope down and to the left of the cliffs is poorly cropping out lava with narrow columnar joints dated at 462 ka; this is a lava flow that probably draped the contact between breccias (background) and ice (foreground) and was then cut by the radial dike. Farther left (246°) on the right (west) side of the Inter Glacier are bluffs of indurated breccia over Miocene granodiorite, and from the southwest to the south are the andesites of Mount Ruth unconformably overlying a brownish-weathering undated lava flow, presumably from the Old Desolate stage, that overlies the breccias. The breccias, in turn, unconformably overlie the Tertiary andesite, but the contact is widely concealed by talus. Yellowish surficial ridges on the lower slope to the southwest and south are erosional remnants of the Osceola Mudflow.

The old mining trail continues from here up the Little Ice Age moraine and across the talus slope, passing near one of the remaining mine tunnels, to the foot of the Inter Glacier, where an indistinct spur trail switchbacks up to Saint Elmo Pass (skyline to the west-southwest), but our route heads back down the trail toward the White River Campground, making one last stop to view a thick exposure of the Osceola Mudflow across the Inter Fork. From the meadow, descend slightly more than 1 mile (1.7 km) down the trail looking for a steep yellowish slope across the valley on your right.

Stop 11, Osceola Mudflow Overlook along Trail (46°53.789' N., 121°41.093' W.; UTM 10T, 5194501N, 600175E; 7.5 miles [12 km] from Sunrise)

Across the valley to the south and below us, a ~150 m terrace exposes 40–60 m of Osceola Mudflow overlying Evans Creek till. These thick Osceola Mudflow deposits are a contrast to <2-m-thick deposits that coat steeper slopes and ridges of the surrounding Glacier Basin.

The bright yellowish- to orangish-brown Osceola Mudflow deposit appears thicker than it really is because it has sloughed down the steep slope and covers the glacial deposits. The upper ~4 m of the Osceola Mudflow is weathered and is the source of the brightly colored debris that coats the steep slope. When the weathered slope below the upper 4 m is excavated, the fresh Osceola Mudflow deposit is actually a neutral gray color. It is also extremely clay rich—15 percent by weight and 37 percent of the matrix (sand, silt, and clay) by weight (Vallance and Scott, 1997). John and others (2008) documented relatively deeply formed magmatic-hydrothermal alteration minerals in clasts and matrix

of the Osceola Mudflow, which include quartz (residual silica), quartz+alunite, quartz+topaz, quartz+pyrophyllite, quartz+dickite/kaolinite, and quartz+illite (all with pyrite) assemblages. Clasts of smectite+pyrite and steam-heated opal+alunite+kaolinite assemblages are also common in the Osceola Mudflow. An avalanche collapse that excavated intensively altered rock as much as ~1 km below the surface of the pre-Osceola edifice is consistent with this hydrothermal mineral assemblage. Even proximal (~3 miles [5 km] from source) deposits, such as this one, show no evidence of the classic hummocky debris-avalanche morphology that would normally be apparent in a deposit resulting from a ~2.5 km^3 edifice collapse. Apparently, the clay-rich avalanche was sufficiently weak and water rich to completely transform to fluid lahar as it deformed during collapse.

The remainder of the walk is down the trail another 2.1 miles (3.5 km) to the White River Campground hiker's parking lot to pick up the vehicles. The section of the trail from about 5,050 to 4,900 ft (1,539 to 1,493 m) elevation is on the outboard side of the 1550–1600 C.E. moraine. The Emmons Moraine Trail branches to the right at about 4,750 ft (1,448 m) elevation and heads south and west initially between the 1835–1850 C.E. moraine on the north and 1900 C.E. moraine on the south (left, heading up the trail), then crosses an outflow channel, after which it is flanked by 1745 C.E. moraine on the west and 1835–1850 C.E. moraine on the east (left, heading up the trail) (Sigafoos and Hendricks, 1972). To walk back up to Sunrise, take the Wonderland Trail that starts near the west end of the loop road on the north side of the campground.

Day 3. Stevens Canyon, Reflection Lakes, and Hike from Paradise to the Old Paradise Ice Caves Area Observing Pleistocene Growth of Mount Rainier, Holocene Tephras, and Edifice Collapse Lahars along Golden Gate Trail

This day is mainly to look at Holocene lahars and tephras on the volcano's south flank near Paradise, but it begins and ends with stops related to ice-marginal volcanism. The first stop is along the roadside in Stevens Canyon. If driving east from Longmire or Paradise, set the odometer at the parking area on the south shore of Reflection Lakes, then drive 5.1–5.3 miles (8.2–8.5 km) down into Stevens Canyon, stopping at one of several pullouts on the right side of the road. The road passes through a tunnel at 5.5 miles (8.9 km), and if you reach this, you have gone slightly too far and should turn around where safe. If driving west from the Ohanapecosh entrance to Mount Rainier National Park, set the odometer at the Box Canyon parking area, then continue 1.8–2.2 miles (2.9–3.6 km), passing through two tunnels, and then stopping at one of several pullouts on the left. The rock-lined pullout is perhaps the best single viewpoint.

Stop 1, Stevens Canyon Overlook (46°46.060′ N., 121°40.461′ W.; UTM 10T, 5180199N, 601219E)

The purpose of this stop is to view the products of Quaternary ice-confined volcanism. The geology (Fiske and others, 1963) underlying the lower approximately one-third of the canyon and Stevens Ridge (uphill from the road) consists of rhyolite tuff of the late Oligocene Stevens Ridge Formation intruded by Miocene granodiorite of the Stevens pluton. The pluton occupies the upper part of the canyon and upper Stevens Ridge. The high peaks across the canyon to the southwest are the Tatoosh Range. In the southeast (left, as viewed) these peaks consist of Oligocene Ohanapecosh Formation andesitic lavas and breccias overlain in the high peaks by Stevens Ridge Formation rhyolite tuff. In the northwest (right, as viewed), again, is the intrusive Stevens pluton, except for the tops of some of the highest peaks where pieces of the Stevens Ridge Formation rhyolite tuff remain as erosionally isolated remnants of the pluton's roof. The canyon is parallel to joints in the intrusive rocks, which likely accounts for its straight orientation.

The Quaternary geology (fig. 41) consists of dacitic lava on the opposite side of the canyon that forms two benches and the elongate ridge directly across the canyon from the viewpoint. Fiske and others (1963) interpreted the lava benches and ridge as an example of progressive entrenchment of a canyon, into which lava occasionally flowed, leaving a succession of benches that were younger with greater proximity to the canyon floor. That reasonable interpretation preceded the advent of high-precision argon geochronology and the availability of relatively inexpensive and rapid whole-rock chemical analyses. Later geologic mapping, supported by K-Ar and then $^{40}Ar/^{39}Ar$ dating, as well as geochemistry, showed that both benches and the ridge, as well as lava on the crest of Mazama Ridge uphill to the north, are the same lava flow, and another explanation was required to account for the various lava benches. Take a look and come up with some ideas, then read on.

The long band of cliffs in the foreground across the canyon exposes dacite lava, with the top of the flow at about our level. The crest of this lava ridge is about 700 ft (215 m) above the floor of Stevens Canyon. The base of the lava is concealed by talus in the slope facing you, but exposures of lava and Tertiary rocks closely approach one another on the back side of the ridge, establishing a flow thickness of about 400 ft (120 m); because the opposite canyon wall slopes toward us, this is a minimum thickness for the proximal side of the lava flow. The lower end of the ridge exposes exceptionally long columns that are gracefully curved and gently inclined, and at least two protuberances on the side of the lava facing you that have flat-lying columns on their steep left and right sides, all consistent with an ice-marginal lava flow. Looking up and across the canyon to the right, one sees a higher flat-topped platform with low lava cliffs along its upper edge, giving way downslope to talus; this is the intermediate level lava bench. Its flat top lies about 720 ft (220 m) above the crest of the lava ridge in the lower canyon, and the platform is about 0.25 km wide by 0.5 km long. Behind and upcanyon from this is the highest platform, known as The Bench, which supports Bench Lake (The Bench is visible indistinctly from pullouts in the mid-canyon, but not from the pullout in the lower canyon by the mouth of the tunnel). The top of The Bench is about 0.25 km across by 0.75 km long and stands about 230 ft (70 m) above the top of the intermediate level lava platform.

Coherence of whole-rock chemical compositions, appearance (abundant andesitic quenched inclusions), and consistent ages close to 90 ka for samples from up and down the canyon, atop Mazama Ridge, and to as high as the apex of Cowlitz Rocks near the terminus of the Paradise Glacier, establish that all the aforementioned lava benches and ridge are the same lava flow, known as the dacite of Mazama Ridge. Lescinsky and Sisson (1998) recognized that The Bench lies immediately upcanyon from the tributary drainage of Unicorn Creek, and the intermediate-level platform lies upcanyon from the tributary drainage of Maple Creek. Both drainages have broad U-shaped cross sections, and Unicorn Creek heads in a cirque above Snow Lake, indicating that both supported glaciers during much of the Pleistocene that descended steeply from the Tatoosh Range and fed the trunk Paradise Glacier in Stevens Canyon. The interpretation put forward is that lava erupted from a site high on the edifice and flowed south down exposed rock, bounded on the east by the Paradise Glacier and

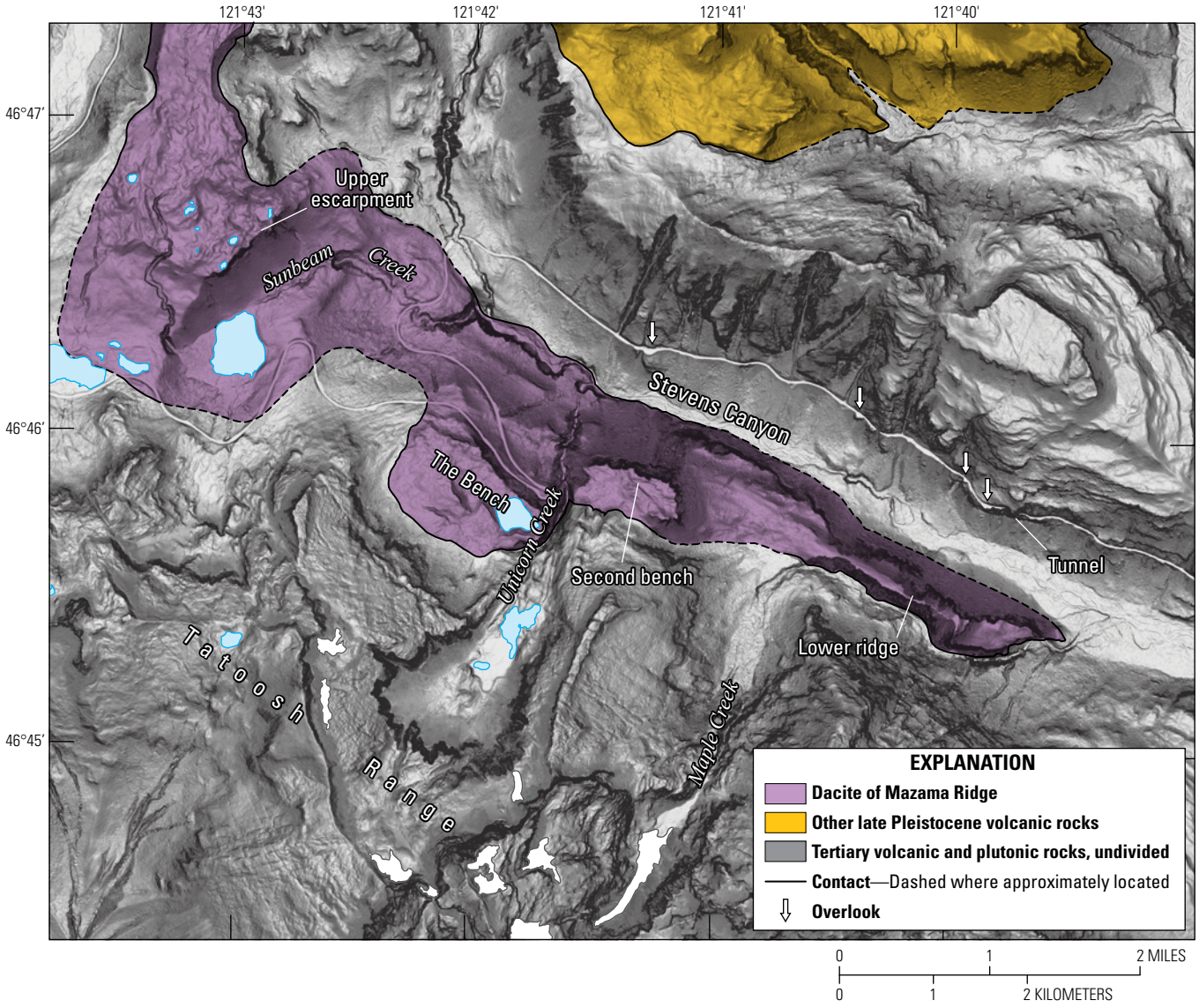

Figure 41. Simplified geologic map of lower Mazama Ridge and Stevens Canyon on the south-southeast side of Mount Rainier showing ice-impounded lava benches upstream from former glacial tributaries to the Pleistocene Paradise Glacier. The dacite of Mazama Ridge (purple) erupted about 90 thousand years ago and flowed south from the volcano, bounded on the east by the then-expanded Paradise Glacier that occupied Stevens Canyon. Tributary glaciers descended northeast from the Tatoosh Range, filling the valleys of Sunbeam, Unicorn, and Maple Creeks. The lava flow stalled upon encountering each successive tributary glacier, thereby building an upper escarpment, The Bench, and then an informally named second bench. After cutting the tributary Maple Creek glacier, the lava descended the southwest margin of the main Paradise Glacier, perhaps within a meltwater-incised ice canyon, creating a narrow lower ridge. Other Pleistocene volcanic rocks are shown in yellow, and Tertiary volcanic and plutonic rocks, undivided, are shown in gray. Geologic mapping after Fiske and others (1963), Lescinsky and Sisson (1998), and by T.W. Sisson. Base image is a slope map (darker is steeper) created from the light detection and ranging (lidar) digital topography of the Mount Rainier area of Robinson and others (2010).

on the west by an unnamed glacier that occupied the valley of Paradise Creek. The lava eventually reached the barrier of the Tatoosh Range and diverted east into Stevens Canyon, bounded between the trunk Paradise Glacier on the northeast and by the Tatoosh Range on the southwest. Lava advanced along the glacier margin until reaching the tributary Unicorn Glacier in the Unicorn Creek drainage that arrested forward progress. Lava accumulated behind this ice dam, building the platform of The Bench. Eventually the lava melted through the Unicorn Glacier and continued its advance down the southwest margin of the trunk Paradise Glacier until reaching the tributary Maple Creek glacier in the Maple Creek drainage. Again, the tributary glacier arrested lava advance, lava accumulated behind the ice dam and constructed the intermediate bench (labeled second bench on fig. 41), then eventually melted through the Maple glacier and continued down the southwest edge of the main Paradise Glacier until the eruption ended and lava advance ceased. The sweeping columns at the lower end of the ridge mark where the end of the lava flow abutted thick ice of the trunk glacier, and the protuberances on the side of the flow with their horizontal columns, are regions where the lava injected short distances laterally into the glacier, possibly at the sites of major crevasses.

Stop 2, Reflection Lakes, at the Westernmost of Two Pullout Areas (46°46.100′ N., 121°43.856′ W.; UTM 10T, 5180202N, 596897E)

From SR 123, 17.7 miles (28.5 km) along the Stevens Canyon Road is the Reflection Lakes parking area on the right side of the road. Park at the second of two pullout areas.

This is primarily a scenic stop. The Reflection Lakes lahar (7,250–7,000 cal. yr B.P.) is one of three generated by avalanches of hydrothermally altered rock that inundated the south flank of Mount Rainier prior to the Osceola Mudflow. The Reflection Lakes lahar swept through a notch in Mazama Ridge to the northwest of us and into Reflection Lakes basin. It did not descend Stevens Canyon east of here; rather, the bulk of the flow remained in Paradise and Nisqually River valleys west of the ridge. The lahar was triggered during eruptions of the Cowlitz Park period.

Travel 1.3 miles (2.1 km) to Paradise Road and follow that road 2.2 miles (3.5 km) to Paradise, park, and walk to the Henry M. Jackson Memorial Visitor Center.

Stop 3, Paradise Lahar near Henry M. Jackson Memorial Visitor Center (46°47.619′ N., 121°44.008′ W.; UTM 10T, 5183013N, 596658E)

From the visitor center, follow the Skyline Trail northeast 0.5 miles (0.8 km) almost to Edith Creek bridge, then walk left 0.2 miles (0.3 km) along a road leading north that is closed to the public. Permission to walk this service road must be obtained in advance from the National Park Service. On reaching a small National Park Service building at the end of this service road, go left about 50 m to a 70-cm tephra section.

The section exposes Summerland and Osceola period tephras overlying the Paradise lahar (~5,700 cal. yr B.P.). Tephra layers are thinner here, and some units are missing entirely because prevailing winds are generally from the west or southwest and most tephra lobes are thickest to the east and northeast. The Paradise lahar is the last of several rock avalanche-induced lahars that inundated the south flank of the volcano. Nearby streamcuts show that the lahar deposit is generally 1–2 m thick in this area. The lahar overtopped the so-called “Skyline Ridge” (between Alta Vista and Panorama Point) to our west and descended the Paradise River valley to the south. The Paradise lahar was the last of the three that resulted from avalanches of water-saturated debris that came from supergene (shallow) hydrothermally altered source rock that once cropped out high on the south flank of the volcano. Debris from this and the other two south-side avalanche-induced lahars (Reflection Lakes and Van Trump Park) all contain altered rock characteristic of a shallow near-surface hydrothermal system (John and others, 2008). This source slid away when the Osceola edifice collapse carried the pre-5,600 cal. yr B.P. summit of Mount Rainier away to the northeast. The volcano has generated no such avalanche-induced lahars on its south side in the past 5,600 years.

Stop 4, Paradise Lahar Pinchout along Golden Gate Trail (46°47.731′ N., 121°43.696′ W.; UTM 10T, 5183227N, 597052E)

Return to the Skyline Trail, cross Edith Creek, and go left on the Golden Gate Trail 0.3–0.4 miles (~2,000 ft [610 m]).

Along trail cuts, the Paradise lahar thins to about 20 cm then pinches out entirely. This is the inundation limit of the Paradise lahar. As the Paradise lahar thins, another similar lahar appears in section beneath it; this is the Reflection Lakes lahar. Just up trail, we can see tephra layer F in section. Unlike at Sunrise, hydrothermal clay is absent in layer F here; it consists entirely of coarse pumiceous ash and lapilli in a ~1 cm layer.

Stop 5, Reflection Lakes Lahar in Cowlitz Park Section, Mazama Ash Below, along Golden Gate Trail (46°47.834′ N., 121°43.604′ W.; UTM 10T, 5183419N, 597166E)

Continue up Golden Gate Trail a distance of about 1,000 ft (305 m) to an outcrop along a trail cut (fig. 42). The outcrop exposes the complete Osceola (5,600–4,500 cal. yr B.P.) and Cowlitz Park (7,400–6,400 cal. yr B.P.) tephra sections, with Mazama ash at the base (7,600 cal. yr B.P.) (fig. 42). All the tephras are SVG ashes except layer F, the basal Osceola period tephra.

About 40 cm of the Reflection Lakes lahar is interbedded in the Cowlitz Park section. We can trace this lahar at least 60 m higher along trail switchbacks. To the south, we can see the notch in Mazama Ridge by means of which the lahar flowed into Reflection Lakes basin. The lahar came within 15 m of overtopping Panorama Point to the northwest. Judging from runup limits, the Refection Lakes lahar must temporarily have filled this

valley to depths of as much as 200 m. The flow was as deep or deeper in neighboring Nisqually River valley to the west.

Stop 6, Former Paradise Ice Caves along Paradise Glacier Trail (near 46°47.995' N., 121°42.840' W.; UTM 10T, 5183733N, 598133E)

Continue up the steep Golden Gate Trail through switchbacks to its intersection with the Skyline Trail. Shortly before the intersection, you pass from the andesite of Pebble Creek (214 ka) to the overlying dacite of Mazama Ridge (90 ka). Turn right on the Skyline Trail and descend 0.6 miles (1 km) to its junction with the Paradise Glacier Trail. Turn left and ascend the Paradise Glacier Trail, noting the quenched magmatic inclusions that are abundant throughout the dacite of Mazama Ridge. Follow the Paradise Glacier Trail up about 0.6 miles (1 km) to the right (east) side of a low bluff decorated with dark, narrow, columns. Until late summer a north-trending snowbank may lie along the east side of this low bluff. This outcrop is the east edge of the dacite of Mazama Ridge, seen earlier today in Stevens Canyon, and is a locality where the active lava flow tucked its edge beneath the margin of the then-much-larger Paradise Glacier. Erosional remnants of the dacite of Mazama Ridge also cap the ridge up and across the valley to the northeast, including the craggy crest of Cowlitz Rocks. This is a good place to examine ice marginal chilling. Look for some columns developed on the top of the lava flow indicating it was sub-glacial in this area.

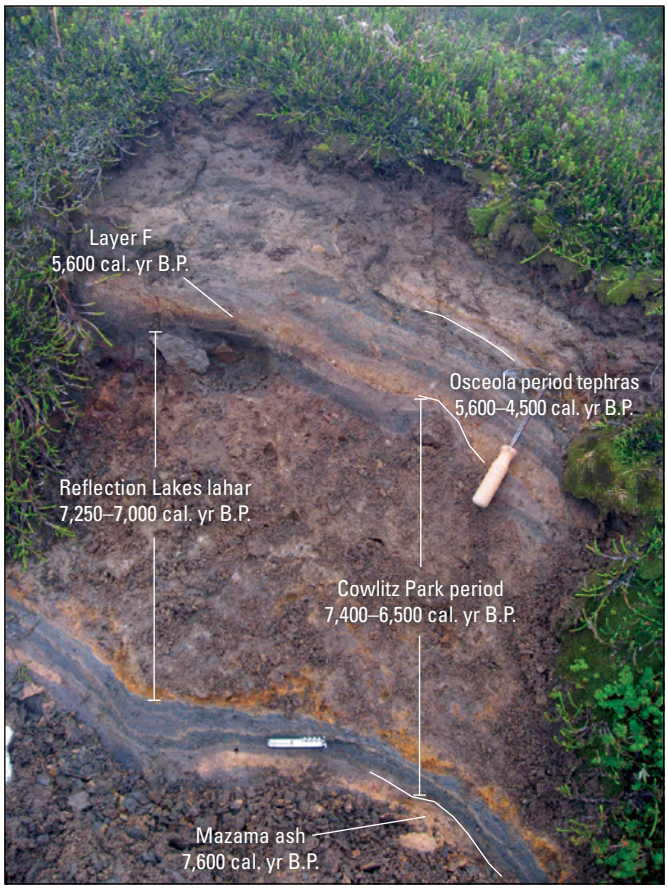

Figure 42. Photograph of Golden Gate Trail cut that shows deposits of the Osceola and Cowlitz Park eruptive periods (day 3, stop 5). Cowlitz Park age tephras sandwich the Reflection Lakes lahar and overlie the Mazama ash. Upsection is a sequence of tephras of the Osceola eruptive period. The lowermost of these tephras, layer F, erupted during the Osceola edifice collapse. Layer F here is thin and consists entirely of pumice, unlike the thick and clayey deposits near Sunrise in Yakima Park. Summerland age tephras are present in this area but at this outcrop are disturbed by soil and hillslope processes. All tephra units are relatively thin here on the south flank of the volcano because the predominant wind direction is from west to east. Ages given in calendar years before present (cal. yr B.P.). Photograph by Jim Vallance, U.S. Geological Survey.

The Paradise Glacier Trail was originally established to provide access to an ice cave network in the lower Paradise Glacier. In the early 20th century, the Paradise Glacier filled the basin in the foreground uphill from the field trip stop, continuous with the present Paradise Glacier, the toe of which can be seen on the upper left side of the valley. In the 1930s, the glacier thinned to the degree that it separated into an upper active glacier and a lower region of stagnant ice. Park visitors would hike to about the field trip stop location where they could enter a large cave in the ice along the main meltwater stream. This lower glacier differed from most areas of stagnant ice in the park by its lack of a thick carapace of till, with the result that the danger of falling rocks was less than at most glacier termini. The meltwater stream was also smaller than most, with a low gradient, so entering the cave was neither difficult nor obviously dangerous. By the late 1980s, the lower glacier and its ice cave system had melted away. The Paradise Glacier was even larger during the Little Ice Age when it also filled the low, flat basin downstream to the southeast to about the brink of the steep drop-off into Stevens Canyon. That area of ice also appears to have melted largely in place, with little surficial moraine, leaving low ribs of rock debris, elongate in the former flow direction of the ice. These are features left from the bed of the glacier, and it is as though the glacier was simply lifted away, exposing its floor. After enjoying the view and speculating on the complicated little columns, return to Paradise by the path of your choice. Following the Skyline Trail counterclockwise back to Paradise affords many opportunities to examine Mount Rainier lava flows and some breccias up close, as well as providing exceptional views of the Nisqually Glacier and of the upper south flank of Mount Rainier.

Day 4. Mildred Point: All Day Hike

This is an entirely hiking day on Mount Rainier's south flank to see ice contact features on the face of a late Pleistocene lava flow, passing the beautiful and popular Comet Falls, and ascending to a vantage point where Mount Rainier's largest known pyroclastic flow deposit can be viewed. The hike commences at the parking pullout (46°46.719' N., 121°47.037' W.; UTM 10T, 5181284N, 592831E) for the Comet Falls Trail along the road from Longmire to Paradise and climbs 2,300 ft (700 m) in less than 3 miles (4.7 km) to Mildred Point (5,940 ft [1,811 m]), which

overlooks the canyon at the head of Kautz Creek. Parts of the trail are steep, and at a moderate pace this trip will occupy the better part of a day round trip, so carry food, water, and adequate clothing. If the weather is low overcast, the upper half of the hike may be in dense fog. The lower half of the walk is still worthwhile, and in summer months low overcast in the mornings commonly gives way to sunny afternoons, so a probing optimistic effort may be rewarded. Consult the map (fig. 43) for summary geology and itinerary.

Commence hiking up the stairs at the northeast end of the parking pullout. This pullout is just southwest (toward Longmire and Ashford) from Christine Falls on the road to Paradise. The

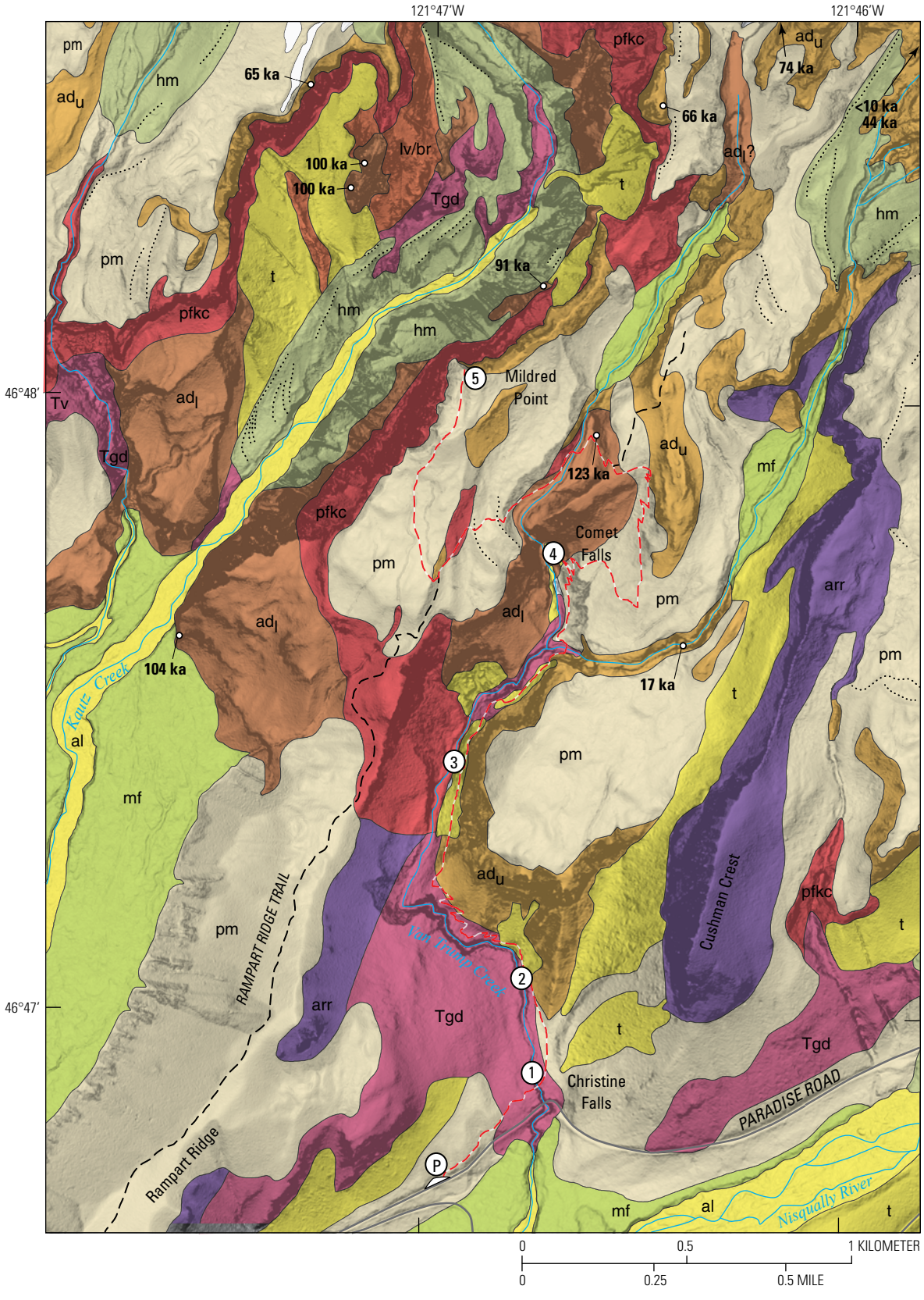

initial several hundred meters of the trail are in poorly exposed Pleistocene moraine and covering slope wash and talus, but an outcrop of the Nisqually granodiorite (of the Tatoosh intrusive suite) soon appears, followed by a wooden bridge over the slot canyon cut by Van Trump Creek into the granodiorite.

Stop 1, Bridge over Van Trump Creek near the Trailhead (46°46.908′ N., 121°46.800′ W.; UTM 10T, 5181639N, 593128E)

The wood bridge over Van Trump Creek is a good place to view the granodiorite. The Tatoosh intrusive suite encompasses the various exposures of Miocene granitic-textured (hypidiomorphic-granular) intrusive rocks in the immediate Mount Rainier area. These rocks span from quartz diorite to granite, and they were originally referred to collectively as the Tatoosh pluton (Fiske and others, 1963), but later detailed mapping and U-Pb zircon geochronology (Wright, 1961; Mattinson, 1977; Thompson, 1983; du Bray and others, 2011) showed that those on the south side of the volcano could be subdivided into four dominant intrusions, from south to north and from oldest to youngest (rounded to nearest 0.5 Ma): the Stevens pluton (19 Ma), the Reflection and Pyramid plutons (18.5 Ma), and the Nisqually pluton (17.5 Ma). Mount Rainier obscures the northern limits of these intrusions, but similar granitic rocks appear from beneath the north foot of the volcano in the upper White River, with a U-Pb age of 14 Ma (Mattinson, 1977), so emplacement of the suite spanned approximately 5 million years. Although the rocks look in hand sample like ordinary granodiorites, some have granophyric groundmass textures indicating rapid final solidification. Portions of the roof of the Stevens pluton are preserved in the higher peaks of the Tatoosh Range as erosionally isolated remnants of the late Oligocene Stevens Ridge Formation intruded by the underlying granodiorite. Numerous small, brecciated regions and veining in the plutons and in associated roof rocks result from explosive loss of volatiles from the solidifying intrusions. Such evidence for volatile loss, volatile expansion, and rapid solidification are consistent with emplacement at shallow depths (low confining pressures and low wall rock temperatures). Stratigraphic reconstruction of the thickness of the late Oligocene to early Miocene Fifes Peak Formation, which overlies the Stevens Ridge Formation, allows for 1–2 km of overburden (du Bray and others, 2011), but the top of the Fifes Peak Formation is

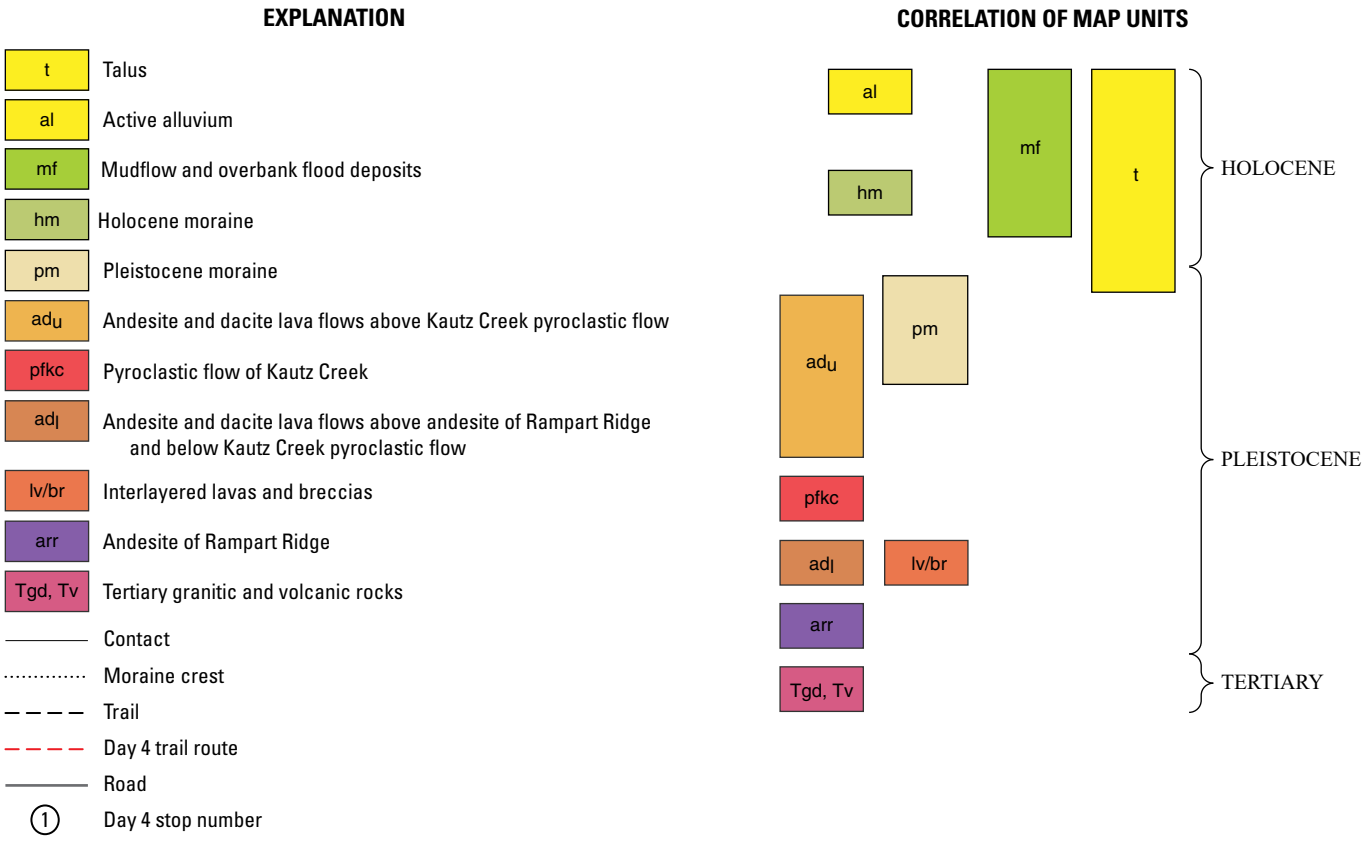

Figure 43. Geologic map of the Van Trump Creek, Kautz Creek, and Mildred Point areas. Circled numbers show stops for day 4 of the field trip. Small circles show samples collected for geochronologic dating; ages are given in kilo-annum (ka). Geologic mapping from Fiske and others (1963) and by T.W. Sisson. Base is a slope map (darker is steeper) from light detection and ranging (lidar) digital topography of the Mount Rainier area of Robinson and others (2010).

eroded, and as a volcanic deposit, its thickness was probably quite variable spatially, so these are minimum estimates. The Fifes Peak Formation is overlain disconformably along the east side of the southern Washington Cascade Range by the early to middle Miocene Grande Ronde Basalt of the Columbia River Basalt Group. Projecting the regional east to southeast dips (3–8°) of the Grande Ronde Basalt (Schasse, 1987), the 45–55 km to the Mount Rainier area would place the top of the Fifes Peak Formation 3–6 km above the present ground surface. From these considerations, the emplacement depth of the exposed level of the Tatoosh intrusive suite is estimated loosely at 1–6 km, indicating average exhumation rates in the range of 0.05–0.4 mm/yr.

After viewing the slot canyon from the bridge, continue walking a short distance up the trail, stopping where the forest opens and reveals a low ridge on the right made up of black, glassy columns and a dark cliff directly ahead (north).

Stop 2, Dacite of Van Trump Creek, along Comet Falls Trail (46°47.053′ N., 121°46.811′ W.; UTM 10T, 5181907N, 593110E)

The dark cliff is the front face of the dacite of Van Trump Creek (63.0 weight percent SiO_2), which erupted at 17±2 ka, and the low ridge on the right (east) side of the trail is a finger of columnar jointed lava extending south from the end of the flow, albeit largely degraded into talus. The lava flow forms a bench on the east side of Van Trump Creek, about 650 ft (200 m) tall and about 0.3 miles (0.5 km) across. Rock cliffs on the front face and west side of the bench, as well as the low finger extending to the south, are dark owing to abundant groundmass glass, and all the steep faces of the bench are decorated with columnar joints. These features result from the lava having embanked against the then-larger Nisqually Glacier, as well as against a small tributary glacier then occupying the lower Van Trump Creek drainage; lava accumulated behind the impounding ice, building the bench. The top of the bench is at about 4,800 ft (1,460 m) elevation, which would have been close to the surface of the Nisqually Glacier at the time of eruption. The low ridge trending south from the flow front may mark the location of a meltwater channel beneath the ice, enlarged and exploited by the advancing lava flow. This lava flow erupted during the time of rapid worldwide deglaciation after the last glacial maximum, with global ice volume estimated within the window of uncertainty for the eruption age as 66–91 percent (at 18–14 ka, respectively) of that at the last glacial maximum (Lambeck and others, 2014). The high ridge to the right (east) of the bench is known as Cushman Crest and is an arm of the andesite of Rampart Ridge, which erupted at about 335 ka.

Continue along the trail as it bends to the west (left), encountering small exposures of granodiorite at trail level, then switchback up and to the north to the pass along the steep west face of the lava flow.

Stop 3, Lava Bench along Comet Falls Trail (46°47.326′ N., 121°46.998′ W.; UTM 10T, 5182409N, 592864E)

As you traverse the steep west face of the lava bench, look back and above the trail for a buttress of black, columnar jointed lava showing through the vine maples. Note the horizontal orientation of the columns, indicating that the lava here was cooling through its side, and that the steep side of the flow is its original margin. Not well exposed, but discernable through the trees across Van Trump Creek, are rough, somewhat rounded exposures of block-and-ash-flow breccia. We will see these breccias more clearly later in the hike from Mildred Point, so do not concern yourself searching for a better view.

Continuing north up the trail along the west wall of the lava bench, you will pass columns at trail level, and then you will cross small outcrops of granodiorite, showing that the trail is built at about the level of the base of the lava flow. Across the creek you will see a southeast-facing alcove with lava cliffs. These are part of the dacite of Comet Falls that unconformably underlies the block-and-ash-flow breccia. The dacite of Comet Falls is better exposed at stop 4, so continue up the trail, crossing a log bridge over the east fork of Van Trump Creek to a good view of Comet Falls. Look upstream from the log bridge to see the dacite of Van Trump Creek crossing the creek, defining a waterfall above the granodiorite.

Stop 4, Comet Falls (46°47.751′ N., 121°46.775′ W.; UTM 10T, 5183202N, 593135E) and Vicinity

Depending on the severity of spray, either view the falls from the sheltered stand of trees just past the bridge or continue up the trail and out a side path to near the base of the falls, stopping at the limit of one's willingness to get wet. Comet Falls drops freely 380 ft (116 m) through the eponymous dacite of Comet Falls that erupted at 123 ka. The thick dacite flow overlies several thinner, apparently conformable flow units exposed in the creek bed that, in turn, overlie granodiorite. No ice contact features have been found preserved on the surfaces of the dacite, but its thickness, its vertical cliff-forming sides, and the rib-and-chute morphology near the top of the flow are reminiscent of ice-marginal lava flows elsewhere on Mount Rainier.

Rib-and-chute structures consist of steep-sided rock ribs at the upper edge of a lava flow, with the ribs oriented approximately parallel to one another and perpendicular to the flow margin. Ribs are spaced about 10–50 m apart and are separated by broad chutes that incline steeply down the top edge of the flow. On some ice-marginal lava flows at Mount Rainier, the sides of ribs and floors of chutes are lined by columnar joints with their long axes oriented perpendicular to the rib and chute surfaces; that is, such columns are radial to the rib and chute surfaces. Columnar jointed chutes can be interpreted as former channels where glacial meltwater cascaded over the surface of the still-hot lava flow, and then down over the flow margin into the trench between the lava and

confining ice. Cascades of meltwater chilled the floors of channels more than the banks, and some banks remained hot enough to extrude into channel-parallel spines (ribs) as molten lava continued to inflate the flow against the confining glacier.

From Comet Falls, the trail begins a long switchbacking climb through the trees with little exposure until reaching the ridge crest southeast of, and slightly higher than, the top of the falls. A couple of isolated outcrops of andesitic lava are passed in open areas near the top of the climb. Their location is consistent with being younger than the dacite of Comet Falls, but poor exposures preclude more detailed geologic interpretations. On clear days one can see Mount St. Helens to the south, which enlivens this otherwise monotonous section of the hike. Eventually the switchbacks end, and the trail trends west to attain the crest of the ridge above and southeast of Comet Falls where you will meet a trail junction (46°47.876' N., 121°46.627' W.; UTM 10T, 5183435N, 593320E). The right fork continues up the ridge to a small, designated camping area and beyond, petering out at snowfields, talus, and till on lower Wapowety Cleaver. Our route takes the left fork (west and northwest), dropping to the bed of the west fork of Van Trump Creek. The bed of the creek is filled with deposits from small-volume debris flows, with fines variably washed out by later stream activity, leaving jumbled boulders. A lava flow crosses from the west to the east banks of the creek above a small exposure of unconsolidated diamict. The lava flow and diamictite unconformably overlie the dacite of Comet Falls, and this lava probably underlies the block-and-ash-flow deposits that will be seen from Mildred Point, but the exposure of this flow is too small to merit radiometric dating. The trail heads southwest and crosses the creek, with the upper surface of the dacite of Comet Falls exposed in the creek bed toward the brink of the falls. After leaving the creek, the trail climbs slightly onto Pleistocene moraine on the west bank. You will then pass one outcrop of indurated breccia on the right side of the trail (west), before reaching an intersection with a path on the right (46°47.713' N., 121°47.048' W.; UTM 10T, 5183125N, 592789E) that ascends steeply to Mildred Point. Follow this non-maintained path generally north through Pleistocene till and reworked Holocene tephra to the top of Mildred Point for a view and well-earned rest.

Stop 5, Mildred Point (46°48.035' N., 121°46.994' W.; UTM 10T, 5183722N, 592849E)

Mildred Point overlooks the canyon at the head of Kautz Creek, with the creek nearly 1,000 ft (300 m) below you. When the USGS prepared a 1-inch to 1-mile scale topographic map of Mount Rainier National Park, published in 1955, the terminus of the Kautz Glacier lay about directly below you at close to 4,850 ft (1,478 m) elevation, but by the 1970 map revision, at 2.5-inches to 1-mile scale, released in 1971, the terminus had retreated 1.3 km (0.8 miles) up the canyon to about 6,000 ft (1,829 m) elevation, and as of 2016, it lay another 0.6 km (0.4 miles) up the canyon at about 7,050 ft (2,149 m), or about 1.7 km (1.05 miles) directly north of Mildred Point. Such retreats are typical for glaciers on the volcano's south flank (Sisson and others, 2011).

Two sketches of the simplified geology visible from Mildred Point are presented in figure 44 (the west perspective) and figure 45 (the east perspective). Miocene granodiorite of the Tatoosh intrusive suite floors the canyon, mantled thinly by Holocene glacial moraine; multiple moraine crests are visible, but their ages have not been investigated. Overlying the granodiorite are (clockwise from southwest to northeast) a thick andesite lava flow (age on the southeast side of the Kautz Creek is 104 ka) that creates a restriction or narrows that separates the deep canyon of upper Kautz Creek from its broad lower valley, a complex of lava flows and interstratified sintered breccias (100 ka; labeled lv/br on fig. 44), and weakly consolidated breccia (labeled br on fig. 44) on the northeast bank just overlooking Kautz Creek, overlain by a lava flow dated at 91 ka. Contact relations between the 104–100 ka lavas and breccias and the 91 ka lava are exposed only in the upper canyon of Kautz Creek and have not been visited because of rockfall hazards.

Above these lavas lies the block-and-ash-flow deposit (pf on fig. 44) that forms the tall, columnar jointed cliffs encircling upper Kautz Creek, including the columnar jointed cliffs located just beneath you. Across the canyon to the northwest, the cliffs attain their greatest heights of 450–500 ft (135–150 m). Columnar joints pass continuously through that section with no breaks, showing that the deposit cooled as a single unit. The induration and columnar jointing are reminiscent of welded tuffs, but no densely welded regions have been found, and the deposit is more properly considered as sintered, with vapor-phase silica partly filling pore spaces and cementing ash grains, and with limited flattening of sparse, pumiceous ash that is only discernable in thin sections. The prominent columnar joints led to the name Basalt Cliff being applied to the bluffs in view across the valley to the northwest, although juvenile glassy clasts in the deposit are actually dacite. The block-and-ash-flow deposit has not been dated directly because of its inappropriately glassy and porous texture, but it has been traced east as far as the west wall of the Nisqually River valley, where it is stratigraphically higher than a lava flow dated at 83±2 ka. In the gully just east of Cushman Crest, the sintered block-and-ash-flow deposit is overlain conformably (or disconformably) by a small-volume, unconsolidated pumiceous pyroclastic flow, similar in phenocryst assemblage and bulk composition to the dacite pumice fall of Sunset Amphitheater, dated at 85±6 ka (Sisson and others, 2019). If that correlation is correct, these results lead to the not-unreasonable interpretation that the largest pumiceous fall and the largest pyroclastic flow in the past 100,000 years at Mount Rainier were produced by the same eruption. In the headwaters of Kautz Creek, the block-and-ash-flow deposit is overlain disconformably by andesite and dacite lava flows, two samples of which from opposite sides of the canyon are dated at 65 and 66 ka. These erupted early in the Point Success substage, during which the upper south and north flanks of the volcano were constructed.

Based on the considerable thickness of the pyroclastic flow cooling unit in upper Kautz Creek, one might expect the deposit to be preserved for great distances down-canyon, but this is not so. The deposit continues only another 0.5 miles (0.8 km) to the

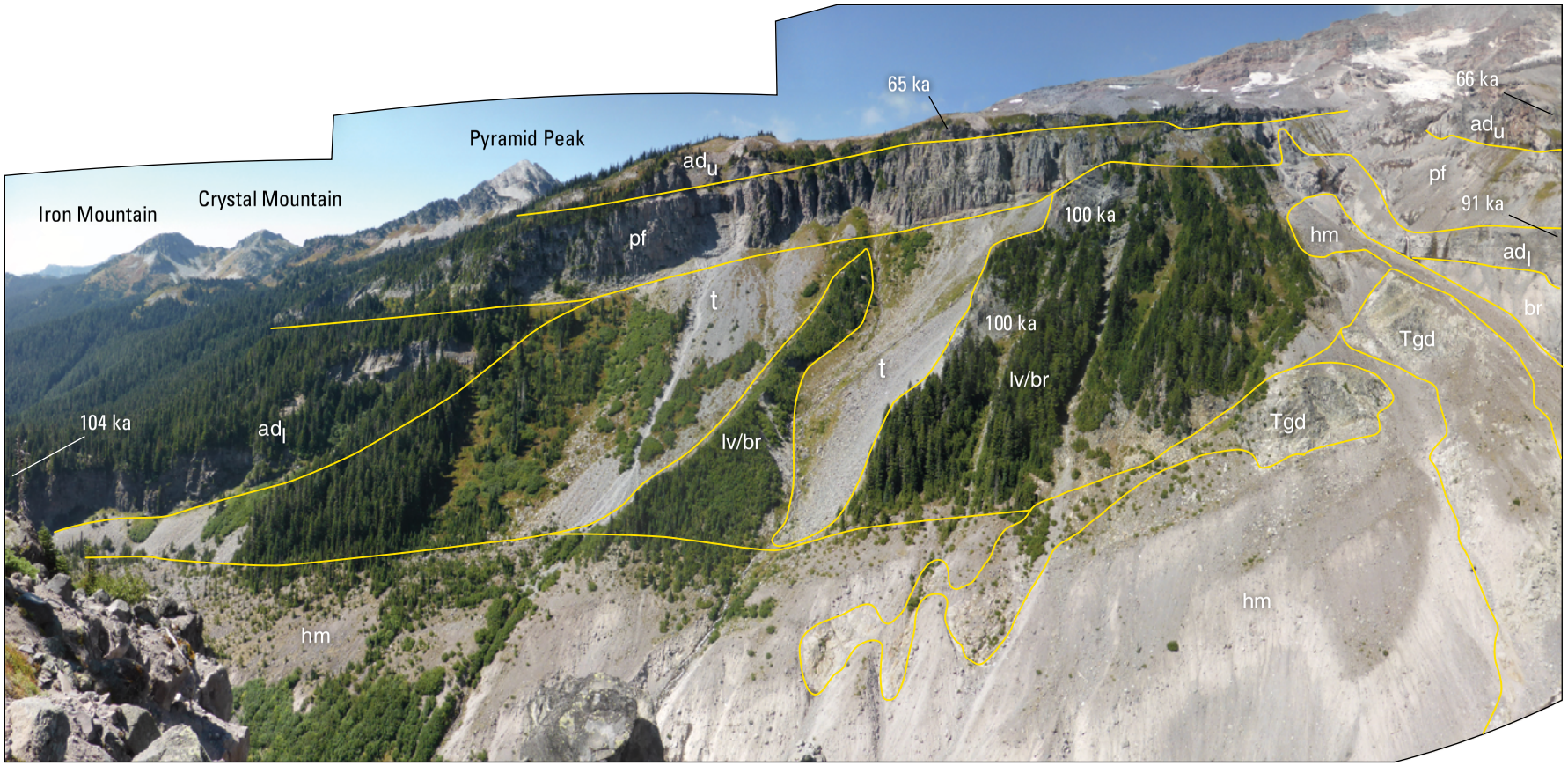

Figure 44. Annotated photograph looking west from Mildred Point (day 4, stop 5). Pyramid Peak, Crystal Mountain, and Iron Mountain are composed of Tertiary volcanic rocks. Andesite from ~65 thousand years ago (ka; labeled ad_u) that caps the ridge to the west overlies pyroclastic-flow deposits (pf), which in turn overlie lavas ranging in age from 104 to 91 ka (ad_l). Other labeled units are Tertiary granodiorite (Tgd), breccia (br), interlayered lava and breccia (lv/br), Holocene moraine (hm), and talus (t). Photograph by Tom Sisson, U.S. Geological Survey.

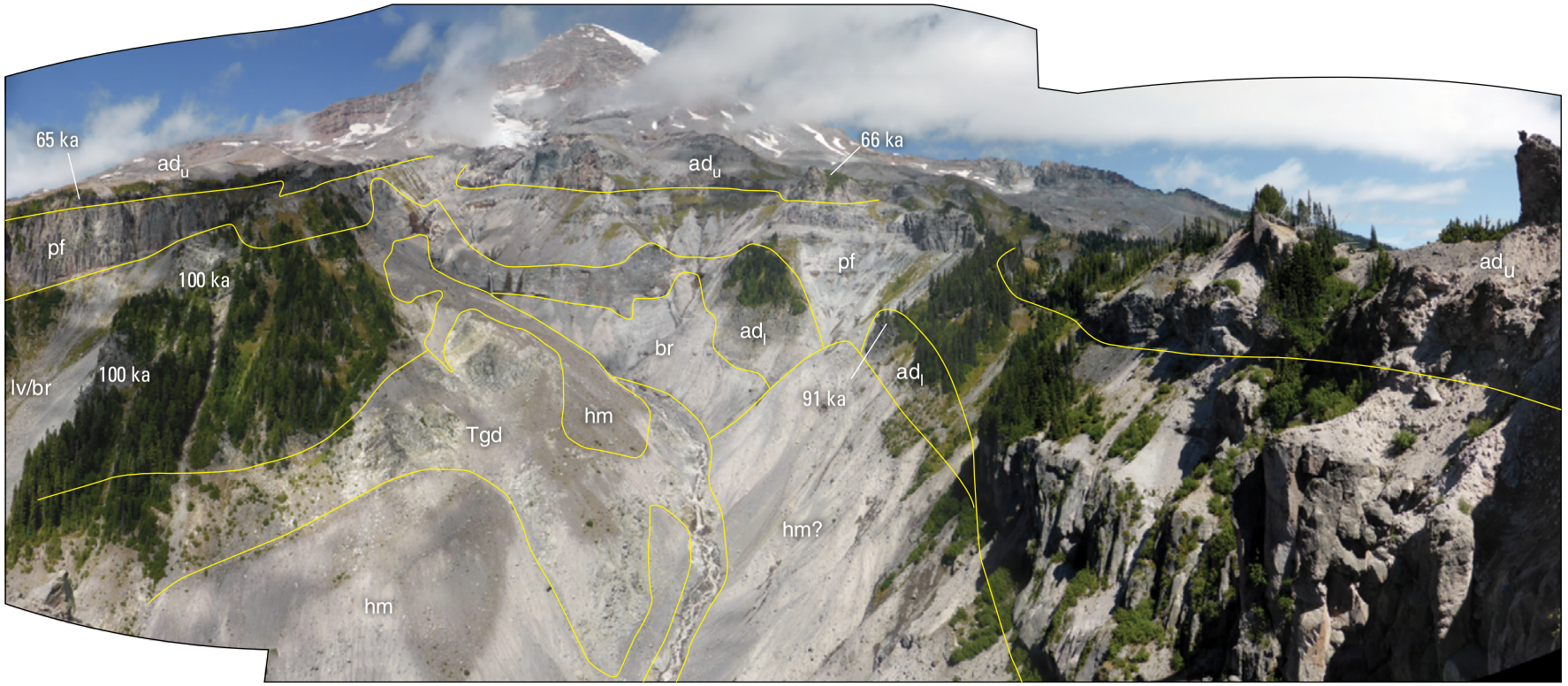

Figure 45. Annotated photograph looking north toward Mount Rainier from Mildred Point (day 4, stop 5). Andesite from ~65 thousand years ago (ka; labeled ad_u) that caps the ridge to the west overlies pyroclastic-flow deposits (pf), which in turn overlie lavas ranging in age from 104 to 91 ka (ad_l). Other labeled units are Tertiary granodiorite, (Tgd), breccia (br), interlayered lava and breccia (lv/br), and Holocene moraine (hm). Photograph by Tom Sisson, U.S. Geological Survey.

southwest from the lower end of the prominent cliffs across the canyon. The sintered and jointed deposit supports Pearl Falls, 400 ft (120 m) tall, and then thins and is lost from exposure. A possible explanation for the considerable thickness of the deposit in the headwaters of Kautz Creek, as well as its failure to continue far from the volcano, is that early phases of the eruption melted a basin through the head of the then larger Kautz Glacier but could not melt the thick valley glacier farther downstream. Block and ash debris embanked behind the beheaded valley glacier, filling the basin of the upper Kautz Creek with as much as 500 ft (150 m) of hot pyroclastic debris that then cooled, sintered, shrank, and cracked. Pyroclastic debris that traveled farther onto the surface of the valley glacier was later carried away and lost from the geologic rock record, and reestablishment of the upper glacier also removed the pyroclastic deposit from the axis of the upper basin.

It is possible to continue northeast from Mildred Point (toward the volcano) to reach cliffs in the sintered and jointed block and ash breccias. This involves traversing the crest of the ridge, in places keeping right to avoid bushes and overly steep sections, and takes about 20 minutes, but is off-trail and requires agility, fitness, and proper boots or sturdy trail shoes. If not so inclined, retrace the route past Comet Falls and lower Van Trump Creek to the parking area.

Day 5. Holocene Lahars in Nisqually River Drainage

Stop 1, Ricksecker Point, Paradise Lahar, and 43-ka Lava Flow

From the road between Longmire and Paradise (SR 706) turn onto the scenic loop road for Ricksecker Point (fig. 46). Starting from Longmire, this turn is 6.2 miles (10 km) toward Paradise, and is 5.2 miles (8.4 km) toward Longmire from Paradise. Ricksecker Point is named for Eugene Ricksecker, who, commencing in 1903, designed and surveyed the route now followed by the road between Longmire and Paradise. By 1910, road construction was sufficient that Paradise could be reached on horseback and by stock-drawn wagons, but construction was not fully completed and the road open to regular use by public automobiles until 1915. On October 8, 1911, President William Howard Taft reached Paradise in an automobile, although mules were required to pull his car through the mud some of the last 2 miles (3.2 km). Taft had been Secretary of War when the road was initiated, and he had assigned its construction to the U.S. Army Corps of Engineers that engaged Ricksecker. Eugene Ricksecker was also involved in design and excavation of the Lake Washington ship canal in Seattle and in dredging to improve the Port of Tacoma. Before these projects, Ricksecker was employed by the USGS to survey parts of the Pacific Northwest, including producing a detailed topographic map of Mount Shasta published in 1897 as Shasta Special Map, California (scale 1:62,500).

The first turnout along the one-way loop road offers a clear view of Mount Rainier, the upper Nisqually River valley, and Nisqually Glacier. This will be a scenic stop if the weather is clear.

This promontory consists of a thick Mount Rainier lava flow whose steep, jointed edge borders the road down to the Nisqually River bridge. This is the youngest large lava flow at the volcano, with a radiometric age of about 43 ka. Ice-contact columns locally preserved on the steep sides of the flow, as well as its position high above the valley floors, show that the lava was impounded between flanking glaciers that filled the valleys of the Nisqually River and Paradise Creek (Lescinsky and Sisson, 1998).

About 0.9 miles (1.5 km) from the beginning of the loop, park to the right so that traffic can pass safely (46°46.103’ N., 121°46.419’ W.; UTM 10T, 5180156N, 593636E).

The Paradise lahar deposit can be identified from the road as the approximately 1-m-thick (3.3 ft) layer that sits on a thin (2–10 cm [0.8–4 inch]) orange band of volcanic ash from Mount Mazama, (~7,600 cal. yr B.P.). Mount St. Helens tephra layers Yn and Wn are the most visible deposits that overlie the Paradise lahar near the top of this outcrop. The deposit is about 270 m (800 ft) above the valley floor of the Paradise River at this location, indicating the lahar was at least temporarily that deep. Downstream at Longmire, the lahar remained more than 70 m (230 ft) deep, but its deposit is 1.2 m (4 ft) thick. The low ratio of deposit thickness to flow depth, combined with the wide variation in clay content, suggest the Paradise lahar may have been very fluid. Crandell (1971) observed that the Paradise lahar generally is a very thin deposit and lacks constructional topography.

Stop 2, Van Trump Creek Cutbank at Second Switchback above Cougar Rock Campground (46°46.589’ N., 121°46.942’ W.; UTM 10T 5181046N, 592956E)

From where the Ricksecker Point loop road rejoins the Longmire-Paradise Road, turn left, and drive 3.3 miles (5.3 km) down toward Longmire, crossing the Nisqually River, passing Christine Falls and the Comet Falls trailhead, to pull over in a car park on the west side of the road (right, heading downhill), shortly past a sharp hairpin turn (fig. 46). This site is also a 3.3-mile (5.3-km) drive above Longmire toward Paradise. From the pullout, cross the road and walk down its shoulder toward an opening in the trees overlooking the valley of Van Trump Creek. Take particular care crossing the road because of the blind corner for traffic ascending from Longmire, commonly heavy on the weekends. Walk about 50 ft to the edge of Van Trump Creek, drop over the cutbank and then move about 30 ft left (upvalley) to the outcrop (46°46.578’ N., 121°46.870’ W.; UTM 10T, 5181026N, 593048E).

The National lahar (2,300 cal. yr B.P.) and another Summerland lahar (~2,500 cal. yr B.P.) overlie two Mount St. Helens Pine Creek (P) ash layers (~2,600 cal. yr B.P.) and alluvium and underlie Mount St. Helens ash layer Wn (1479 C.E.). The earliest Summerland tephra is interbedded between the two P ash layers at the base of the lahars. These Summerland lahars were generated by interaction of hot rock and snow and ice during eruptions from the summit of the volcano. Although previous Summerland eruptions generated lahars to the northeast, lahars of

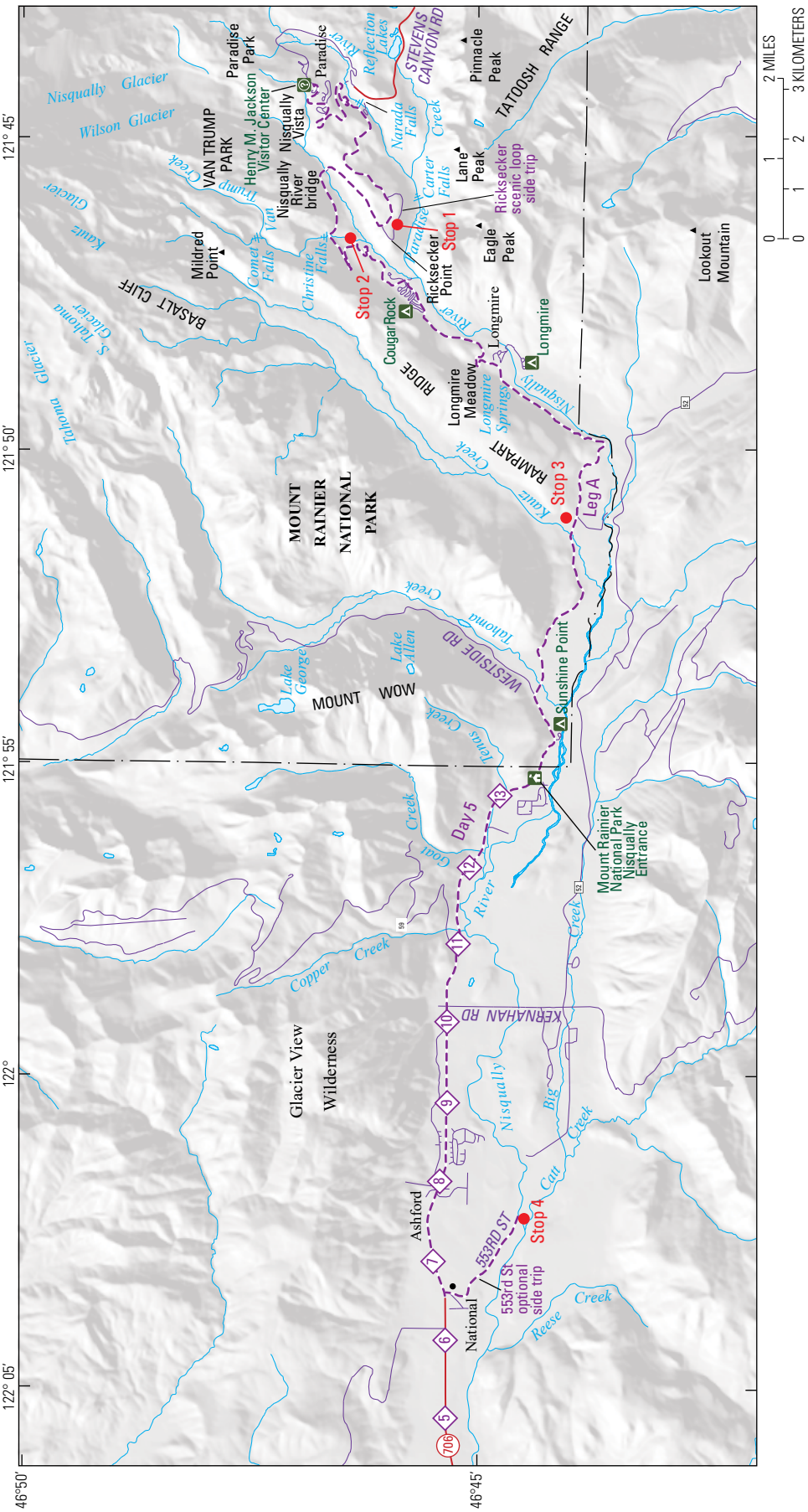

Figure 46. Map showing day 5 stops along the Nisqually River drainage. Diamond boxes are mileage markers. Modified from Pringle (2008).

this age are not present to the south. Apparently until middle to late Summerland time, the summit cone had not built itself sufficiently high that lahars and pyroclastic flows could escape the Osceola amphitheater and spill southward. As the summit cone grew during later Summerland time, pyroclastic flows and lahars began to spill into the upper Nisqually River catchment and then moved downstream. The C tephra eruption also generated the National lahar, a voluminous lahar that descended the Nisqually River to its delta at Puget Sound.

Stop 3, Kautz Creek Parking Area, 1947 Debris Flow and Older Lahars Exposed 100 Meters Upstream (46°44.163' N., 121°51.366' W.; UTM 10T, 5176469N, 587393E)

From the pullout at stop 2, drive 6.3 miles (10.1 km) down the road, past Longmire, to a large parking area with restrooms on the south side of the road just before (east of) Kautz Creek bridge. This parking area is also 3.5 miles (5.6 km) east of the Nisqually entrance to Mount Rainier National Park. Kautz Creek abandoned its channel during floods of 2006 and now intersects the highway about 0.2 miles (0.35 km) east of the bridge. The channel shifting point is about a mile (1.5 km) upstream. Many tall snags near the Kautz Creek parking lot and observation point (north of the road and slightly east of the bridge) are remnants of a forest that was killed by a debris flow on October 2 and 3, 1947. The debris flow buried the old road with 20 ft (6 m) of rock and mud and temporarily dammed the Nisqually River. Crandell (1971) suggested that the 1947 debris flow was the result of intense downpours combined with the release of additional water from Kautz Glacier. The toe of the glacier was severely broken up during events of the storm and flood. Debris flows like this are common at Mount Rainier but usually smaller in scale than the 1947 event. At Mount Rainier, debris flows are commonly triggered by severe rainstorms during atmospheric river events (locally known as "Pineapple Express" storms). Other debris flows initiate during extended periods of hot, dry weather owing to sudden release of water from glacier termini or margins. Such glacier outburst events are common at Mount Rainier and are associated generally with retreat of glaciers since the Little Ice Age maximum, exposing copious periglacial sediments that are remobilized by heavy stream flows during intense rainfall and melting events. It is likely that global warming, owing to human activity, has accelerated glacial recession and contributed at least indirectly to the frequency of small debris flows at Mount Rainier.

In November 2006 during a torrential rainstorm, Kautz Creek abandoned its course under the bridge and carved a new channel 0.2 miles (0.3 km) eastward. The new channel incised the 1947 debris fan and cut the highway. As a result of this and other damage in 2006, Mount Rainier National Park was closed to the public for 6 months.

North of the bridge about 100 m along the west bank of Kautz Creek (46°44.248' N., 121°51.399' W.; UTM 10T, 5176625N, 587348E), deposits of the 1947 debris flow and of previous lahars are exposed (fig. 47). The neutral gray deposit at the top of the section is the 1947 debris flow. Beneath it are two Mount St. Helens pumice falls, Wn (1479 C.E.) and Yn (3,700 cal. yr B.P.). The lower part of the sequence includes the Reflection Lakes lahar, Mazama ash, Van Trump lahar (10,050 cal. yr B.P.), and an unknown lahar. The Van Trump lahar was emplaced during the Sunrise eruptive period and is the oldest of three avalanche-induced lahars located on the south flank of Mount Rainier.

Stop 4, National Bridge, National and Paradise or Reflection Lake Lahars (46°44.689' N., 122°2.837' W.; UTM 10T, 5177268N, 572796E).

At National (an old townsite) intersection, or mile 6.6 on SR 706, turn on 553rd Street (labeled "South District Access") and drive 1.1 miles (1.8 km) south to the Nisqually River bridge. This bridge was washed out in the flood of November 2006 but has since been rebuilt.

At the southeast bridge abutment, lahar deposits interbedded with Mount St. Helens tephra layer Yn (3,700 cal. yr B.P.) overlie glacial outwash of Evans Creek age. The gray 1-m-thick top layer is a clay-poor Summerland lahar (probably the National lahar, 2,300 cal. yr B.P.) cropping out along an 8-m terrace (fig. 48). Abundant C tephra within the lahar suggests that the VEI-4 eruption that produced layer C also generated the lahar. The clay-poor lahar deposit overlies Mount St. Helens pumice lapilli and an orangish-brown lahar, which could be either the Reflection Lakes or Paradise lahar from Mount Rainier. The Mazama ash (7,600 cal. yr B.P.) underlies the orangish-brown lahar and overlies glacial outwash.

Near here, a 2–3-m-thick sandy gravel deposited by the same Summerland lahar caps a terrace that is 60 ft (18 m) higher than this location and indicates peak inundation at this site. The flood wave of the Summerland lahar was high enough to have buried trees at least as far downstream from Mount Rainier as McKenna, near Yelm, more than 35 miles (56 km) away, and probably reached the Nisqually River delta (Pringle, 2008).

This is the end of the field trip.

Acknowledgments

We thank reviewers Willie Scott, Lee Siebert, and Dan Dzurisin; their comments greatly improved this field guide, as did editorial comments from Claire Landowski and Monica Erdman. We are particularly grateful to Pat Pringle, who provided us with original files of figures and other material from his guidebook, "Roadside Geology of Mount Rainier National Park and Vicinity," (Pringle, 2008). Several figures used in this field guide are adapted from Pat's previous guide.

Figure 47. Photograph illustrating a stream-cut outcrop along Kautz Creek drainage about 100 meters south of Paradise Road (day 5, stop 3). The outcrop exposes a debris-flow deposit emplaced in 1947, Mount St. Helens tephras Wn and Yn, the Reflection Lakes lahar, the Mazama ash, and the Van Trump Park lahar. Ages given in calendar years before present (cal. yr B.P.) or Common Era (C.E.). Photograph by Jim Vallance, U.S. Geological Survey.

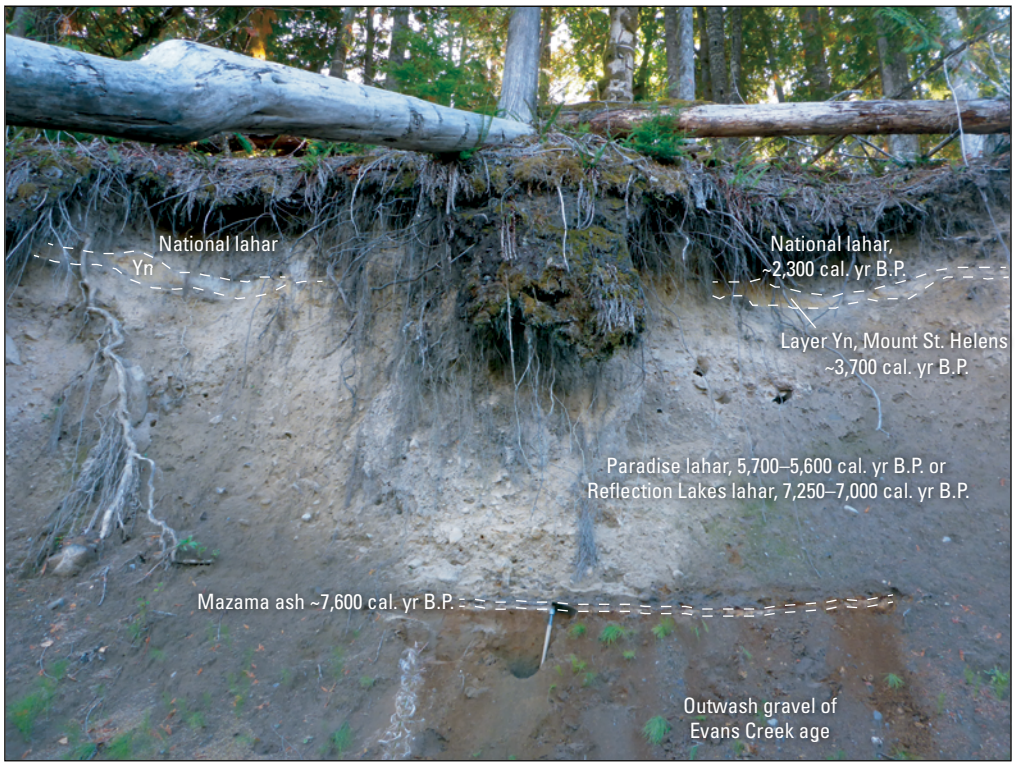

Figure 48. Photograph illustrating a Nisqually River cut at bridge across Nisqually River near National (day 5, stop 4). The outcrop exposes a lahar, which is probably the National lahar (about 2,300 calendar years before present [cal. yr B.P.]), Mount St. Helens layer Yn, the Paradise or Reflection Lakes lahar, the Mazama ash, and Evans Creek age outwash gravel. Photograph by Jim Vallance, U.S. Geological Survey.

References Cited

Armentrout, J.M., 1987, Cenozoic sequence stratigraphy, unconformity-bounded sequences, and tectonic history of southwest Washington, *in* Schuster, J.E., ed., Selected papers on the geology of Washington: Washington Division of Geology and Earth Resources Bulletin 77, p. 291–320.

Bacon, C.R., 1986, Magmatic inclusions in silicic and intermediate volcanic rocks: Journal of Geophysical Research, v. 91, p. 6091–6112.

Bacon, C.R., Bruggman, P.E., Christiansen, R.L., Clynne, M.A., Donnelly-Nolan, J.W., and Hildreth, W., 1997, Primitive magmas at five Cascade volcanic fields—Melts from hot, heterogeneous sub-arc mantle: Canadian Mineralogist, v. 35, p. 397–423.

Blunt, D.J., Easterbrook, D.J., and Rutter, N.W., 1987, Chronology of Pleistocene sediments in the Puget Lowland, Washington *in* Schuster, J.E., ed., Selected papers on the geology of Washington: Washington Division of Geologic and Earth Resources Bulletin 77, p. 321–353.

Buckovic W.A., 1979, The Eocene deltaic system of west-central Washington, *in* Armentrout J.M., Cole M.R., TerBest H., eds., Cenozoic paleogeography of the western United States: Society of Economic Paleontologists and Mineralogists, Pacific Coast Paleogeography Symposium 3, p. 147–163.

Burbank, D.W., 1981, A chronology of late Holocene glacier fluctuations on Mount Rainier, Washington: Arctic and Alpine Research, v. 13, p. 369–386.

Cary, A.S., 1966, Puget Sound basin planning—Vashon stade maximum in the Puget Lowland; Glacial Lake Russell in the Puget Lowland; Marginal drainage and lakes between Vashon ice and mountain front; Ice invades the Puget Lowland: U.S. Army Corps of Engineers [Seattle], 4 sheets, scale 1:250,000.

Clynne, M.A., Calvert, A.T., Wolfe, E.W., Evarts, R.C., Fleck, R.J., and Lanphere, M.A., 2008, The Pleistocene eruptive history of Mount St. Helens, Washington, from 300,000 to 12,800 years before present, *in* Sherrod, D.R., Scott, W.E., and Stauffer, P.H., eds., A volcano rekindled—The renewed eruption of Mount St. Helens, 2004–2006: U.S. Geological Survey Professional Paper 1750, p. 593–628.

Conrey, R.M., Sherrod, D.R., Hooper, P.R., and Swanson, D.A., 1997, Diverse magmas in the Cascade arc, northern Oregon and southern Washington: Canadian Mineralogist, v. 35, p. 367–396.

Crandell, D. R., 1963, Surficial geology and geomorphology of the Lake Tapps quadrangle, Washington: U.S. Geological Survey Professional Paper 388-A, 84 p., 2 plates, scales 1:24,000 and 1:62,500. [Also available online at https://doi.org/10.3133/pp388A.]

Crandell, D. R., 1969, Surficial geology of Mount Rainier National Park, Washington: U.S. Geological Survey Bulletin 1288, 41 p., 1 plate, scale 1:48,000. [Also available online at https://doi.org/10.3133/b1288.]

Crandell, D.R., 1971, Postglacial lahars from Mount Rainier volcano, Washington: U.S. Geological Survey Professional Paper 677, 75 p.

Crandell, D.R., and Fahnestock, R.K., 1965, Rockfalls and avalanches from Little Tahoma Peak on Mount Rainier, Washington: U.S. Geological Survey Bulletin 1221-A, 30 p.

Crandell, D.R., and Miller, R.D., 1964, Post-hypsithermal glacier advances at Mount Rainier, Washington: U.S. Geological Survey Professional Paper 501-D, p. D110–D114.

Crandell, D.R., and Miller, R.D., 1974, Quaternary stratigraphy and extent of glaciation in the Mount Rainier region, Washington: U.S. Geological Survey Professional Paper 847, 59 p., 2 plates, scales 1:250,000 and 1:48,000. [Also available online at https://doi.org/10.3133/pp847.]

Crandell, D.R., and Waldron, H.H., 1956, A recent volcanic mudflow of exceptional dimensions from Mt. Rainier, Washington: American Journal of Science, v. 254, no. 6, p. 349–362.

Dragovich, J.D., Pringle, P.T., and Walsh, T.J., 1994, Extent and geometry of the mid-Holocene Osceola mudflow in the Puget Lowland—Implications for Holocene sedimentation and paleogeography: Washington Geology, v. 22, no. 3, p. 3–26.

Driedger, C.L., 1986, A visitor's guide to Mount Rainier glaciers: Pacific Northwest National Parks and Forests Association, 80 p.

du Bray, E.A., Bacon, C.R., John, D.A., Wooden, J.L., and Mazdab, F.K., 2011, Episodic intrusion, internal differentiation, and hydrothermal alteration of the Miocene Tatoosh intrusive suite south of Mount Rainier, Washington: Geological Society of America Bulletin, v. 123, no. 3–4, p. 534–561. [Also available online at https://doi.org/10.1130/B30095.1.]

Duncan R.A., 1982, A captured island chain in the coast range of Oregon and Washington: Journal of Geophysical Research, v. 87, p. 10,827–10,837. [Also available online at https://doi.org/10.1029/JB087iB13p10827.]

Evarts, R.C., Clynne, M.A., Fleck R.J., Lanphere, M.A., Calvert, A.T., and Sarna-Wojcicki, A.M., 2003, The antiquity of Mount St. Helens and age of the Hayden Creek Drift [abs.]: Geological Society of America Abstracts with Programs, v. 35, no. 6, p. 80.

Finn, C.A., Sisson, T.W., and Deszcz-Pan, M., 2001, Aerogeophysical measurements of collapse-prone hydrothermally altered zones at Mount Rainier volcano: Nature, v. 409, no. 6820, p. 600–603.

Fiske, R.S., Hopson, C.A., and Waters, A.C., 1963, Geology of Mount Rainier National Park, Washington: U.S. Geological Survey Professional Paper 444, 93 p.

Foxworthy, B. L., and Hill, Mary, 1982, Volcanic eruptions of 1980 at Mount St. Helens—The first 100 days: U.S. Geological Survey Professional Paper 1249, 125 p.

Frizzell V.A., Tabor R.W., Zartman R.E., and Blome, C.D., 1987, Late Mesozoic or early Tertiary mélanges in the western Cascades of Washington, *in* Schuster, J.E., ed., Selected papers on the geology of Washington: Washington Division of Geology and Earth Resources Bulletin 77, p. 129–148.

Gardner, J.E., Carey, S., Rutherford, M.J., and Sigurdsson, H., 1995, Petrologic diversity in Mount St. Helens dacites during the last 4000 years—Implications for magma mixing: Contributions to Mineralogy and Petrology, v. 119, p. 224–238.

Gill, J.B., 1981, Orogenic andesites and plate tectonics: Berlin, Heidelberg, New York, Springer, 390 p.

Halliday, A.N., Fallick, A.E., Dickin, A.P., MacKenzie, A.B., Stephens, W.E., and Hildreth, W., 1983, The isotopic and chemical evolution of Mount St. Helens: Earth and Planetary Science Letters, v. 63, p. 241–256.

Hammond, P.E., and Korosec, M.A., 1983, Geochemical analyses, age dates, and flow-volume estimates for Quaternary volcanic rocks, southern Cascade Mountains, Washington: Washington Division of Geology and Earth Resources Open-File Report 83–13, 36 p.

Heller, P.L., Peterman, Z.E., O'Neil, J.R., and Shafiqullah, M., 1985, Isotopic provenance of sandstones from the Eocene Tyee Formation, Oregon Coast Range: Geological Society of America Bulletin, v. 96, p. 770–780.

Hildreth, W., 1996, Kulshan caldera—A Quaternary postglacial caldera in the North Cascades, Washington: Geological Society of America Bulletin, v. 108, p. 786–793. [Also available online at https://doi.org/10.1130/0016-7606(1996)108<0786:KCAQSC>2.3.CO;2.]

Hoblitt, R.P., Walder, J.S., Driedger, C.L., Scott, K.M., Pringle, P.T., and Vallance, J.W., 1998, Volcano hazards from Mount Rainier, Washington [revised 1998]: U.S. Geological Survey Open-File Report 98-428, 11 p., 2 plates. [Also available online at https://doi.org/10.3133/ofr98428.]

Hyndman, R.D., and Wang, K., 1993, Thermal constraints on the zone of major thrust earthquake failure—The Cascadia subduction zone: Journal of Geophysical Research, v. 98, no. B2, p. 2039–2060.

Jicha, B.R., Hart, G.L., Johnson, C.M., Hildreth, W., Beard, B.L., Shirey, S.B., and Valley, J.W., 2009, Isotopic and trace element constraints on the petrogenesis of lavas from the Mount Adams volcanic field, Washington: Contributions to Mineralogy and Petrology, v. 157, p. 189–207.

John, D.A., Rytuba, J.J., Ashley, R.P., Blakely, R.J., Vallance, J.W., Newport, G.R., and Heinemeyer, G.R., 2003, Field guide to hydrothermal alteration in the White River altered areas and in the Osceola Mudflow, Washington: U.S. Geological Survey Bulletin 2217, 52 p.

John, D.A., Sisson, T.W., Breit, G.N., Rye, G.O., and Vallance, J.W., 2008, Characteristics, extent and origin of hydrothermal alteration at Mount Rainier Volcano, Cascades Arc, USA—Implications for debris-flow hazards and mineral deposits: Journal of Volcanology and Geophysical Research, v. 175, p. 289–314.

Koppes, M.N., and Montgomery, D.R, 2009, The relative efficiency of fluvial and glacial erosion over modern orogenic timescales: Nature Geoscience, v. 2, p. 644–647.

Lambeck, K., Fouby, H., Purcell, A., and Sun, Y., 2014, Sea level and global ice volumes from the last glacial maximum to the Holocene: Proceedings of the National Academy of Sciences of the United States of America, v. 111, no. 43, p. 15,296–15,303. [Also available at https://doi.org/10.1073/pnas.1411762111.]

Leeman, W.P., Lewis, J.F., Evarts, R.C., Conrey, R.M., and Streck, M.J., 2005, Petrologic constraints on the thermal structure of the Cascades arc: Journal of Volcanology and Geothermal Research, v. 140, p. 67–105.

Leeman, W.P., Smith, D.R., Hildreth, W., Palacz, Z., and Rogers, N., 1990, Compositional diversity of late Cenozoic basalts in a transect across the southern Washington Cascades—Implications for subduction zone magmatism: Journal of Geophysical Research, v. 95, B12, p. 19,561–19,582.

Leeman, W.P., Tonarini, S., Chan, L.H., and Borg, L.E., 2004, Boron and lithium isotopic variations in a hot subduction zone—The southern Washington Cascades: Chemical Geology, v. 212, p. 101–124.

Lescinsky, D.T., and Sisson, T.W., 1998, Ridge-forming, ice-bounded lava flows at Mount Rainier, Washington: Geology, v. 26, no. 4, p. 351–354.

Lisiecki, L.E., and Raymo, M.E., 2005, A Pliocene-Pleistocene stack of 57 globally distributed benthic $\delta^{18}O$ records: Paleoceanography, v. 20, no. PA1003. [Also available online at https://doi.org/10.1029/2004PA001071.]

Lisiecki, L.E., and Stern, J.V., 2016, Regional and global benthic $\delta^{18}O$ stacks for the last glacial cycle: Paleoceanography, v. 31, p. 1368–1394. [Also available online at https://doi.org/10.1002/2016PA003002.]

Mattinson, J.M., 1977, Emplacement history of the Tatoosh volcano-plutonic complex, Washington—Ages of zircons: Geological Society of America Bulletin, v. 88, p. 1509–1514.

McKenna, J.M., 1994, Geochemistry and petrology of Mount Rainier magmas—Petrogenesis at an arc-related stratovolcano with multiple vents: Seattle, University of Washington, M.Sc. thesis, 244 p.

Miller, R.B., 1989, The Mesozoic Rimrock Lake inlier, southern Washington Cascades—Implications for the basement of the Columbia embayment: Geological Society of America Bulletin, v. 101, p. 1289–1305.

Miyashiro, A., 1974, Volcanic rock series in island arcs and active continental margins: American Journal of Science, v. 274, p. 321–355.

Morrison, R.B., 1991, Introduction *in* Morrison, R.B., ed., Quaternary nonglacial geology—Conterminous U.S.: Geological Society of America, Decade of North American Geology, Geology of North America, v. K-2, p. 1–2.

Mullineaux, D.R., 1974, Pumice and other pyroclastic deposits in Mount Rainier National Park, Washington: U.S. Geological Survey Bulletin 1326, 83 p.

Mullineaux, D.R., 1996, Pre-1980 tephra-fall deposits erupted from Mount St. Helens, Washington: U.S. Geological Survey Professional Paper 1563, 98 p.

Murphy, M.T., and Marsh, B.D., 1993, Textures and magmatic evolution of intermediate-composition dome complexes—Evidence from the northern Tatoosh complex, southern Washington Cascades: Journal of Volcanology and Geothermal Research, v. 54, p. 197–220. [Also available online at https://doi.org/10.1016/0377-0273(93)90064-X.]

Nathenson, M., 2017, Revised tephra volumes for Cascade Range volcanoes: Journal of Volcanology and Geophysical Research, v. 341, p. 42–52. [Also available online at https://doi.org/10.1016/j.jvolgeores.2017.04.021.]

Parsons, T., Trehu, A.M., Luetgert, J.H., Miller, K., Kilbride, F., Wells, R.E., Fisher, M.A., Flueh, E., ten Brink, U.S., and Christensen, N.I., 1998, A new view into the Cascadia subduction zone and volcanic arc—Implications for earthquake hazards along the Washington margin: Geology, v. 26, p. 199–202.

Porter, S.C., and Swanson, T.W., 1998, Radiocarbon age constraints on rates of advance and retreat of the Puget lobe of the Cordilleran ice sheet during the last glaciation: Quaternary Research, v. 50, no. 3, p. 205–213.

Pringle, P.T., 2000, Buried forests of Mount Rainier volcano—Evidence for extensive Holocene inundation by lahars in the White, Puyallup, Nisqually, and Cowlitz River valleys [abs.]: Washington Geology, v. 28, no. 1/2, p. 28. [Also available online at http://www.dnr.wa.gov/publications/ger_washington_geology_2000_v28_no1-2.pdf.]

Pringle, P.T., 2008, Roadside geology of Mount Rainier National Park and vicinity: Washington Division of Geology and Earth Resources Information Circular 107, 190 p.

Reid, M.E., Sisson, T.W., and Brien, D.L., 2001, Volcano collapse promoted by hydrothermal alteration and edifice shape, Mount Rainier, Washington: Geology, v. 29, p. 779–782. [Also available online at https://doi.org/10.1130/0091-7613(2001)029<0779:VCPBHA>2.0.CO;2.]

Reiners, P.W., Hammond, P.E., McKenna, J.E., and Duncan, R.A., 2000, Young basalts of the central Washington Cascades, flux melting of the mantle, and trace element signatures of primary arc magmas: Contributions to Mineralogy and Petrology, v. 138, p. 249–264.

Ripp, B., 1999, Mount Rainier mining company: Tacoma, Washington, The News Tribune, May 30, 1999.

Robinson, J.E., Sisson, T.W., and Swinney, D.D., 2010, Digital topographic map showing the extents of glacial ice and perennial snowfields at Mount Rainier, Washington, based on the LiDAR survey of September 2007 to October 2008: U.S. Geological Survey Data Series 549, https://pubs.usgs.gov/ds/549.

Samolczyk, M.A., Osborn, G., Menounos, B., Clague, J., Davis, P.T., Riedel, J., and Koch, J., 2010, A comparison of glacier fluctuations on Mount Rainier to regional glacial histories: American Association of Petroleum Geologists Search and Discovery Article no. 90172, Canadian Society of Exploration Geophysicists GeoConvention 2010.

Samolczyk, M.A., Vallance, J.W., Cubley, J.F., Osborn, G.D., and Clark, D.H., 2016, Geochemical characterization and dating of R tephra, a postglacial marker bed in Mount Rainier National Park, Washington, USA: Canadian Journal of Earth Sciences, v. 53, p. 202–217. [Also available online at https://doi.org/10.1139/cjes-2015-0115.]

Schasse, H.W., 1987, Geologic map of the Mount Rainier quadrangle, Washington: Washington Division of Geology and Earth Resources Open File Report 87–16, 1 sheet, 1:100,000 scale, 43 p. pamphlet.

Schuster, E.J., 2005, Geologic map of Washington State: Washington Division of Geology and Earth Resources Geologic Map GM-53, 1 sheet, scale 1:500,000, pamphlet 44 p.

Scott, K.M., 1988, Origins, behavior, and sedimentology of lahars and lahar-runout flows in the Toutle-Cowlitz River system: U.S. Geological Survey Professional Paper 1447-A, 74 p.

Scott, K.M., and Vallance, J.W., 1995, Debris-flow, debris-avalanche, and flood hazards at and downstream from Mount Rainier, Washington: U.S. Geological Survey Hydrologic Investigations Atlas HA 729, 9 p., 2 plates.

Scott, K.M., Vallance, J.W., and Pringle, P.T., 1995, Sedimentology, behavior, and hazards of debris flows at Mount Rainier, Washington: U.S. Geological Survey Professional Paper 1547, 56 p., 1 plate.

Sigafoos, R.S. and Hendricks, E.L., 1961, Botanical evidence of the modern history of Nisqually Glacier, Washington: U.S. Geological Survey Professional Paper 387-A, 20 p.

Sigafoos, R.S. and Hendricks, E.L., 1972, Recent activity of glaciers of Mount Rainier, Washington: U.S. Geological Survey Professional Paper 387- B, 24 p., 7 plates.

Sisson, T.W., Robinson, J.E., and Swinney, D.D., 2011, Whole-edifice ice volume change A.D. 1970 to 2007/2008 at Mount Rainier, Washington, based on LiDAR surveying: Geology, v. 39, p. 639–642, https://doi.org/10.1130/G31902.1.

Sisson, T.W., Salters, V.J.M., and Larson, P.B., 2013, Petrogenesis of Mount Rainier andesite—Magma flux and geologic controls on the contrasting differentiation styles at stratovolcanoes of the southern Washington Cascades: Geological Society of America Bulletin, v. 126, no. 1/2, p. 122–144, https://doi.org/10.1130/B30852.1.

Sisson, T.W., Schmitt, A.K., Danišík, M., Calvert, A.T., Pempena, N., Huang, C.-Y., and Shen, C.-C., 2019, Age of the dacite of Sunset Amphitheater, a voluminous Pleistocene tephra from Mount Rainier (USA), and implications for Cascade glacial stratigraphy: Journal of Volcanology and Geothermal Research, v. 376, p. 27-43.

Sisson, T.W., and Vallance, J.W., 2009, Frequent eruptions of Mount Rainier over the last ~2,600 years: Bulletin of Volcanology, v. 71, p. 595–618, https://doi.org/10.1007/s00445-008-0245-7.

Sisson, T.W., Vallance, J.W., and Pringle, P.T., 2001, Progress made in understanding Mount Rainier's hazards: Eos, American Geophysical Union Transactions, v. 82, no. 9, p. 113, 118–120.

Smith, D.R., and Leeman, W.P., 1987, Petrogenesis of Mount St. Helens dacitic magmas: Journal of Geophysical Research, v. B92, p. 10,313–10,334.

Smith, D.R., and Leeman, W.P., 1993, The origin of Mount St. Helens andesites: Journal of Volcanology and Geothermal Research, v. 55, p. 271–303.

Smith, D.R., and Leeman, W.P., 2005, Chromium spinel-olivine phase chemistry and the origin of primitive basalts of the southern Washington Cascades: Journal of Volcanology and Geothermal Research, v. 140, p. 49–66.

Southon, J., Noronha, A.L., Cheng, H., Edwards, R.L., and Wang, Y., 2012, A high-resolution record of atmospheric ^{14}C based on Hulu Cave speleothem H82: Quaternary Science Reviews, v. 33, p. 32–41. [Also available online at https://doi.org/10.1016/j.quascirev.2011.11.022.]

Stanley, D., Johnson, S.Y., and Nuccio, V.F., 1994, Analysis of deep seismic reflection and other data from the southern Washington Cascades: U.S. Geological Survey Open-File Report 94–159, 180 p.

Stanley, D., Villasenor, A., and Benz, H., 1999, Subduction zone and crustal dynamics of western Washington—A tectonic model for earthquake hazards: U.S. Geological Survey Open-File Report 99-311, accessed August 2018 at http://pubs.usgs.gov/of/1999/ofr-99-0311.

Stockstill K.R., Vogel T.A., and Sisson, T.W., 2002, Origin and emplacement of the andesite of Burroughs Mountain, a zoned, large-volume lava flow at Mount Rainier, Washington: Journal of Volcanology and Geothermal Research, v. 119, p. 275–296. [Also available online at https://doi.org/10.1016/S0377-0273(02)00358-X.]

Tabor, R.W., Frizzell, V.A., Booth, D.B, and Waitt, R.B., 2000, Geologic map of the Snoqualmie Pass 30 x 60 minute quadrangle, Washington: U.S. Geological Survey Geologic Investigations Series I-2538.

Thompson, M.E., 1983, Solidification in magmas—Part 1. The magmatic history of the Tatoosh volcanic-plutonic complex, Mount Rainier National Park; Part 2. Numerical simulation of heat and mass transfer in solidifying magmas: Eugene, University of Oregon, M.S. thesis, 227 p.

Uyeda, Seiya, 1978, The new view of the Earth—Moving continents and moving oceans: W.H. Freeman and Company, 217 p.

Vallance, J.W., 2000, Lahars, *in* Sigurdsson, H., Houghton, B., Rymer, H., Stix, J., McNutt, S., eds., The encyclopedia of volcanoes: Academic Press, p. 601–616.

Vallance, J.W., Cunico, M.L., and Schilling, S.P., 2003, Debris-flow hazards caused by hydrologic events at Mount Rainier, Washington: U.S. Geological Survey Open-File Report 03–368, 4 p., 2 plates.

Vallance, J.W., and Iverson, R.M., 2015, Lahars and their deposits, *in* Sigurdsson, H., Houghton, B., Rymer, H., Stix, J., McNutt, S., eds., The Encyclopedia of Volcanoes, 2d ed.: Academic Press, p. 649–664.

Vallance, J.W., and Pringle, P.T., 2008, Lahars, tephra, and buried forests—The postglacial history of Mount Rainier, *in* Pringle, P.T., Roadside geology of Mount Rainier National Park and vicinity: Washington Division of Geology and Earth Resources Information Circular 107, 191 p.

Vallance, J.W., and Scott, K.M., 1997, The Osceola Mudflow from Mount Rainier—Sedimentology and hazard implications of a huge clay-rich debris flow: Geological Society of America Bulletin, v. 109, p. 143–163.

Vance, J.A., Clayton, G.A., Mattinson, J.M., and Naeser, C.W., 1987, Early and middle Cenozoic stratigraphy of the Mount Rainier-Tieton River area, southern Washington Cascades, *in* Schuster, J.E., ed., Selected papers on the geology of Washington: Washington Division of Geology and Earth Resources, Bulletin 77, p. 269–290.

Venezky, D.Y., and Rutherford, M.J., 1997, Preeruption conditions and timing of dacite-andesite magma mixing in the 2.2 ka eruption at Mount Rainier: Journal of Geophysical Research, v. 102(B9), p. 20,069–20,086, https://doi.org/10.1029/97JB01590.

Waitt, R.B., Jr., and Thorson, R.M., 1983, The Cordilleran ice sheet in Washington, Idaho, and Montana, *in* Porter, S.C., and Wright, H.E., Jr., eds., Late-Quaternary environments of the United States: University of Minnesota Press, v. 1, p. 53–70.

Walder, J. S., and Driedger, C.L., 1995, Frequent outburst floods from South Tahoma Glacier, Mount Rainier, U.S.A.—Relation to debris flows, meteorological origin and implications for subglacial hydrology: Journal of Glaciology, v. 41, no. 137, p. 1–10.

Walker, G.W., and MacLeod, N.S., 1991, Geologic map of Oregon: U.S. Geological Survey, 2 sheets, scale 1:500,000.

Walsh, T.J., Korosec, M.A., Phillips, W.M., Logan, R.L., and Schasse, H.W., 1987, Geologic map of Washington—Southwest quadrant: Washington Division of Geology and Earth Resources Geologic Map GM-34, 28 p. text, 2 sheets, scale 1:250,000.

Wells, R.E., Blakely, R.J., and Weaver, C.S., 2002, Cascadia microplate models and within-slab earthquakes, *in* Kirby, S.H., Wang, K., and Dunlop, Susan, eds., The Cascadia subduction zone and related subduction systems—Seismic structure, intraslab earthquakes and processes, and earthquake hazards: U.S. Geological Survey Open-File Report 02–328 and Geological Survey of Canada Open File 4350, p. 17–23, accessed August 1, 2018, at https://pubs.usgs.gov/of/2002/0328.

Wells, R.E., Weaver, C.S., and Blakely, R.J., 1998, Fore-arc migration in Cascadia and its neotectonic significance: Geology, v. 26, no. 8, p. 759–762.

Wright T.L., 1961, The mineralogy and petrogenesis of the southern part of the Tatoosh pluton, Mount Rainier National Park, Washington: Baltimore, Maryland, Johns Hopkins University, Ph.D. dissertation, 324 p.

Zehfuss, P.H., Atwater, B.F., Vallance, J.W., Brenniman, H., and Brown, T.A., 2003, Holocene lahars and their by-products along the historical path of the White River between Mount Rainier and Seattle, *in* Swanson, T.W., Western Cordillera and adjacent areas: Geological Society of America Field-Trip Guide 4, p. 209–223.

Zimbelman, D.R., Watters, R.J., Crowley, J.K., and Rye, R.O., 2000, Non-uniform distribution of volcanic hazards, Mount Rainier [abs.]: Washington Geology, v. 28, no. 1/2, p. 29. [Also available online at http://www.dnr.wa.gov/Publications/ger_washington_geology_2000_v28_no1-2.pdf.]

Moffett Field Publishing Service Center
Manuscript approved August 18, 2022
Edited by Claire Landowski and Monica Erdman
Illustration support by JoJo Mangano
Layout by Cory Hurd

ISSN 2328-0328 (online)
https://doi.org/10.3133/sir20175022A